Three-dimensional Finite Element Analysis of the Pile Foundation Behavior in Unsaturated Expansive Soil

Xingyi Wu

Thesis submitted to the University of Ottawa

in partial fulfillment of the requirements for the degree of

MASTER OF APPLIED SCIENCE

in

Civil Engineering

Department of Civil Engineering

Faculty of Engineering

University of Ottawa

ABSTRACT

Expansive soils, which are widely referred to as problematic soils are extensively found in many countries of the world, especially in semi-arid and arid regions. Several billions of dollars are spent annually for maintenance or for repairs to the structures constructed with and within expansive soils. The major problems of expansive soils can be attributed to the volume changes associated with the alternate wetting and drying conditions due to the influence of environmental factors. Pile foundations have been widely accepted by practicing engineers as a reasonably good solution to reduce the damages to the structures constructed on expansive soils. Typically, piles foundations are extended through the active layer of expansive soil to reach the bedrock or placed on a soil-bearing stratum of good quality. Such a design and construction approach typically facilitates pile foundations to safely carry the loads from the superstructures and reduce the settlement. However, in many scenarios, damages associated with the pile foundations are due to the expansion of the soil that is predominantly in the active zone that contributes to the pile uplift. Such a behavior can be attributed to the water infiltration into the expansive soil, which is a key factor that is associated with the soil swelling. Due to this phenomenon, expansive soil typically moves upward with respect to the pile. This generates extra positive friction on the pile because of the relative deformation. If the superstructure is light or the applied normal stress on the head of the piles is not significant, it is likely that there will be an uplift of the pile contributing to the damage of the superstructure.

In conventional engineering practice, the traditional design methods that include the rigid pile method and the elastic pile method are the most acceptable in pile foundation design. These methods are typically based on a computational technique that uses simplified assumptions with respect to soil and water content profile and the stiffness and shear strength properties. In other words, the traditional design method has limitations, as they do not take account of the complex hydromechanical behavior of the in-situ expansive soils. With the recent developments, it is possible to alleviate these limitations by using numerical modeling techniques such as finite element methods. In this thesis, a three-dimensional finite element method was used to study the hydro-mechanical behavior of a single pile in expansive soils during the infiltration process.

In this thesis, a coupled hydro-mechanical model for the unsaturated expansive soil is implemented into Abaqus software for analysis of the behavior of single piles in expansive soils during water infiltration. A rigorous continuum mechanics based approach in terms of two independent stress state variables; namely, net normal stress and suction are used to form two three-dimensional constitutive surfaces for describing the changes in the void ratio and water content of unsaturated expansive soils. The elasticity parameters for soil structure and water content in unsaturated soil were obtained by differentiating the mathematical equations of constitutive surfaces. The seepage and stress-deformation of expansive soil are described by the coupled hydro-mechanical model and the Darcy's law. To develop the subroutines, the coupled hydro-mechanical model is transferred into the coupled thermal-mechanical model. Five user-material subroutines are used in this program. The user-defined field subroutine (USDFILD) in Abaqus is used to change and transfer parameters. Three subroutines including user-defined material subroutine (UMAT), user-defined thermal material subroutine (UMATHT), and user-defined thermal expansion subroutine (UEXPAN) are developed and used to calculate the stress-deformation, the hydraulic behavior, and the expansion strain, respectively. Except for the coupled hydro-mechanical model of unsaturated expansive soils, a soil-structure interface model is implemented into the user-defined friction behavior subroutine (FRIC) to calculate the friction between soil and pile. The program is verified by using an experimental study on a single pile in Regina clay. The results show that for the single pile in expansive soil under a vertical load, water infiltration can cause a reduction in the pile shaft friction. More pile head load is transferred to the pile at greater depth, which increases the pile head settlement and pile base resistance. In future, the proposed method can also be extended for verification of other case studies from the literature. In addition, complex scenarios can be investigated to understand the behavior of piles in expansive soils.

ACKNOWLEDGMENTS

I would like to express my deepest appreciation to my supervisor Prof. Sai K. Vanapalli for his support and encouragement during my study and research. His encouragement, insightful suggestions, and continuous supports have enlightened my way towards exploring the unsaturated soils and have broadened my vision. Besides his instruction on my research, he also gave me a huge help on my growing. He gave me a lot of suggestions to me on how to act as a real man. I also will remember his great tolerance to me; he forgave me again and again when I made some mistakes. He also tried his best to help me to purse a Ph.D. position, contacting potential supervisors for me and provided several helpful suggestions on my future. Without Prof. Sai, both this thesis and I could not have reached its present stage. I sincerely appreciate what Prof. Sai did for me in past two and half years and I will remember his help forever!

I am also grateful to Professors Mehdi Pouragha and Rozalina Dimitrova for serving as committee members and providing insightful comments and suggestions. Your comments were helpful for me to improve this thesis.

My appreciations extend to my colleagues at the University of Ottawa for their friendship and support. These individuals include; Yunlong Liu, Mohammed Al-Khazaali, Ping Li, Xiaokun Hou, Junping Ren, Penghai Yin, Xiuhan Yang, Mingshu Cheng, Mengxi Tan, Xinting Cheng, Wenjun Zhang, Yao Li, Junjie Wang, Aolin Zhang, Yu Bai, Kenneth O. Omenogor, Luqiang Ding, Dr. Ruixia He, and Dr. Jian Xu.

I am extremely thankful for my parents, who not only supported me with the finances to go to Canada to pursue my studies and dreams but inspired me when I had some troubles in my life. This thesis would not have been possible without their love, support and inspiration.

CONTENT

LIST OF FIGURES

LIST OF TABLES

CHAPTER 1
INTRODUCTION

1.1 Background

Expansive soil is a term that is widely used for describing soils that undergo significant volume changes due to the variation of the water content (Nelson and Miller 1997). A typical expansive soil is made up of several clay minerals; which include montmorillonite, illite, or kaolinite in addition to other minerals. Montmorillonite is a clay mineral that has a high ability to absorb a large quantity of water. A water content increase in the expansive soil associated with rainfall or other modes of infiltration is absorbed between the clay sheets of clay minerals, resulting in the swelling of the soil. When the water content is reduced by evaporation or other factors, the water between clay sheets is released, which will induce shrinkage characteristics to the expansive soil. Therefore, the composition of the clay minerals has a dramatic influence on the volume change behavior of expansive soils due to water content changes. The volume change characteristics contribute to significant damages to infrastructure constructed within or with expansive soils; due to this reason, they are considered by geotechnical engineers as problematic soils.

Expansive soils are widely distributed around the world (Chen 1975; Ng et al. 2003). Many countries have expansive soil deposits; for example, Argentina, Australia, Burma, Canada, China, Cuba, Ghana, Great Britain, India, Iran, Kenya, Mexico, Morocco, Rhodesia, South Africa, Spain, Turkey, USA, and Venezuela (Chen 1975). The distribution of expansive soil around the world is shown in Figure 1.1.

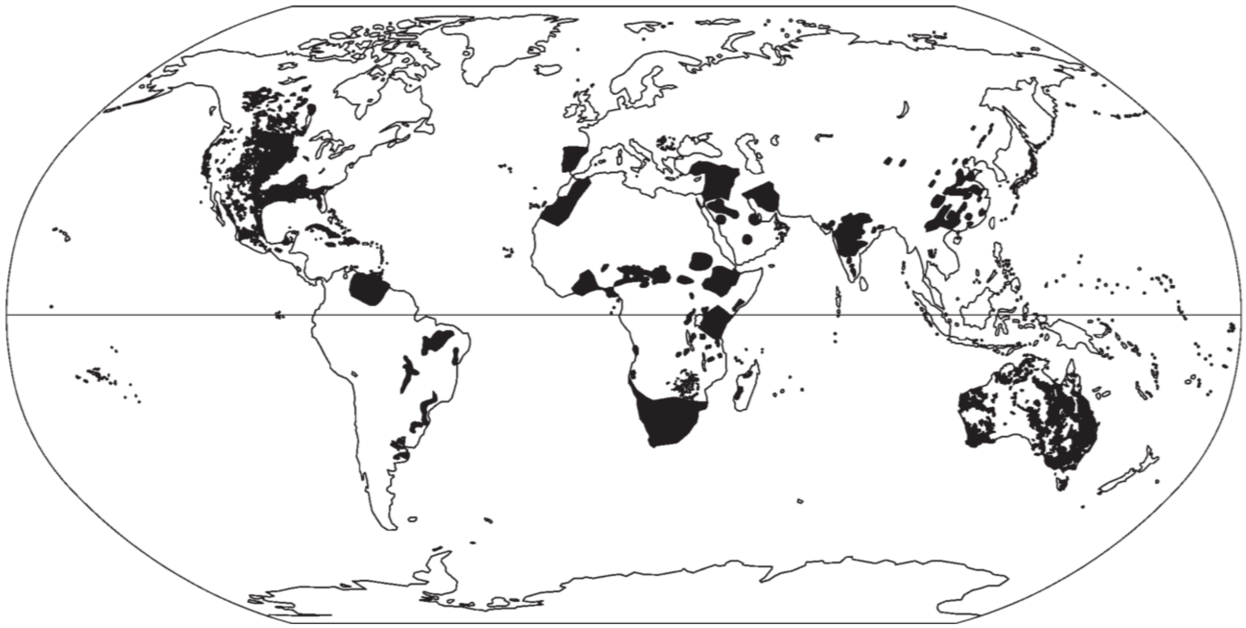

Figure 1.1 Global distribution of expansive soils (Nelson et al. 2015).

As discussed earlier, expansive soil volume change behavior can result in many engineering problems and have been widely reported in the literature (Steinberg 1998). The first recognized problem in engineering practice associated with expansive soils was reported in 1938 by the U.S. Bureau of Reclamation (Chen 1975). This was related to a foundation problem for a steel siphon. Such problems are not only limited to the foundations, but also other infrastructure in expansive soils and contribute to damages. For example, the swelling-induced softening behavior can result in the failure of the expansive soil slope (Qi and Vanapalli 2016). The swelling of expansive soil can cause additional earth lateral pressure on the retaining wall, which may result in the deformation and bending and the possible failure of the retaining walls (Al-Busoda et al. 2017).

The problems associated with the expansive soils result in enormous economic costs annually around the world. For example, Puppala and Cerato (2009) reported that the cost of damage due to expansive soils in the USA is approximately $13 billion, each year. In China, according to an incomplete estimation, economic losses associated with the expansive soil are over $1 billion per year (Shi et al. 2002). Vanapalli and Adem (2013) summarized the annual costs associated with the expansive soil problems for different regions in the world (see Table 1.1) which highlight the significant losses.

Table 1.1 The annual cost associated with the expansive soil for different regions in the world (Vanapalli and Adem 2013).

Region	Cost of damage per year
USA	$13 billion
UK	£400 million
France	€3.3 billion
Saudi Arabia	$300 million
China	¥100 million
Victoria, Australia	$150 million

Pile foundations are widely used as they reduce damages and ensure the safety of buildings constructed in expansive soil areas (Poulos 1993; Xiao et al. 2011). These foundations are typically slender columns that penetrate through the expansive soil layers to reach the bedrock or a firm soil layer that is not affected by the variation in the water contents (Soundara and Robinson 2017; Liu 2019). Even though the expansive soil swells, the bedrock or the soil layer that is not sensitive to the variation of water content support the loads from the superstructure by the pile foundation alleviating settlement problems.

Geotechnical engineers should be able to interpret the hydromechanical behavior of expansive soils such that rational design procedures can be proposed for the design of pile foundations in expansive soils. Figure 1.2 illustrates the behavior of the pile foundation in expansive soil prior to and after the water infiltration. Typically, a positive friction contribution arises along the length of the pile in expansive soils due to surcharge prior to the infiltration of water. The bedrock or the firm soil that is not affected by the variation in water content can offer end-bearing resistance. However, when there is an increase in water content due to rainfall or other modes of water infiltration, the expansive soil swells. The ground heave occurs resulting in an increase in the natural ground surface (i.e. in the vertical direction). In addition, expansive soil moves in the upward direction relative to the pile. The positive friction may increase due to the increase in the relative movement between the soil and pile. Typically, pile under the light loaded structure may get uplifted due to the increase in the positive friction. The bedrock or soil layer that is not affected by variation in water content will not swell when the water flows into the soil, because it is not sensitive to the changes in water content. The pile moves upward relative to the bedrock or the soil layer that is not affected by variation in water content due to the uplift of the pile associated with the infiltration. Due to the relative deformation, negative friction may distribute along a portion of the pile length closer to the base. The end bearing resistance may decrease during the infiltration due to the uplift of the pile.

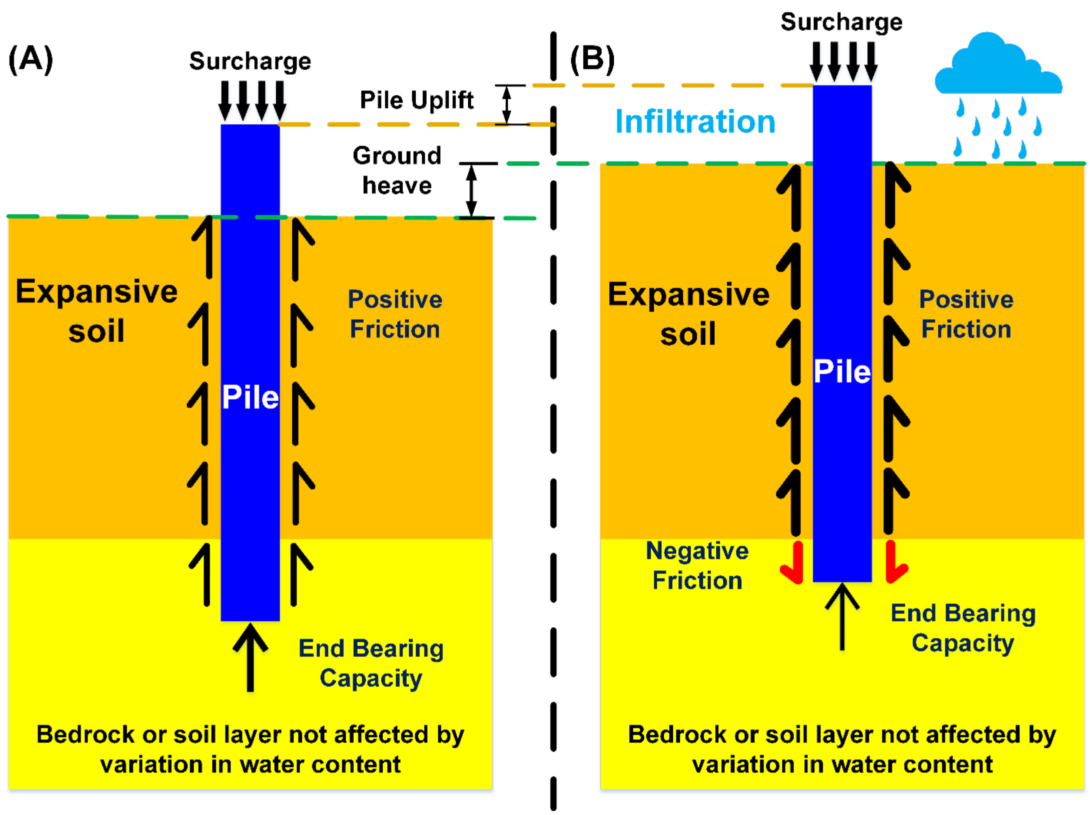

Figure 1.2 The mechanical behavior of the pile foundation in expansive soils (A) before infiltration; (B) after infiltration (modified from Liu and Vanapalli 2017).

The mechanical behavior of single piles in expansive soils, as discussed above, has been widely accepted in the literature (for example, Jiang et al., 2020; Mohamedzein et al., 1999).

However, in this behavior, the shear stress in pile-soil interface was assumed to increase as the increase in the relative displacement between pile and soil, as shown in Figure 1.3. In addition, the stress-relative displacement relation in the pile-soil interface was assumed to be independent to the suction or pore water pressure of the interface. In other words, the effect of the pore water pressure on the mechanical behavior of the pile-soil interface and the softening behavior of the shear strength of the interface were not included. Borana et al. (2017) conducted a series of pullout tests on smooth and rough model piles in a compacted soil with different water contents. The results of this study suggest that the soil water content (as well as suction) has a significant influence on the skin friction of the model pile. The average shear stress along the length of the pile decreases with an increase in soil water content. The lower initial water content can be associated with a higher suction that contributes to a larger pile skin friction (or the higher the interface shear strength). This study supports that the mechanical behavior of the pile foundations in unsaturated expansive soils can be rationally interpreted by considering the influence of water pressure or suction changes associated with water content changes.

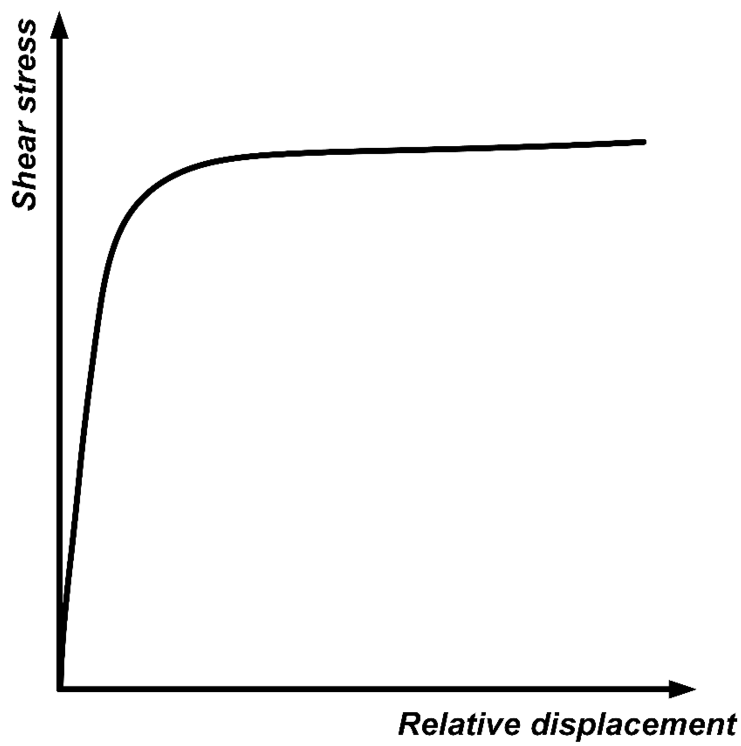

Figure 1.3 The hardening behavior of the shear stress of the pile-soil interface.

Three different methods are widely used for the design of the pile foundation in expansive soils (Nelson et al. 2012). These methods are, namely; (i) the rigid pile method, (ii) elastic pile method, and (iii) the numerical modeling method.

In the rigid pile method, the pile is assumed as rigid and the movement of the pile head is assumed as zero. The positive friction exerted on the pile by the swelling of expansive soils is equal to the sum of the applied head load and the negative friction below the depth of the potential expansion soil (Chen 1988; O'Neill 1988).

In the elastic pile method, the pile heave is allowed. The expansive soil is assumed as an elastic half-space. The pile heave is calculated by assuming the pile is in the stiff part of the elastic half-space. However, both the rigid and the elastic pile methods do not facilitate numerical modeling of the hydromechanical behavior of unsaturated expansive soils. Due to this reason, the variation of shaft friction distribution, end bearing resistance, axis force distribution of the pile foundation at the different stages of the water infiltration cannot be reliably modeled.

The finite element method is a powerful tool that overcomes the shortcomings of the first two methods. This method makes it possible to couple for the hydromechanical behavior of unsaturated expansive soil along with unsaturated pile-soil interface through use of valid constitutive models. Due to the coupling, the finite element method is capable of simulating the complex hydraulic behavior of in-situ expansive soils and the mechanical behavior of the pile foundation upon the infiltration. This thesis aims to study the variation of the mechanical properties of the pile foundation in the expansive soil upon the water infiltration by using the finite element method.

1.2 Objective and Scope of Study

The key objective of this thesis is to use the finite element method to simulate the behavior of the pile foundation in unsaturated expansive soil upon water infiltration. The commercial software Abaqus is used in this study to conduct the numerical simulations. Compared with the two-dimensional (2D) numerical analysis, the three-dimensional (3D) numerical analysis can take into account the appropriate geometry and boundary conditions. Therefore, the 3D numerical analysis can provide more realistic results (Shen and Karakus 2014). In this thesis, the 3D numerical analysis of the pile foundation was conducted. Presently, Abaqus does not have the 3D coupled hydro-mechanical constitutive models for simulating unsaturated expansive soils behavior. For this reason, a 3D coupled hydro-mechanical constitutive model for the unsaturated expansive soil is developed in this thesis. In addition to the constitutive model for the unsaturated expansive soil, a constitutive model for the unsaturated pile-soil interface is also required for performing the numerical analysis.

For achieving the objective, a constitutive model for unsaturated soil is required in numerical modeling. Matyas and Radhakrishna (1968) are the pioneers who introduced the concept of constitutive state surface for the unsaturated soil. By extending this approach, the void ratio and water content can be plotted as the functions of two stress state variables; namely, net normal stress and suction. Later studies have highlighted the use of net normal stress, $(\sigma - u_a)$ and suction $(u_a - u_w)$ as two independent stress variables to rationally interpret the hydro-mechanical behavior of unsaturated soils (Fredlund and Morgenstern, 1976). Assuming the unsaturated expansive soils behavior as elastic, Fredlund and Morgenstern (1976) proposed two constitutive equations for unsaturated soils in terms of independent stress state variables (i.e. net normal stress, $(\sigma - u_a)$ and suction $(u_a - u_w)$). The first equation describes the soil structure (i.e. void ratio) deformation and the second equation describes the water content. A series of elastic parameters are included in these constitutive equations. In other words, the void ratio and the water content of unsaturated soils are presented as the functions of the net normal stress and suction (i.e. three-dimensional surfaces). Vu (2003) proposed mathematical equations to fit these surfaces. The elastic parameters included in constitutive equations can be determined by differentiating the mathematical equations. When the elastic parameters are determined, the hydromechanical behavior of unsaturated expansive soil can be simulated using the constitutive equations proposed by Fredlund and Morgenstern (1976). The flow of water in unsaturated soil can be simulated by Darcy’s law. The coupled hydro-mechanical analysis can be carried out by combining the constitutive equations for the unsaturated soils and Darcy’s law. In this thesis, the equations for the constitutive relations and Darcy’s law for the unsaturated soils, and the governing equations for the coupled hydro-mechanical problems are introduced. The determination of the elastic parameters is also introduced in this thesis.

In addition to the constitutive models for rationally interpreting the unsaturated soil behavior, a reasonable constitutive model is also required for the pile-soil interface in numerical modeling. In engineering practice, the shaft resistance degradation has been investigated from several field tests (Zhang et al. 2010, 2011; Zhao et al. 2009). The skin friction along the pile surface increases with an increase in the relative displacement and approaches the peak value. After approaching the peak value, the skin friction decreases to a residual value. Zhang and Zhang (2012) proposed a hyperbolic model to simulate the degradation behavior of skin friction. For the unsaturated soil-structure interface, the shear strength is not only influenced by the net normal stress but also by the suction. Hamid and Miller (2009) proposed an equation to formulate the shear strength of the unsaturated soil-structure interface in terms of two stress state variables by modifying the shear strength equation proposed for unsaturated soils by Vanapalli et al. (1996). Liu and Vanapalli (2019) modified the Zhang and Zhang (2012) model to simulate the behavior of the unsaturated pile-soil interface. In this model, the equation proposed by Hamid and Miller (2009) is used to calculate the peak stress of the unsaturated pile-soil interface. The constitutive model for the unsaturated pile-soil interface proposed by Liu and Vanapalli (2019) is employed in this thesis. In this thesis, the equations of the unsaturated pile-soil interface are introduced. The determination of the parameter of the interface is also discussed in this thesis.

Abaqus is one of the most widely used commercial software to conduct numerical modeling for geotechnical engineering problems. Many problems, for example, slope stability analysis (Yang et al. 2012), pile foundation (Sinha and Hanna 2017), liquefaction (Wang et al. 2019), and other geotechnical problems, have been studied using Abaqus software. To use Abaqus program for numerical simulations, the similarity of the coupled thermo-mechanical problems and the coupled hydro-mechanical problems is exploited (Zhang 2004). In the coupled hydro-mechanical problems, the water flow behavior in soils is modeled using Darcy's law. The heat conduction follows Fourier's law in the coupled thermo-mechanical problems. Darcy's law is similar to Fourier's law in principle and form. Both these equations relate the driving forces (i.e. the gradient of pressure head, the gradient of temperature) to their conjugated flux (i.e. water flux, heat flux) (Groenevelt 2003). Because of the similarity, it is possible to simulate the water flow by using Fourier's law. In the coupled hydro-mechanical problems, the strain of the soil structure for the unsaturated soil can be induced by external stress and suction. In the coupled thermo-mechanical problems, the strain is induced by external stress and temperature. Therefore, the strain-stress relation for the coupled hydro-mechanical problems is similar to the strain-stress relation for the coupled thermo-mechanical problems. In other words, it is possible to simulate the coupled hydro-mechanical problems by processing the coupled thermo-mechanical analysis. In this study, the equations for the coupled thermo-mechanical problems are derived. These are constitutive relationships for soil, energy variation as well as heat conduction and other governing equations for modeling the coupled thermo-mechanical problems. The equations for the hydro-mechanical problems are compared with the equations for the coupled thermo-mechanical problems. In addition, parameters used in the coupled hydro-mechanical problems and the coupled thermo-mechanical problems are compared and their similarities are detailed in this thesis. By exploiting the similarity features, the software Abaqus is used as a tool to simulate the coupled hydro-mechanical problems of unsaturated expansive soils.

Abaqus provides different types of user-defined subroutines whereby users can define the complex behavior of materials in a general way (Huang 1991). Based on the similarity of the coupled hydro-mechanical problems and coupled thermo-mechanical problems, five user-defined subroutines are used to develop the program. The user-defined field subroutine USDFILD is used to change and transfer parameters. Three subroutines including user-defined material subroutine UMAT, user-defined thermal material subroutine UMATHT, and user-defined thermal expansion subroutine UEXPAN are used to calculate the stress-deformation, the hydraulic behavior, and the expansion strain, respectively. The soil-structure interface model is implemented into user-defined friction behavior subroutine FRIC to calculate the friction between soil and pile.

Liu (2019) conducted a large-scale comprehensive model pile test at the University of Ottawa. The test results are used to verify the developed subroutines and simulate the behavior of model pile behavior. The mechanical properties of the pile foundation (i.e. the distribution of the shaft friction, the distribution of the axis force, the displacement of the pile head) are analyzed.

1.3 Structure of Thesis

The thesis consists of six chapters.

This Chapter entitled, Introduction presents the background, the objective, and the scope of the thesis.

Chapter II presents the literature review, highlighting (i) the design method for the pile foundation in expansive soils; (ii) the constitutive models for unsaturated soils; (iii) the constitutive model for explaining the soil-structure interface.

Chapter III introduces the constitutive models that are developed in the user-defined subroutines. This chapter includes (i) the constitutive relation for the unsaturated expansive soil; (ii) the flow law for the water phase in the unsaturated expansive soil; (iii) the differential equations governing the mechanical behavior and flow behavior of the unsaturated expansive soils; (iv) the constitutive model for the unsaturated pile-soil interface.

Chapter IV introduces the theoretical development of user-defined subroutines for the constitutive models of unsaturated expansive soil and the pile-soil interface. This chapter includes (i) the constitutive relation and heat transfer law for the coupled thermo-mechanical problems; (ii) the differential governing equations for the coupled thermo-mechanical problems; (iii) the similarity of the coupled hydro-mechanical problems and the coupled thermo-mechanical problems; (ii) the layout of five developed subroutines.

Chapter V introduces the experimental program of the large-scale model pile test performed by Liu (2019) in expansive clay from Regina. The developed subroutines are used along with Abaqus to conduct the coupled hydro-mechanical analysis of unsaturated expansive soils and the analysis of behavior of the pile foundation. This chapter includes (i) a brief introduction of the experimental study; (ii) the introduction of the simulation including the input values, boundary conditions, and the analysis; (iii) comparison between the experimental and numerical simulation results.

Chapter VI presents the summary and conclusions. This chapter also suggests future studies that can be performed.

CHAPTER 2
LITERATURE REVIEW

2.1 Introduction

There is an urgent need for reliable methods that provide rational procedures for the design of pile foundations in expansive soils for use in conventional engineering practice. One of the most widely used foundations to reduce the damages to the structures constructed in various types of soils is pile foundations (Sorochan 1974). Three methods are commonly used for the design of pile foundations, namely: (i) the rigid pile method, (ii) the elastic pile method, and (iii) the finite element based method. These methods are briefly reviewed in this chapter. Of these three methods, the finite element method is a flexible method that can simulate the behavior of pile during the swelling process associated with water infiltration in unsaturated expansive soils. In the finite element analysis, the constitutive models for the unsaturated expansive soils and the unsaturated pile-soil interface are required in the numerical modeling; therefore, these models are also reviewed in this chapter.

2.2 Design methods for the pile foundation in expansive soils

Nelson et al. (2007, 2012) studies highlight three methods that are commonly used for the design of the pile foundation in expansive soils, which are succinctly summarized below.

2.2.1 Rigid pile method

Chen (1988) and O'Neill (1988) proposed the rigid pile method. In this method, the pile is assumed as rigid and no displacement will occur at the pile head. The uplift friction induced by the swelling of the expansive soil is considered equal to the summation of the negative friction in the soil layers below the active zone and the surcharge. Chen (1988) and O'Neill (1988) assumed the uplift skin friction stress was constant in the active zone and suggested that the friction stress, f_u can be calculated by the following equation.

$$f_{\mathrm{u}} = \alpha_1 \sigma_{\mathrm{s}}' \tag{2.1}$$

where α_1 is the coefficient of the uplift friction, σ_{s}' is the swelling pressure.

O'Neill (1988) suggested using the following equation for calculating the friction stress. The coefficient of the uplift friction, α_1, is presented as the function of the coefficient of the uplift friction, α_2, and the effective friction angle for the residual strength of the soils.

$$f_{\mathrm{u}} = \alpha_2 \sigma_{\mathrm{s}}' \tan\ \varphi_r' \tag{2.2}$$

where α_2 is the coefficient of the uplift friction, φ_r' is the effective friction angle for the residual strength of the soils.

The uplift force, U, can be calculated by the following equation.

$$U = \pi d f_{\mathrm{u}} z_{\mathrm{a}} \tag{2.3}$$

where d is the diameter of the pile and z_{a} is the depth of the active zone.

The summary of the surcharge and the negative force below the active zone, W, can be calculated by the following equation.

$$W = \frac{\pi d^2}{4} q_{\mathrm{dl}} + \pi d f_{\mathrm{s}} (L - z_{\mathrm{a}}) \tag{2.4}$$

where q_{dl} is the applied surcharge, L is the length of the pile, and f_{s} is the friction between the pile and soil below the active zone. As the uplift friction is assumed equal to sum of the surcharge and the negative force below the active zone, Equation (2.3) was set to be equal to Equation (2.4). The length of the pile can be determined by letting Equation (2.3) to be equal to Equation (2.4).

The rigid pile method was effective to design the pile foundation in the expansive soil. However, in practice, it is well known that there is going to be some displacement in the foundation, which is not accounted in this method. Therefore, the rigid pile method is not a reliable method as the heave of the pile head is considered in the design procedure.

2.2.2 Elastic pile method

Poulos and Davis (1980) proposed a basic framework for the elastic pile method. In this method, the soil is assumed as an elastic, homogenous half-space and allows the pile head displacement (i.e. pile-soil slip can be accommodated). The heave of the soil is assumed distributed linearly to the depth of the active zone. The soil displacement is calculated by the stiffness of the soil and the interface shear stress. The effects of the pile-soil slip along the interface was allowed for by specifying the limit value of the shear stress, and a limiting base pressure equal to the bearing capacity. The solution was cycled until the shaft friction and the end bearing resistance do not exceed the limit values. For extending this approach in practice, Poulos and Davis (1980) provided design charts. Nelson et al. (2007) extended this approach and provided additional design charts that facilitate the design of straight shaft pile and belled pile. Nelson et al. (2007) predicted the heave of the expansive soil by using the heave index, stress state, swelling pressure, initial void ratio, and the layer thickness. The heave index was determined from the consolidation-swell test data.

Fan et al. (2007) proposed the load-displacement transfer law for a single pile in expansive soil under the applied load. Both the pile and soil were assumed as elastic. The displacement of soil around the pile is related not only with the depth but also with the distance away from the pile axes. The heave of expansive soil is assumed distributed linearly along with the depth. Two different scenarios are possible are likely in the behavior of piles in expansive soils based on the assumption used in the analysis. In the first scenario, the pile can move downward under the applied load if the expansion in the soil is neglected. In the second scenario, the pile may move upward due to the swelling of soil when the applied load is ignored. The actual behavior of the pile in the expansive soil can be obtained by combing these two scenarios. Such an approach is proposed by extending the assumption that the displacement is influenced by the soil depth but also the distance from the pile axes. The relation between the displacement of soil and the distance away from the pile axes was assumed to follow a logarithmical equation. According to the displacement compatible condition (Figure 2.1), the displacement of soil at the radius of the pile radius should be equal to the displacement of the pile. Therefore, the pile displacement can possibly be given from the equation for the soil displacement. The interface shear stress can be calculated by the stiffness of the soil and the displacement of soil. The pile was divided into several elements. By considering the static equilibrium, it is possible to calculate the pile displacement. The pile displacement in two scenarios can be calculated in this way. It is possible to calculate the pile displacement in the actual state by superposing these two scenarios. Xiao et al. (2011) employed this model to study the behavior of pile in expansive soil. The effects of the length, the diameter of the pile, the shear modulus of soil, and the applied load on the behavior of the pile were studied. Jiang et al. (2020) modified this model by considering the shear modulus of the soil changing with depth. The shear modulus of soil was assumed to increase linearly with the depth. The effects of pile length and pile diameter were studied.

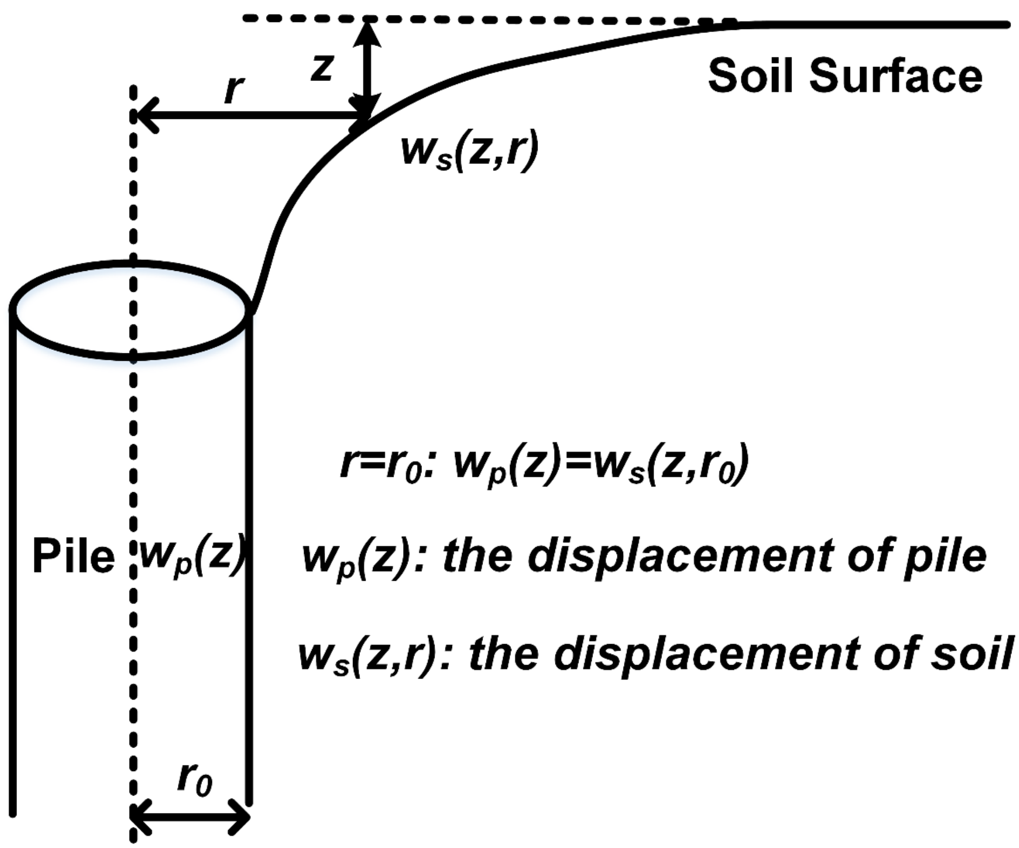

Figure 2.1 The displacement compatible condition of soil and pile (Xiao et al. 2011).

Liu and Vanapalli (2017) may be the first researchers who introduced the unsaturated soil mechanics into the elastic design method. A new equation for the lateral earth pressure was proposed in this study. The lateral earth pressure was calculated from information of the vertical swelling pressure and the vertical load induced by the soil unit weight and surcharge. The equation for the lateral earth pressure was combined with the equation for the unsaturated soil-structure interface shear strength to calculate the friction stress in the pile-soil interface. In a recent study, Liu and Vanapalli (2019b) modified the method proposed by Liu and Vanapalli (2017). The modified method facilitates the calculation of the lateral earth pressure taking account of the influence of variation of the soil swelling associated with different suction values. In addition, Liu and Vanapalli (2019a) proposed a new pile-soil interface model. This new model is capable of simulating the behavior of the unsaturated pile-soil interface taking account of the influence of suction (Liu and Vanapalli 2019a). These methods were proved effective to simulate the behavior of the pile.

The elastic pile design method was simple to conduct. However, the elastic design method was just suitable for the pile whose ratio between the length and diameter was less than 20 (Nelson et al. 2012). Therefore, the method that is more flexible is required for the practice.

2.2.3 Finite element based method

Finite element methods are widely used in the pile-soil analysis for all soils including expansive soils and are capable of modelling complex soil profile and soil behavior (Nelson et al. 2012). The finite element methods are also flexible for simulating the pile with different sizes and properties. In addition, the influence soil-structure interaction in general and pile-soil interaction in particular can be taken into account in these methods (Abhishek and Sharma 2019; Al-Busoda et al. 2017; Justo et al. 1984; Mohamedzein 2006; Mohamedzein et al. 1999).

Amir and Sokolov (1976) developed a two-dimensional finite element model to simulate the pile in expansive media. Both flow and elastic behavior were assumed linear. The volume change of soil can result in the evident displacement of the pile. The results also showed that the deeper piles had smaller displacements. Lytton (1977) assumed the soil was linear elastic. Darcy's law was employed to calculate the water flow. The coupled and uncoupled hydro-mechanical analysis was carried out. Justo et al. (1984) conducted a three-dimensional finite element analysis. In this study, the soil was assumed as isotropic, nonlinear, and nonhomogeneous. The nonlinear and nonhomogeneous due to the stress state was considered by employing the dependence of the initial swelling and oedometric modulus on the vertical stress. The results showed that the stress state had a great influence on the calculated heave and pile stresses that should be considered in practice.

Mohamedzein et al. (1999) studied the mechanical behavior of the short pile in expansive soil. In this study, the soil is modeled as a nonlinear elastic by using the Duncan-Chang model and modified Duncan-Change model. The relation of the swelling strain and the suction in $\varepsilon - \log s$ space is assumed linear. The slope of the $\varepsilon - \log s$ line was the suction compression index. The suction compression index was obtained by conducting the one-dimensional consolidation tests. In this study, the slip in the pile-soil interface was assumed to be less than 40 mm. The results illustrated that an increase in the pile length and the applied axial compressive load can decrease the upward vertical displacement of the pile due to the soil swelling assuming full contact between pile and the soil. The finite element based method is effective and flexible to study the behavior of the pile in expansive soil. However, at the present, the studies based on the finite element method were limit.

Nelson et al. (2012) suggested that the constitutive relationships used for modeling the soil behavior should be able to calculate the strain induced by the external stress and the strain induced by the variation of suction. In addition, the finite element method should take into account the pile-soil interface to model the slip between pile and soil.

In this study, the finite element analyses were carried out to model the pile-soil behavior in unsaturated expansive soils. The required background related to constitutive models and the unsaturated pile-soil interface properties is summarized in the following section.

2.3 Constitutive model for the unsaturated expansive soil

The rational concepts of soil mechanics were developed based on Terzaghi effective stress (Skempton 1960). In the traditional soil mechanics, soils are assumed to be saturated either with water or other types of fluid (e.g. air). Therefore, the classic soil mechanics focused on conventional soils, such as saturated sand, silt, clay, or dry sand (Fredlund et al. 2012). However, the arid and semi-arid zones cover 40% of the global land surface (Figure 2.2). Therefore, there are numerous soils encountered in the practice who were not saturated. Therefore, it is necessary to expand the spectrum of soil mechanics to include unsaturated soils.

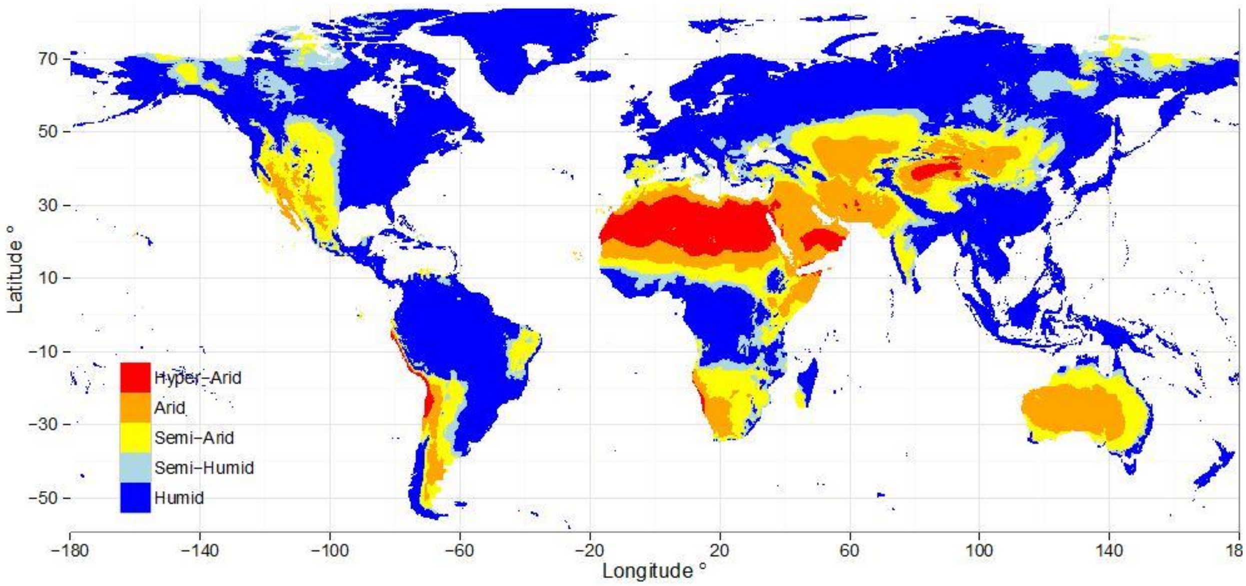

Figure 2.2 Map of the global distribution of climatic zones (Source: http://ozewex.org/semi-arid-ecosystems-particularly-sensitive-to-mega-droughts/).

Compared with the saturated soils which consist of two phases including solid phase (i.e. soil particle) and fluid phase (e.g. water), the unsaturated soils are typically made up of three phases including solid phase (i.e. soil particles), fluid phase (e.g. water), and air phase, as plotted in Figure 2.3. Therefore, to describe the behavior of the unsaturated soils, the properties of the air phase for example the pore air pressure, u_a, should be considered in addition to the water phase.

Bishop (1959) first introduced the concept "suction", $(u_a - u_w)$, into the stress variable to interpret the shear strength of soils. Since then, many constitutive models have been developed to interpret the behavior of unsaturated soils (Alonso et al. 1990; Fredlund and Morgenstern 1976; Gallipoli et al. 2003; Khalili and Selvadurai 2003; Wheeler et al. 2003; Zhang and Lytton 2009a).

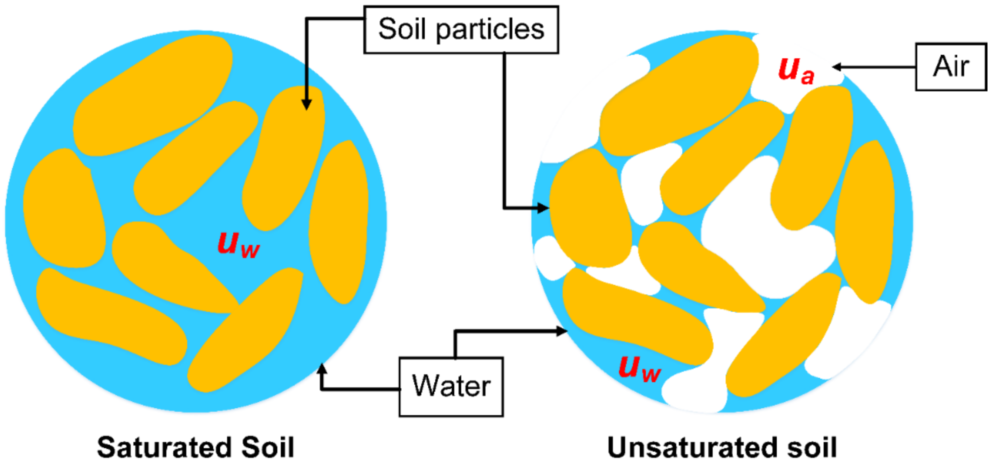

Figure 2.3 The composition of the saturated soils and unsaturated soils.

2.3.1 State surface model

Bishop (1959) proposed the effective stress equation, σ', for unsaturated soils, which is expressed as follows.

$$\sigma' = (\sigma_n - u_a) + \chi(u_a - u_w) \tag{2.5}$$

where σ_n is the total normal stress. u_w is the pore water pressure. u_a is the pore air pressure. The total normal stress in excess to the pore air pressure is defined as the net normal stress, $(\sigma_n - u_a)$. The suction is defined as the excess of the pore air pressure to the pore water pressure, $(u_a - u_w)$. χ is defined as the effective stress parameter or Bishop's parameter.

The effective stress parameter varies from a value of 0 for the dry soil to a value of 1 for the saturated soil, enabling the simple transition from the unsaturated to the saturated state (Nuth and Laloui 2008). However, measured χ values for several types of soil from independent volume change and the shear strength tests were not identical (Bishop et al. 1960). Similar trends in results were also reported in the research of Jennings and Burland (1962). Therefore, there are some limitations to employ the Bishop effective stress equation to explain the mechanical behavior of the unsaturated soils.

Matyas and Radhakrishna (1968) suggested that a single three-dimensional surface be used to present the complete history of the void ratio of the unsaturated soils. The surface is contained by three axes showing the magnitude of the net normal stress, $(\sigma_n - u_a)$, the suction, $(u_a - u_w)$, and the void ratio, e. The three-dimensional surface is referred in the literature as the state surface. Matyas and Radhakrishna (1968) were the earliest researchers who proposed the concept of the state surface and proposed that suction probably should be used as an independent stress variable to the net normal stress. Fredlund (1973) conducted null experiments and the results supported that the net normal stress, $(\sigma_n - u_a)$, the suction, $(u_a - u_w)$, can be used as two independent stress state variables to rationally explain the mechanical behavior of unsaturated soils.

The framework to use $(\sigma_n - u_a)$, and $(u_a - u_w)$, as two independent variables was followed by many researchers (for example, Fredlund and Morgenstern 1976; Lloret and Alonso 1985; Vanapalli et al. 1996; Adem and Vanapalli 2013) in the literature. By using the two independent stress variables, the void ratio and the water content (i.e. gravimetric water content, volumetric water content, degree of saturation) can be presented as the functions of the net normal stress and suction. The complete history of the void ratio and water content can be presented by the state surfaces. The state surfaces were measured by many researchers. For example, Shuai (1996) measured the state surfaces of a expansive soil, Regina clay, under different stress states. Pereira and Fredlund (2000) measured the void ratio and degree of saturated state surface for a collapsible soil. The state surfaces were expressed using different mathematical equations. These equations have been used for different types of soils, for example, silt (Ho 1988), expansive soil (Vu 2003), and modified to reduce the numerical issue at the low net normal stress and suction (Vu 2003).

Fredlund and Morgenstern (1976) proposed linear equations to formulate the constitutive relations for the void ratio and water content in terms of $(\sigma_n - u_a)$ and $(u_a - u_w)$. In other words, the unsaturated soil in this model was assumed as a linear elastic material. Therefore, this constitutive model has a form similar to Hooke's law. Two elastic moduli including the elastic modulus with respect to net normal stress and the elastic modulus with respect to suction were employed in this model. These equations first introduced to propose a simple yet fundamental framework for the constitutive models of unsaturated soils. The linear formulas do not correspond to the nonlinear behavior of the unsaturated soil. However, when the increments in stress and strain are infinitesimal, the linear formulas are capable of describing the nonlinear behavior. The elastic moduli at any stress (net stress and suction) level can be obtained by differentiating the void ratio and water content state surfaces with an assumed Poisson's ratio (Cho and Lee 2001; Vu 2003; Zhang 2004). The framework was used by many researchers to study the behavior of unsaturated soils. Shuai (1996) developed a program based on this framework to simulate the swelling pressure of the expansive soils. The developed program is able to accommodate various boundary conditions and various stress paths. Vu (2003) developed the consolidation/swelling theory of unsaturated soils into programs to predict the volume change associated with unsaturated expansive soils. Zhang (2005) developed the framework into four subroutines and used the subroutines in the commercial software Abaqus to simulate the behavior of the residential buildings on expansive soils. These results clearly showed that the framework is effective to simulate the behavior of unsaturated soils.

Some elastoplastic models based on the state surface concept were also developed. Zhang and Lytton (2009a; b) proposed a modified state surface model based on the state surface concept. Two surfaces were included in this model: one was the elastic rebound surface, the other one was the plastic hardening surface. The plastic hardening surface was presented by the traditional void ratio surface. The modified state surface model is capable of simulating the irrecoverable volume change behaviour of unsaturated soils. Qi and Vanapalli (2016) extended the Mohr-Coulomb criterion to study the mechanical behavior of the expansive soil. In the extended Mohr-Coulomb criterion, the state surfaces for the expansive soil were used to determine the elastic moduli. The stability analysis of the expansive soil slope was carried out by using the extended Mohr-Coulomb criterion. The results clearly showed that the softening induced by the swelling of the expansive soil in the infiltration can induce slope failures in expansive soils (Qi and Vanapalli 2016).

The state surface model is simple and can be used to simulate the different stress states of the expansive soils. Therefore, in this thesis, the state surface model was employed to study the behavior of a single pile in expansive soils.

2.3.2 Elastoplastic model

In addition to the state surface model, a series of the elastoplastic models have been proposed (Alonso et al. 1990, 1999; Gallipoli et al. 2003; Gens and Alonso 1992; Khalili and Selvadurai 2003; Mašín 2013; Sheng et al. 2008; Tamagnini 2004; Wang and Wei 2014; Wheeler et al. 2003).

Alonso et al. (1990) proposed a widely used constitutive model for unsaturated soils, which is referred to as the Barcelona Basic Model (BBM) in the literature. The BBM can be considered as an extension of the modified Cam Clay model, which is used for modeling saturated soil behavior. In the BBM, suction was used as the second stress state variable for modeling the behavior of unsaturated soils. As shown in Figure 2.4, the virgin compression curve for the unsaturated soil is assumed as a straight line in the $v - \ln p$ space, where v is the specific volume and $v = 1 + e$, which is consistent with the Modified Cam Clay model. However, the slope and the intercept of the virgin compression curve at a certain value of net stress is different for the different values of suction. For a certain value of net stress, the virgin compression curve has higher values of the slope and intercept at the higher suction. In the elastic domain, the slopes of the loading-unloading line and the suction unloading line are assumed as two constants. The relation of the preconsolidation stress (yield stress, p_0) and suction is presented as the loading-collapse curve (LC), as plotted in Figure 2.5.

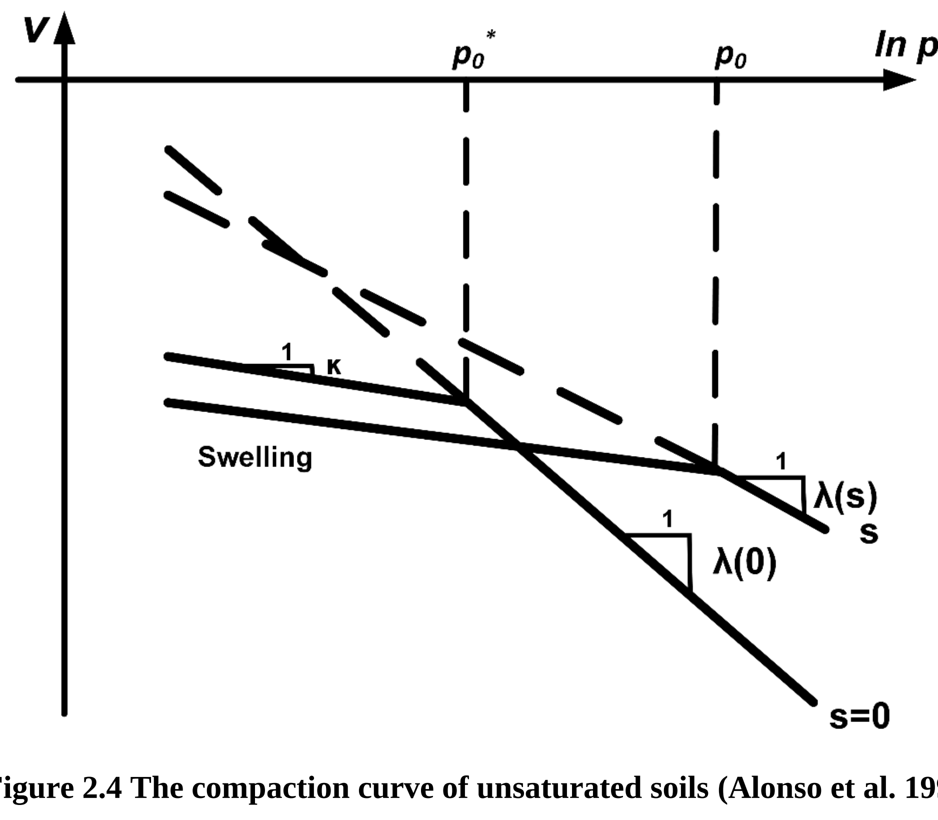

Figure 2.4 The compaction curve of unsaturated soils (Alonso et al. 1990).

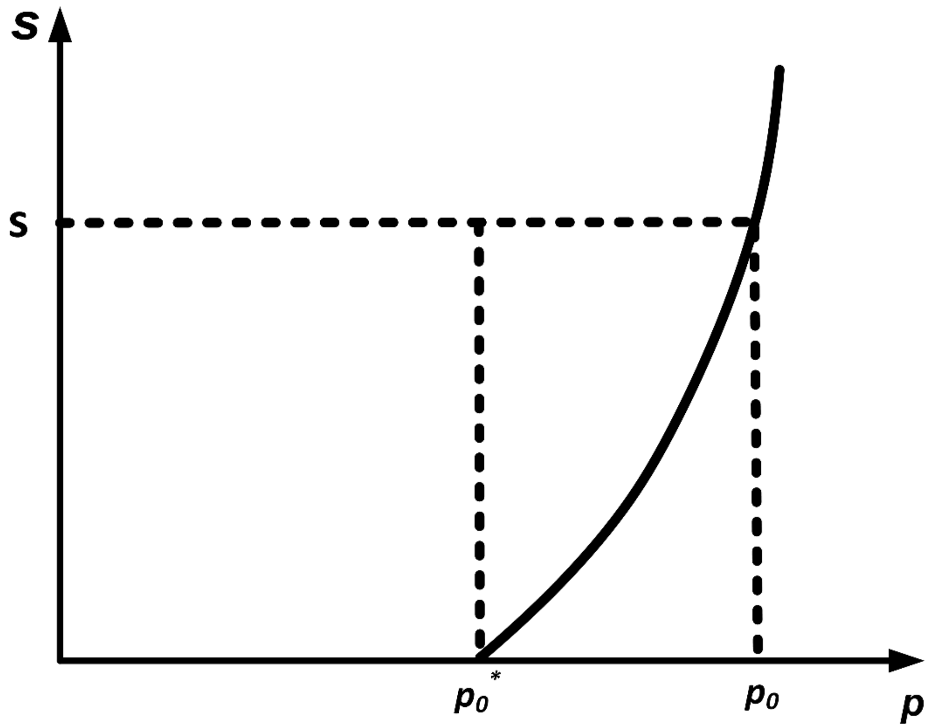

Figure 2.5 The loading collapse curve (LC) (Alonso et al. 1990).

Apart from the loading induced irrecoverable strain, the increase in the suction may also induce irrecoverable strain. The yield curve in $p-s$ space is assumed parallel to the $p-$ axis, which is defined as the suction increase curve (SI). The specific volume-suction relation is also assumed linear. For a saturated soil, the Modified Cam Clay is used to describe the soil behavior. For the unsaturated soil, the yield surfaces are assumed to exhibit ellipse shape similar to the Modified Cam Clay. The failure state for the unsaturated soil was also considered in this model. For the saturated soil, the critical state line (CSL) is used to represent the failure state, which is consistent with the Modified Cam Clay. The critical state lines for the unsaturated soil at different suctions are assumed parallel to the CSL for the saturated soil. The cohesion of the CSL is assumed to increase linearly with an increase in the suction. Due to this assumption, the intercept of the ellipses and the p axis increased linearly with an increase in the values of suction. The LC curve, the SI curve, the Modified Cam Clay, and the relation of the intercept and the suction constituted the yield space for the unsaturated soils, as given in Figure 2.6. Most other elastoplastic constitutive models were based largely on the Barcelona Basic Model (Cui and Delage 1996; Gallipoli et al. 2003; Wheeler et al. 2003; Wheeler and Sivakumar 1995).

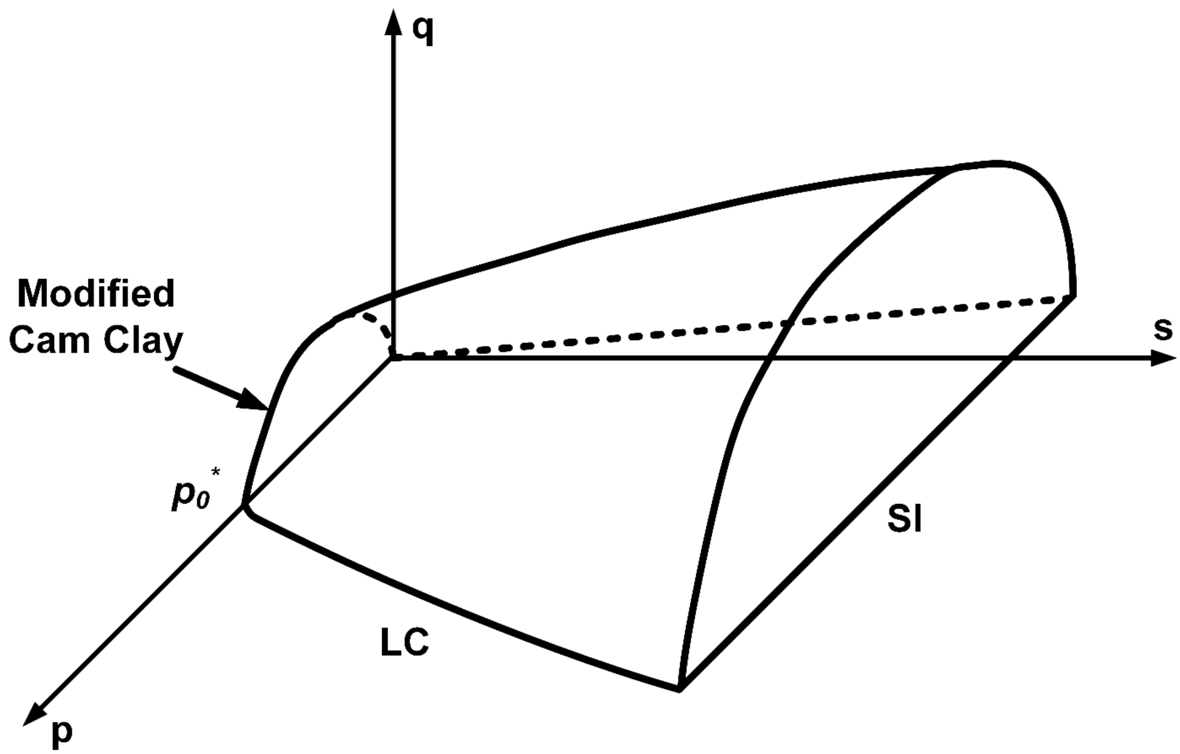

Figure 2.6 The yield surface of the Barcelona Basic Model (Alonso et al. 1990).

The Barcelona Basic Model was improved to simulate the behavior of expansive soils taking into account the influence of both the macro and microstructure. The microstructure of the expansive soils was employed to simulate the volume change behavior of expansive soils on the macro scale. For rigorous analysis, macro and microstructure information is derived from the pore-size distribution using Mercury Intrusion Porosimetry (MIP) results. There is an agreement in the literature that there are typically two pore sizes; which are referred to as micropore and macropore in the expansive soils (Cui et al. 2002; Koliji et al. 2006, 2010; Nowamooz and Masrouri 2010; Seiphoori et al. 2014; Tang et al. 2018; Wang et al. 2013; Zemenu et al. 2009). The structure that consisted of two pores of different sizes is defined as the double structure. Typically, the micropores are assumed the pore pores within aggregates or intra-aggregates pores, while the pores between aggregates (inter-aggregates) were assumed as the macropores. The concept of the double structure is plotted in Figure 2.7. The concept of the double structure was employed in the constitutive models of expansive soils.

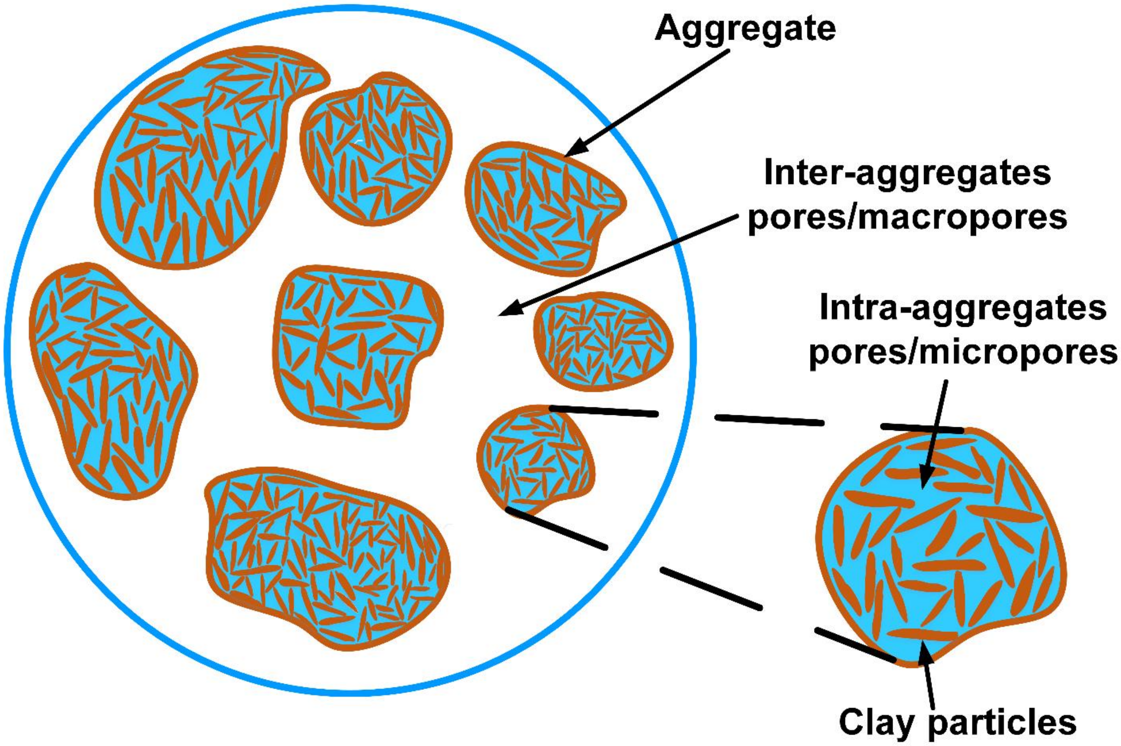

Figure 2.7 The concept of double structure (Likos and Wayllace 2010).

Gens and Alonso (1992) may be the earliest researchers who introduced the concept of double structure into the framework of the unsaturated soil constitutive models to analyze the behavior of the expansive soils. The microstructure deformation was used to describe the swelling of the clay mineral and the macrostructure deformation was used to describe the rearrangement of the soil particles. The micropores were assumed saturated in this framework. Therefore, the effective principle was still valid for the micropores. The microstructural deformation was assumed as reversible. Hence, the microstructure deformation depended only on the change in the mean effective stress, $dp' = d(p - u_w) = d(p - u_a + u_a - u_w) = d(p + s)$. This relation can be used to describe not only the suction decrease induced swelling but the external stress induced compaction. In this framework, the microstructural deformation was independent of the macrostructural deformation, however, the reverse was not. The macrostructural deformation was plastic and affected not only by the variation in the suction and external stress but the deformation in the microstructure. In the swelling process, the swelling in the microstructure can affect the soil skeleton and increasing the macrostructural void ratio. The plastic volume change can result in the movement of the loading collapse curve (LC) (the swelling induced softening). The framework was named as Barcelona Model for Expansive Soils (BExM). The BExM framework is widely used to simulate the behavior of the expansive soils in the literature. Alonso et al. (1999) introduced the ratio between the microstructural strain and the plastic macrostructural strain to the framework. The model was able to simulate the swelling-shrinkage fatigue in wetting-drying cycles. Wang and Wei (2014) introduced swelling-shrinkage coefficients to reversible and irreversible strains in macroscale. These coefficients are dependent on the current stress state and the accumulated irreversible strains. The definition of the coefficients can be used as tools to simulate the fatigue behavior in swelling-shrinkage cycles without measuring the microstructure parameters.

The models based on BBM and BExM are able to simulate the complex stress paths. However, several parameters have to be determined from cumbersome experimental studies and employed in the model for obtaining simulation results. Therefore, these models may not be suitable for use by geotechnical engineers in conventional practice for design of pile foundations in expansive soils.

2.4 Constitutive model for the unsaturated soil-structure interface

Many different constitutive models have been proposed for interpreting the soil-structure interface behavior. The models for dry soil-structure interface include the elastic model, elastoplastic model and disturbed state concept (for example, Goodman 1976; Hu and Pu 2004; Yu et al. 2015). A series of models have been proposed during the last decade for unsaturated soil-structure interface considering the effects of suction (for example, Lashkari 2012; Lashkari and Kadivar 2016; Liu et al. 2017; Farhadi and Lashkari 2017).

2.4.1 Dry soil-structure interface models

The widely used soil-structure interface models for dry soils are elastic model, elastoplastic model, and disturbed state concept (Zhang and Zhang 2009).

The commonly used elastic models include the Mohr-Coulomb model, the hyperbolic model, and the trilinear model. The Mohr-Coulomb model is used as a linear elastic model in several different software including the FLAC and Plaxis to describe the behavior of the interface (Yu et al. 2015). The hyperbolic models are widely used for the interface because of the similar shape of hyperbolic function and the shear stress relation of the interface (Cao et al. 2014; Kim et al. 1997; Lin et al. 2014; Ni et al. 2017; Pelecanos and Soga 2017; Xue et al. 2018; Zhang et al. 2015; Zhang and Zhang 2012; Zhao et al. 2005). Zhang and Zhang (2012) proposed an equation that can simulate the degradation behavior of the shear stress in the pile-soil interface. Three parameters including the peak stress, the relative displacement between the pile and soil with respect to the peak stress, and the ratio between the residual stress and the peak stress are included in this equation. This equation has a simple formation and has a smooth transfer from the peak stress and residual stress. This advantage can contribute to the increase in the simulation efficiency of the finite element method; therefore, this model is employed in this study.

Lin et al. (2014) proposed a softening model for the pile-soil interface. This model is a piecewise function, which makes it difficult to develop the program. Ni et al. (2017) proposed a generalization equation for the shaft friction of the pile-soil interface. In this equation, a single parameter, n, is used to estimate different stages of the friction-displacement curve of the pile-soil interface. This equation is capable of simulating the hardening and softening behavior. However, the transfer from the peak stress to the residual stress is not smooth. Pelecanos and Soga (2017) proposed a degradation and hardening hyperbolic model (DHHM). The DHHM has four parameters which include maximum shear stress, maximum stiffness for displacement, unitless degradation parameter that governs the degradation of the modulus, and unitless hardening parameter. These parameters, however, are difficult to determine and the model has a form that is hard to differentiate.

The different hyperbolic functions proposed by various researchers for the interface are summarized in Table 2.1. The trilinear model is proposed by Goodman (1976) describes the behavior of joints or discontinuities in rock engineering and is widely used in many software. As given in Figure 2.8, based on the curve of the typical shear stress and horizontal displacement curve is separated into three parts using straight lines. The advantage of the elastic model is its simplicity.

Table 2.1 The different hyperbolic models for the soil-structure interface.

Equation	Parameters	References
$\tau_s(z) = \frac{S_s(z)(a + cS_s(z))}{(a + bS_s(z))^2}$ $a = \frac{\beta_s - 1 + \sqrt{1-\beta_s}}{2\beta_s}\frac{S_{su}}{\tau_{su}}$ $b = \frac{1 - \sqrt{1-\beta_s}}{2\beta_s}\frac{1}{\tau_{su}}$ $c = \frac{2 - \beta_s - 2\sqrt{1-\beta_s}}{4\beta_s}\frac{1}{\tau_{su}}$ $\beta_s = \frac{\tau_{sr}}{\tau_{su}}$	$\tau_s(z)$: the interface shear stress (shaft friction) at a depth of z, $S_s(z)$: the relative displacement of pile and soil at a depth of z, S_{su}: the relative displacement with respect to the peak shear strength, τ_{su}: the peak shear stress, β_s: the ratio between the residual shear strength and peak shear strength.	Zhang and Zhang 2012
$\tau_s = \frac{S_s}{a + bS_s} \quad S_s \le S_{su}$ $\tau_s = \tau_{su} - \frac{S_s - S_{su}}{A + B(S_s - S_{su})} \quad S_s > S_{su}$	τ_s: the interface shear stress (shaft friction), S_s: the relative displacement of pile and soil, S_{su}: the relative displacement with respect to the peak shear strength	Lin et al. 2014
$\tau = \frac{k_m z}{\sqrt[d]{1 + (z\frac{k_m}{\tau_m})^{hd}}}$	τ: the interface shear stress (shaft friction), z :the relative displacement of pile and soil, k_m: maximum stiffness for displacement, d: unitless degradation parameter that governs the degradation of the modulus, h: unitless hardening parameter	Pelecanos and Soga 2017
$\tau(z) = \tau_u[(n+1)\left(\frac{z}{z_u}\right)^{\frac{n}{n+1}} - n\frac{z}{z_u}]$	$\tau(z)$: the interface shear stress (shaft friction), z: the relative displacement of pile and soil, τ_u: the peak shear stress, z_u: the relative displacement with respect to the peak shear stress, n: a single parameter used to estimate different stages of the friction-displacement curve of the pile-soil interface	Ni et al. 2017

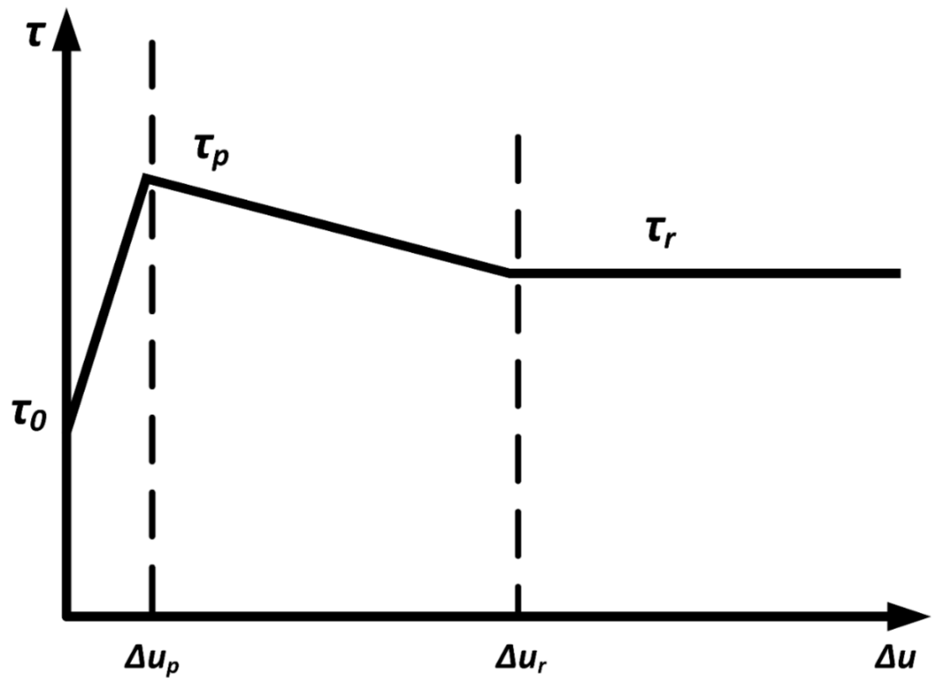

Figure 2.8 The trilinear model (Goodman 1976).

The elastoplastic models are the second most acceptable type of models because they can describe the behavior of the interface precisely. Shahrour and Rezaie (1997) used the Mohr-Coulomb criterion as the failure criterion to model cyclic behavior. The Cam-clay model was used to model a series of problems including the different behavior of interface in constant normal load and constant normal stiffness tests (Ghionna and Mortara 2002) and cyclic and monotonic behavior in the direct shear test, large scale test, and simple test (Hosseinali and Toufigh 2018). Some other models, for example, are Lade`s Single Hardening Model were used as well (Ebrahimian et al. 2012).

Desai proposed the disturbed state concept (DSC) and this concept has been used in the study of the interface (Desai 2000; Desai and Ma 1992; Desai and Rigby 1997; Fakharian and Evgin 2000; Hu and Pu 2004). The DSC considers the interface as the mixture of two different states of soil at any given deformation stage (Desai 2000). The origin state or continuum state is called the relative state and the rest of the part that is degraded or stiffened state is named as the fully adjusted state. Based on this concept, the results from the direct shear test and simple shear test and a sliding block are simulated (Hu and Pu 2004). The cyclic behavior of interface and effects of the stress path and pore water pressure were described by the DSC (Desai and Rigby 1997; Fakharian and Evgin 2000). Apart from this, the DSC was used to describe the behavior of joints (Desai and Ma 1992).

2.4.2 Unsaturated soil-structure interface models

Because of the limited research on the behavior of the unsaturated soil-structure interface, there are not enough models proposed. The presently available unsaturated soil-structure interface models in the literature include the hyperbolic model, elastoplastic model based on critical state and disturbed state concept (Hamid and Miller 2008; Lashkari 2012; Lashkari and Kadivar 2016; Liu and Vanapalli 2019a).

Liu et al. (2017) modified the hyperbolic model to study the behavior of pile in expansive soil. The hyperbolic model proposed by Zhang and Zhang in Table 2.1 is used in the expansive soil-structure interface. In the hyperbolic model, the peak strength is the controlling factor and it is estimated by the unsaturated soil-structure interface proposed by Hamid and Miller (2018) that modifies the unsaturated soil strength proposed by Vanapalli in 1996 (Miller and Hamid 2006; Vanapalli et al. 1996). In expansive soil, because of the infiltration of water, the soil will expand. In the vertical direction, the soil can expand freely on the surface of the ground and expand partially along with the depth. In the horizontal direction, however, the soil cannot expand because of the limitation of structure which results in the occurrence of the horizontal expansion pressure. Liu and Vanapalli (2017, 2019a) proposed the horizontal expansion pressure and modified the shear strength equation for the interface. Liu (2019) used this model to estimate the skin friction and pile axial force of piles in expansive soil successfully. This model is simple; however, it can comprehensively describe the mechanical behavior of the unsaturated soil-structure interface. Therefore, this model was employed in this study to simulate the behavior of the unsaturated pile-soil interface.

Some elastoplastic models were proposed by Lashkari and co-workers (Lashkari 2012; Lashkari and Kadivar 2016; Lashkari and Torkanlou 2016). The critical state concept was used in these models. These models can simulate different soil-structure interface but most of these models are complex. Hamid and Miller (2008) may be the earliest researchers who proposed a model based on the DSC to study the behavior of the unsaturated soil-structure interface. The DSC for unsaturated soil proposed by Geiser et al. 1997 was modified for unsaturated soil-structure interface by Hamid and Miller 2008). This model can simulate the hardening-softening behavior, the dilatancy phenomenon and the effects of suction.

The elastoplastic model and the disturbed state model are capable for simulating the complex mechanical behavior of the interface. However, several parameters are required in these models which are difficult to determine. Due to this reason, these models may not be suitable for use in conventional engineering practice. Therefore, the elastic model proposed by Liu et al. (2017) was used in this study.

2.5 Summary and conclusion

In this chapter, design methods for the pile foundations that can be used for expansive soils were briefly reviewed. The design methods include the rigid methods, the elastic methods, and the finite element based methods. In the rigid method, the pile was assumed as rigid and the displacement of the pile was assumed as zero. The rigid method is simple for use in practice; however, it is conservative for the design of the pile. The displacement of the pile head was allowed in the elastic method. However, the elastic design method was just suitable for the pile whose ratio between the length and diameter was less than 20. The finite element method can reduce these shortcomings of rigid and elastic methods. In the finite element based method, the constitutive models for the unsaturated soils and unsaturated pile-soil interfaces can be included and rigorously analyze the behavior of piles in unsaturated expansive soils. Therefore, the finite element method was employed in this study.

The constitutive models for the unsaturated expansive soils are required in the finite element methods. The constitutive models were reviewed in this chapter. The constitutive models for the unsaturated expansive soils include the state surface models and the elastoplastic models. Most elastoplastic models were based on the Barcelona Basic Model. These models are capable of modeling complex stress paths. However, the parameters used in these models are difficult to determine. Hence, these models may not be suitable for the design. The state surface models were simple and the parameters were easy to determine. Therefore, the state surface model was used in this study.

The constitutive models for the unsaturated soil-structure interface were also reviewed in this chapter. These models included the elastic models, elastoplastic models, and the disturbed state models. The hyperbolic model is one of the elastic models that is simple and can fully simulate the mechanical behavior of the soil-structure interface. Therefore, the hyperbolic model was used in this study.

CHAPTER 3
CONSTITUTIVE RELATIONSHIPS OF UNSATURATED SOIL AND UNSATURATED SOIL-STRUCTURE INTERFACE

3.1 Introduction

In this chapter, a constitutive model from the literature for the unsaturated expansive soils is presented that is capable of explaining the coupled hydro-mechanical problems. The equations for the coupled hydro-mechanical problems include the constitutive relationships for the unsaturated soil, flow law for the water phase, and the differential governing equations.

The concept of state surface based on the two independent stress variables is rational for describing the mechanical behavior of the unsaturated soils. This approach has been widely used by many researchers (for example, Fredlund and Morgenstern 1976; Lloret and Alonso 1985; Zhang and Lytton 2009a). The mechanical behavior of unsaturated soils can also be described by the constitutive surfaces for the soil structure (void ratio) and the water phase (water content or the degree of saturation) (Matyas and Radhakrishna 1968). Fredlund and Morgenstern (1976) proposed the linear equations to describe the constitutive surfaces for the soil structure and water phase. The linear equations are valuable for formulating the nonlinear behavior of the unsaturated soils for infinitesimal stress and strain increments. In this chapter, incremental forms of the equations for the soil structure and water phase constitutive relations are briefly introduced. The flow law is also required in addition to the constitutive relations for the soil structure and water phase for a rational explanation of the flow behavior. For this reason, in this study, the coupled hydro-mechanical behavior for unsaturated soils is analyzed using Darcy’s law for the flow behavior along with the constitutive relationships for mechanical behavior.

The differential governing equations are required to establish the equations for the fully coupled hydro-mechanical problems. The balance equations for each phase (i.e. soil structure and water phase) are introduced first. The balance equations for the soil structure satisfy the requirement of the static equilibrium. The balance equation for the water phase satisfies the requirement of continuity. By incorporating the balance equations and the constitutive relations for each phase (i.e. soil structure and water phase), the governing equations for the coupled hydro-mechanical problems are established (Muraleetharan and Wei 1999). The governing equations can be solved and the solutions for the coupled hydro-mechanical problems can be obtained by specifying appropriate boundary conditions.

As summarized earlier, to conduct the coupled hydro-mechanical analysis, information of the mechanical and hydraulic properties is required. The mechanical properties include the elastic modulus with respect to the net normal stress, E, the elastic modulus with respect to suction, H, the coefficient of water volume change with respect to net normal stress, m_1^w, the coefficient of water volume change with respect to suction, m_2^w. These elastic parameters are functions of the net normal stress and suction. When the constitutive surfaces of the void ratio and the water content are constructed, the elastic parameters can be determined by differentiating the constitutive surfaces. The required hydraulic property is the hydraulic conductivity of the unsaturated soil. Shuai (1996) measured the constitutive surfaces of the void ratio and water content for the unsaturated expansive soil. Vu (2003) proposed equations to fit the constitutive surfaces for the void ratio and water content; these equations were used to determine the elastic parameters. Shuai (1996) measured the hydraulic conductivity of unsaturated expansive soil and proposed an equation to formulate the hydraulic conductivity function by using the saturated hydraulic conductivity, void ratio, and the soil-water characteristic curve. In this chapter, the parameter determination for the coupled hydro-mechanical problems is summarized.

To simulate the behavior of the pile foundation in unsaturated expansive soils, the constitutive relation for the pile-soil interface is also required in the numerical analysis. Zhang and Zhang (2012) proposed a hyperbolic model to formulate the relationship between shear stress and the relative displacement between the pile-soil interface. To simulate the behavior of the unsaturated pile-soil interface, Liu (2019) introduced the equation for the shear stress of the unsaturated soil-structure interface into Zhang and Zhang (2012) model. The details related to the unsaturated pile-soil interface model are introduced in this chapter.

3.2 Constitutive relationship and flow laws for the unsaturated soil

The constitutive relation for soil and the flow law for the water phase are required for the coupled hydro-mechanical analysis of soil. As unsaturated soils are typically comprised of three phases (i.e. soil structure, water phase, and air phase), it is necessary to provide a constitutive relation for each independent phase of the unsaturated soil (Fredlund and Rahardjo 1993). In this model, the air phase is assumed to connect with the atmosphere, and the excessive pore air pressure is assumed to dissipate instantly if the external loading is applied to the soil (Rahardjo and Fredlund 1995). In other words, the air pressure is assumed as constant (Qi and Vanapalli 2015). Therefore, the change in the air phase is ignored in this model. The first part of this section primarily focuses on the constitutive relationship for soil structure and water phase in unsaturated soil to describe the mechanical behavior of unsaturated soil. The flow law is required in the coupled hydro-mechanical analysis to describe the seepage of water in unsaturated soil. In this model, Darcy's law is assumed to be valid for the unsaturated soil (Zhang 2004). Therefore, the second part of this section focuses on Darcy's law for unsaturated soil.

3.2.1 Constitutive relationship for the unsaturated soil

Some assumptions are introduced to describe the constitutive relationships for the soil structure and water phase in the unsaturated soil. The soil structure is assumed as homogenous, isotropic, and elastic. The soil particles and the water phase are assumed as incompressible. The changes in strain and stress are infinitesimal. Based on these assumptions, the elasticity form and the compressibility form for the constitutive relation for the soil structure and water phase are given. Two stress states including three-dimensional stress state and K_0-loading state are introduced in this section.

3.2.1.1 Elasticity form for the constitutive relationship of soil structure

The constitutive relationship for the soil structure of saturated soil under a three-dimensional stress state can be described by the effective stress $(\sigma - u_w)$ in the form of Hooke's law. For the isotropic and linear elastic soil structure, the relationship of strain and stress for the saturated soil structure in $x-$, $y-$, and $z-$ directions can be given by Equation (3.1)-Equation (3.3).

$$\varepsilon_x = \frac{\sigma_x - u_w}{E} - \frac{\mu}{E}(\sigma_y + \sigma_z - 2u_w) \tag{3.1}$$

$$\varepsilon_y = \frac{\sigma_y - u_w}{E} - \frac{\mu}{E}(\sigma_x + \sigma_z - 2u_w) \tag{3.2}$$

$$\varepsilon_z = \frac{\sigma_z - u_w}{E} - \frac{\mu}{E}(\sigma_x + \sigma_y - 2u_w) \tag{3.3}$$

where:

σ_x is the total normal stress in $x-$direction,

σ_y is the total normal stress in $y-$direction,

σ_z is the total normal stress in $z-$direction,

ε_x is the normal strain in $x-$direction,

ε_y is the normal strain in $y-$direction,

ε_z is the normal strain in $z-$direction,

E is the elasticity modulus for the soil structure,

μ is the Poisson's ratio.

The constitutive relationship for the soil structure of the unsaturated soils can be formulated in a similar form by choosing the suitable state stress variables (Fredlund and Morgenstern 1976). The net normal stress $(\sigma - u_a)$ and suction $(u_a - u_w)$ widely used as two independent state stress variables to describe the constitutive relationship for the soil structure. For the unsaturated soil under a three-dimensional stress state, the strain and stress relation can be given by Equation (3.4)-Equation (3.6) (Fredlund and Rahardjo 1993).

$$\varepsilon_x = \frac{\sigma_x - u_a}{E} - \frac{\mu}{E}(\sigma_y + \sigma_z - 2u_a) + \frac{(u_a - u_w)}{H} \tag{3.4}$$

$$\varepsilon_y = \frac{\sigma_y - u_a}{E} - \frac{\mu}{E}(\sigma_x + \sigma_z - 2u_a) + \frac{(u_a - u_w)}{H} \tag{3.5}$$

$$\varepsilon_z = \frac{\sigma_z - u_a}{E} - \frac{\mu}{E}(\sigma_x + \sigma_y - 2u_a) + \frac{(u_a - u_w)}{H} \tag{3.6}$$

where:

E is the elasticity modulus for the soil structure with respect to the net normal stress,

H is the elasticity modulus for the soil structure with respect to the suction.

The constitutive relationship for the shear strain and shear stress of the soil structure can be given by Equation (3.7) thru Equation (3.9).

$$\gamma_{xy} = \frac{\tau_{xy}}{G} \tag{3.7}$$

$$\gamma_{yz} = \frac{\tau_{yz}}{G} \tag{3.8}$$

$$\gamma_{zx} = \frac{\tau_{zx}}{G} \tag{3.9}$$

where:

τ_{xy} is the shear stress on the x −plane in y −direction,

τ_{yz} is the shear stress on the y −plane in z −direction,

τ_{zx} is the shear stress on the z −plane in x −direction,

γ_{xy} is the shear strain on the x −plane in y −direction,

γ_{yz} is the shear strain on the y −plane in z −direction,

γ_{zx} is the shear strain on the z −plane in x −direction,

G is the shear modulus that can be calculated by $G = \frac{E}{2(1+\mu)}$.

The curve of the constitutive relationship for the soil structure of the soil is typically nonlinear. However, when the strain increment and stress increment are infinitesimal, the curve of the constitutive relationship for the soil structure can be assumed as linear. Therefore, the linear elastic strain-stress relation can be applied to represent the nonlinear elastic strain-stress relation when the increment in strain and stress are infinitesimal. The incremental form is normally used to describe the infinitesimal increment in strain and stress. The incremental form of the soil structure constitutive relation under a three-dimensional stress state can be given by Equation (3.10)-Equation (3.15).

$$d\varepsilon_x = \frac{d(\sigma_x - u_a)}{E} - \frac{\mu}{E} d(\sigma_y + \sigma_z - 2u_a) + \frac{d(u_a - u_w)}{H} \tag{3.10}$$

$$d\varepsilon_y = \frac{d(\sigma_y - u_a)}{E} - \frac{\mu}{E} d(\sigma_x + \sigma_z - 2u_a) + \frac{d(u_a - u_w)}{H} \tag{3.11}$$

$$d\varepsilon_z = \frac{d(\sigma_z - u_a)}{E} - \frac{\mu}{E} d(\sigma_x + \sigma_y - 2u_a) + \frac{d(u_a - u_w)}{H} \tag{3.12}$$

$$d\gamma_{xy} = \frac{d\tau_{xy}}{G} \tag{3.13}$$

$$d\gamma_{yz} = \frac{d\tau_{yz}}{G} \tag{3.14}$$

$$d\gamma_{zx} = \frac{d\tau_{zx}}{G} \tag{3.15}$$

For the soil under the K_0-loading state, the incremental form of the soil structure constitutive relation can be derived from the incremental form of the soil structure constitutive relation under a three-dimensional stress state. For the soil under the K_0-loading state, total vertical stress incremental $d\sigma_y$ is applied to the soil, the vertical strain will occur in the vertical direction ($y-$direction) while the strains in the other two directions ($x-$ and $z-$ directions) are not allowed. In other words, $d\varepsilon_x = d\varepsilon_z = 0$ for the soil under the K_0-loading state. The strain conditions of the K_0-loading state can be applied to Equation (3.10) thru Equation (3.12) to obtain the incremental forms of the soil structure constitutive relation under the K_0-loading state.

By substituting $d\varepsilon_x = d\varepsilon_z = 0$ into Equation (3.10)-Equation (3.12), the increment of the vertical strain of soil structure under the K_0-loading state can be obtained by Equation (3.16).

$$d\varepsilon_y = \frac{1-\mu-2\mu^2}{E(1-\mu)} d\left(\sigma_y - u_a\right) + \frac{1+\mu}{H(1-\mu)} d(u_a - u_w) \tag{3.16}$$

The incremental in the volumetric strain of soil structure, $d\varepsilon_v$, can be calculated by the summary of the incremental in normal strains in three directions, as shown in Equation (3.17).

$$d\varepsilon_v = d\varepsilon_x + d\varepsilon_y + d\varepsilon_z \tag{3.17}$$

where:

$d\varepsilon_v$ is the incremental change in the volumetric strain of soil structure.

By substituting Equations (3.10) thru (3.12) to Equation (3.17), the incremental change in the volumetric strain of the soil structure for a three-dimensional stress state can be formulated by the net normal stress in three directions and suction.

$$d\varepsilon_v = 3(\frac{1-2\mu}{E})d(\frac{\sigma_x+\sigma_y+\sigma_z}{3} - u_a) + \frac{3}{H}d(u_a - u_w) \tag{3.18}$$

By defining mean total net normal σ_{mean} as $(\sigma_x + \sigma_y + \sigma_z)/3$, Equation (3.18) can be modified into Equation (3.19).

$$d\varepsilon_v = 3(\frac{1-2\mu}{E})d(\sigma_{\text{mean}} - u_a) + \frac{3}{H}d(u_a - u_w) \tag{3.19}$$

For the soil under the K_0-loading state, the increment of the volumetric strain, $d\varepsilon_v$ is equal to the increment of the vertical strain, $d\varepsilon_y$ as the strains in the other two directions are zero ($d\varepsilon_x = d\varepsilon_z = 0$). Therefore, the volumetric strain of soil structure under the K_0-loading state can be obtained from Equation (3.20).

$$d\varepsilon_v = \frac{1-\mu-2\mu^2}{E(1-\mu)}d\left(\sigma_y - u_a\right) + \frac{1+\mu}{H(1-\mu)}d(u_a - u_w) \tag{3.20}$$

The total volumetric strain of soil structure can be obtained by summarizing the incremental change in the volumetric strain in each increment.

$$\varepsilon_v = \sum d\varepsilon_v \tag{3.21}$$

3.2.1.2 The constitutive relationship for water phase of unsaturated soil

As the unsaturated soil is normally comprised of three phases (i.e. soil structure, water, air), the constitutive relationship of soil structure is not enough to describe the behavior of unsaturated soil. The constitutive relationship for the water phase should be given. In this relationship, the water phase is assumed incompressible (Fredlund and Rahardjo 1993). The constitutive relationship of the water phase should be formulated as the function of the net normal stress $(\sigma - u_a)$ and suction

$(u_a - u_w)$. The constitutive relationship of the water phase can be formulated in a similar form as the function of the constitutive relation of soil structure. The incremental form of the constitutive relation for the water phase of unsaturated soil under a three-dimensional stress state can be given by Equation (3.22).

$$\frac{dV_w}{V_0} = \frac{3}{E_w} d(\sigma_{\text{mean}} - u_a) + \frac{1}{H_w} d(u_a - u_w) \tag{3.22}$$

where:

V_w is the volumetric water content of the unsaturated soil,

V_0 is the initial volume of the unsaturated soil,

E_w is the water volumetric modulus with respect to mean net normal stress $\sigma_{\text{mean}} - u_a$,

H_w is the water volumetric modulus with respect to the suction $u_a - u_w$.

The incremental form of the constitutive relation for the water phase of unsaturated soil under K_0 loading state can be given by Equation (3.23).

$$\frac{dV_w}{V_0} = \frac{1+\mu}{E_w(1-\mu)} d\left(\sigma_{\text{y}} - u_a\right) + \left(\frac{1}{H_w} - \frac{2(E/H)}{E_w(1-\mu)}\right) d(u_a - u_w) \tag{3.23}$$

3.2.1.3 The compressibility forms for the constitutive relationship of unsaturated soil

The compressibility form for the constitutive model of soil structure under the three-dimensional stress state can be obtained by Equation (3.24).

$$d\varepsilon_v = m_1^s d(\sigma_{\text{mean}} - u_a) + m_2^s d(u_a - u_w) \tag{3.24}$$

where:

m_1^s is the coefficient of volume change with respect to net normal stress under three-dimensional stress state,

m_2^s is the coefficient of volume change with respect to the suction under a three-dimensional stress state.

The compressibility form for the constitutive model of soil structure under the K_0 loading state can be obtained by Equation (3.25).

$$d\varepsilon_v = m_{1-1}^s d(\sigma_{\mathrm{y}} - u_a) + m_{1-2}^s d(u_a - u_w) \tag{3.25}$$

where:

m_{1-1}^s is the coefficient of volume change with respect to net normal stress under the K_0 loading state,

m_{1-2}^s is the coefficient of volume change with respect to the suction under the K_0 loading state.

The coefficients of volume change, m_1^s, m_2^s, m_{1-1}^s, and m_{1-2}^s, are the ratio between the change in the volumetric strain and stress state variables. The definition of the coefficients of volume change is plotted in Figure 3.1. As the constitutive curve for the soil structure of the soil is typically nonlinear, the coefficients are not constant. However, the coefficients can be assumed as constants if the increments in strain and stress are infinitesimal.

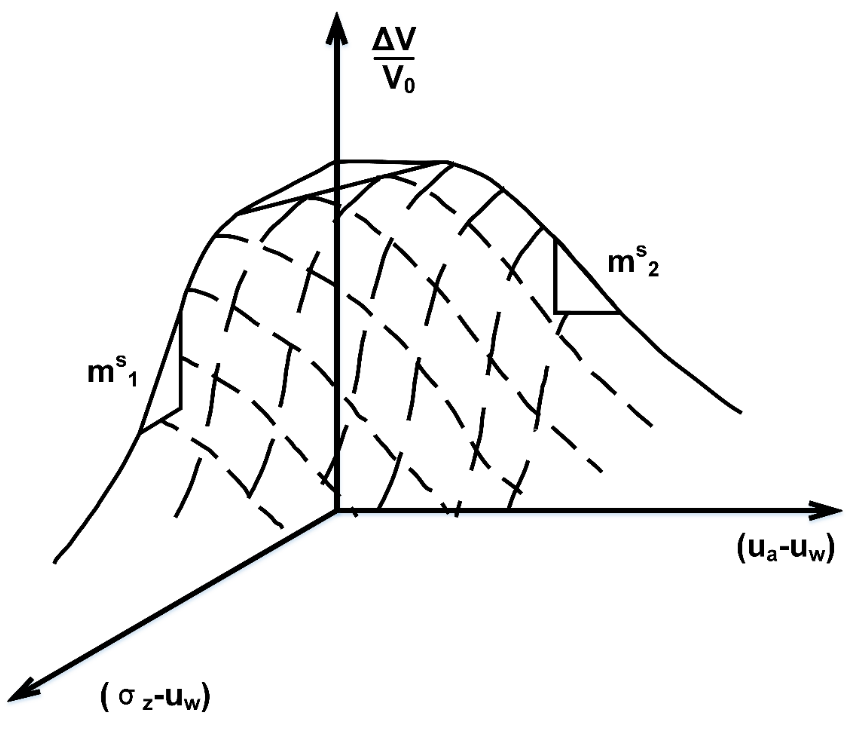

Figure 3.1 The definition of the coefficients of the volume change (modified from Fredlund 1981).

The compressibility form for the constitutive relationship of the water phase in the unsaturated soil under a three-dimensional stress state can be given by Equation (3.26).

$$\frac{dV_w}{V_0} = m_1^w d(\sigma_{\text{mean}} - u_a) + m_2^w d(u_a - u_w) \tag{3.26}$$

where:

m_1^w is the coefficient of water volume change with respect to net normal stress under three-dimensional stress state,

m_2^w is the coefficient of water volume change with respect to the suction under a three-dimensional stress state.

The compressibility form for the constitutive relationship of the water phase in the unsaturated soil under the K_0 loading state can be given by Equation (3.27).

$$\frac{dV_w}{V_0} = m_{1-1}^w d(\sigma_y - u_a) + m_{1-2}^w d(u_a - u_w) \tag{3.27}$$

where:

m_{1-1}^w is the coefficient of water volume change with respect to net normal stress under the K_0 loading state,

m_{1-2}^w is the coefficient of water volume change with respect to the suction under the K_0 loading state.

The coefficients of water volume change, m_1^w, m_2^w, m_{1-1}^w, and m_{1-2}^w, are the ratio between the change in the volume of water and stress state variables. The definition of the coefficients of volume change is plotted in Figure 3.2.

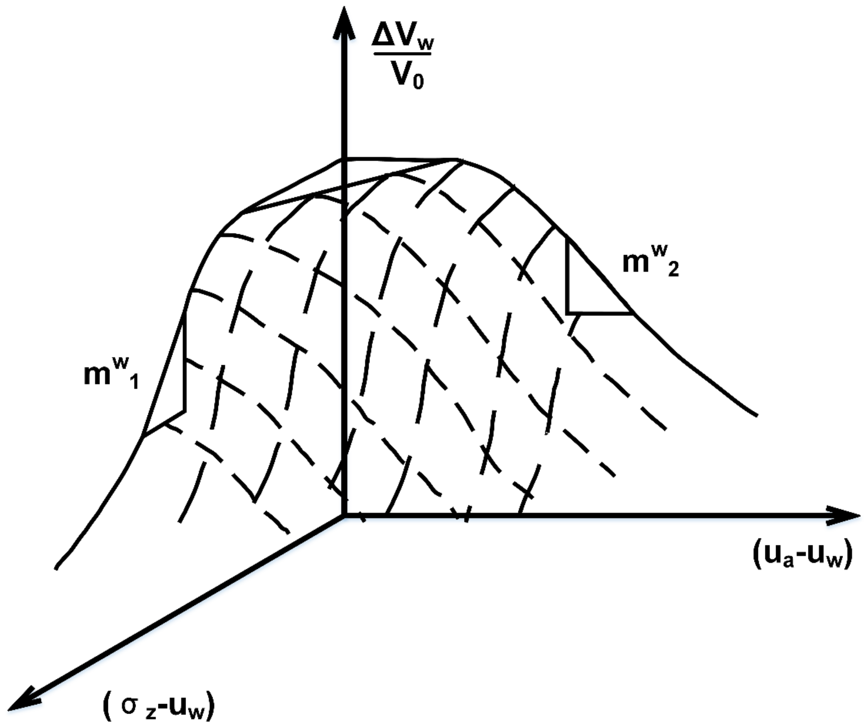

Figure 3.2 The definition of the coefficients of water volume change (modified from Fredlund 1981).

The coefficients of volume change, m_1^s, m_2^s, m_{1-1}^s, and m_{1-2}^s, can be transferred into the elastic modulus of volume change, E, and H. The coefficients of water volume change, m_1^w, m_2^w, m_{1-1}^w, and m_{1-2}^w, can be transferred into the water volumetric modulus, E_w, and H_w. The relations of the coefficient of volume change and elastic modulus are presented in Table 3.1.

Table 3.1 Coefficients of Volume change under three-dimensional stress state and K_0-loading state.

	$\boldsymbol{m_1^s/m_{1-1}^s}$	$\boldsymbol{m_2^s/m_{1-2}^s}$	$\boldsymbol{m_1^w/m_{1-1}^w}$	$\boldsymbol{m_2^w/m_{1-2}^w}$
Three-dimensional stress state	$3(\frac{1-2\mu}{E})$	$\frac{3}{H}$	$\frac{3}{E_w}$	$\frac{1}{H_w}$
K_0 loading state	$\frac{1-\mu-2\mu^2}{E(1-\mu)}$	$\frac{1+\mu}{H(1-\mu)}$	$\frac{1+\mu}{E_w(1-\mu)}$	$\frac{1}{H_w}-\frac{2(E/H)}{E_w(1-\mu)}$

3.2.2 Flow law of water phase

The flow of the water phase is typically calculated by Darcy's law. Darcy's law relates the water flow rate to the hydraulic head (i.e. pressure head, elevation head), as shown in Equation (3.28).

$$q_i = -k_i \frac{\partial}{\partial x_i}\left(\frac{u_w}{\rho_w g} + y\right) \tag{3.28}$$

where:

q_i is the flux in i direction,

k_i is the hydraulic conductivity of the soil in i direction,

u_w is the value of pore water pressure,

ρ_w is the density of water,

g is the gravimetric acceleration,

y is the elevation head.

3.3 Differential equations for the coupled hydro-mechanical problems

Two sets of fundamental equations govern the mechanical behavior of soil structure and the flow behavior of the water phase in unsaturated soil. The fundamental equations are the force equilibrium equations for the soil structure and the continuity equation for the water phase (Khalili and Selvadurai 2003; Qi and Vanapalli 2015; Zhang 2004). In this section, the fundamental equations for the coupled hydro-mechanical analysis of the unsaturated soil are introduced.

3.3.1 Equilibrium equations for the soil structure of the unsaturated soil

The equations of overall static equilibrium for the soil structure of the unsaturated soil can be written as Equation (3.29).

$$\frac{\partial \sigma_{ij}}{\partial x_j} + b_i = 0 \tag{3.29}$$

where:

σ_{ij} are the components of the total stress tensor,

b_i are the components of the body force vector.

Equation (3.30) thru Equation (3.35) (i.e. expressions in terms of net normal stress $\sigma_{ij} - u_a$ and $u_a - u_w$) can be obtained by solving Equation (3.4) thru Equation (3.9).

$$\sigma_x - u_a = \lambda\varepsilon_v + 2G\varepsilon_x + \frac{3\lambda+2G}{H}(u_a - u_w) \tag{3.30}$$

$$\sigma_y - u_a = \lambda\varepsilon_v + 2G\varepsilon_y + \frac{3\lambda+2G}{H}(u_a - u_w) \tag{3.31}$$

$$\sigma_z - u_a = \lambda\varepsilon_v + 2G\varepsilon_z + \frac{3\lambda+2G}{H}(u_a - u_w) \tag{3.32}$$

$$\tau_{xy} = G\gamma_{xy} \tag{3.33}$$

$$\tau_{yz} = G\gamma_{yz} \tag{3.34}$$

$$\tau_{zx} = G\gamma_{zx} \tag{3.35}$$

where:

$\lambda = \frac{E\mu}{1-\mu-2\mu^2}$.

The strain-displacement relation for the soil structure of unsaturated soil can be given by Equation (3.36) thru (3.38).

$$\varepsilon_x = \frac{\partial u}{\partial x}, \gamma_{yz} = \frac{\partial w}{\partial y} + \frac{\partial v}{\partial z} \tag{3.36}$$

$$\varepsilon_y = \frac{\partial v}{\partial y}, \gamma_{xz} = \frac{\partial w}{\partial x} + \frac{\partial u}{\partial z} \tag{3.37}$$

$$\varepsilon_z = \frac{\partial w}{\partial z}, \gamma_{xy} = \frac{\partial v}{\partial x} + \frac{\partial u}{\partial y} \tag{3.38}$$

where:

u, v, w are the displacement in $x-$, $y-$, and $z-$ direction, respectively.

By substituting Equation (3.30) thru (3.38) into Equation (3.29), the differential equations for the soil structure of the unsaturated soil can be given by Equation (3.39) thru (3.41).

$$(\lambda + G)\frac{\partial \varepsilon_v}{\partial x} + G\nabla^2 u - \frac{3\lambda+2G}{H}\frac{\partial (u_a - u_w)}{\partial x} + X = 0 \tag{3.39}$$

$$(\lambda + G)\frac{\partial \varepsilon_v}{\partial y} + G\nabla^2 v - \frac{3\lambda+2G}{H}\frac{\partial (u_a - u_w)}{\partial x} + Y = 0 \tag{3.40}$$

$$(\lambda + G)\frac{\partial \varepsilon_v}{\partial z} + G\nabla^2 w - \frac{3\lambda+2G}{H}\frac{\partial (u_a - u_w)}{\partial x} + Z = 0 \tag{3.41}$$

where:

X, Y, Z are the components of body force in $x-$, $y-$, and $z-$ direction, respectively,

∇^2 is the Laplace operator, $\nabla^2 = \frac{\partial^2}{\partial x^2} + \frac{\partial^2}{\partial y^2} + \frac{\partial^2}{\partial z^2}$.

3.3.2 Continuity equations for the water phase of the unsaturated soil

The water phase is assumed as incompressible and the strain increments are assumed as infinitesimal (Qi and Vanapalli 2015). The continuity equation for the water phase can be given by Equation (3.42).

$$\frac{\partial q_x}{\partial x} + \frac{\partial q_y}{\partial y} + \frac{\partial q_z}{\partial z} + \frac{\partial \theta_w}{\partial t} = 0 \tag{3.42}$$

where:

q_x, q_y, q_z are the flux in $x-$, $y-$, and $z-$ direction, respectively,

θ_w is the volumetric water content,

t is the time.

The volumetric content, θ_w, is typically defined as the ratio of the volume of water, V_w, and the total volume of soil, V. With the infinitesimal assumption of the strain, Equation (3.42) can be modified into Equation (3.43).

$$\frac{\partial q_x}{\partial x} + \frac{\partial q_y}{\partial y} + \frac{\partial q_z}{\partial z} + \frac{\partial (V_w/V_0)}{\partial t} = 0 \tag{3.43}$$

By substituting Equation (3.26) and Equation (3.28) into Equation (3.43), the differential equation for the water phase of the unsaturated soil can be given by Equation (3.44).

$$\frac{\partial}{\partial x}(k_x\frac{\partial}{\partial x}(\frac{u_w}{\rho_w g}))+\frac{\partial}{\partial y}(k_y\frac{\partial}{\partial y}(\frac{u_w}{\rho_w g}))+\frac{\partial}{\partial z}(k_z(\frac{\partial}{\partial z}(\frac{u_w}{\rho_w g})+y))$$
$$=m_1^w\frac{\partial(\sigma_{\text{mean}}-u_a)}{\partial t}+m_2^w\frac{\partial(u_a-u_w)}{\partial t} \tag{3.44}$$

3.4 Parameters determination for the coupled hydro-mechanical analysis

The parameters used for the coupled hydro-mechanical analysis of unsaturated expansive soils include the elastic parameters for the soil structure, the elastic parameters for the water phase, and the hydraulic parameter for Darcy's law of the unsaturated soil, as given by the follows (Vu 2003):

(1) the elasticity modulus for the soil structure with respect to the net normal stress, E, or the coefficient of volume change with respect to net normal stress, m_1^s or m_{1-1}^s,

(2) the elasticity modulus for the soil structure with respect to the suction, H, or the coefficient of volume change with respect to suction, m_2^s or m_{1-2}^s,

(3) the water volumetric modulus with respect to the net normal stress, E_w, or the coefficient of water volume change with respect to net normal stress, m_1^w or m_{1-1}^w,

(4) the water volumetric modulus with respect to the suction, H_w, or the coefficient of water volume change with respect to suction, m_2^w or m_{1-2}^w,

(5) the hydraulic conductivity of the unsaturated expansive soil, k_i,

(6) Poisson ratio, μ.

Determination of these parameters requires the construction of the constitutive surface of soil properties such as void ratio, water content (i.e. the gravimetric water content, the volumetric water content, and the degree of saturation) in terms of stress variables net normal stress and suction, and the hydraulic conductivity determined from laboratory tests.

3.4.1 Determination of the parameters for soil structure and water phase by the soil properties

The volume-mass properties of unsaturated soil (i.e. void ratio, gravimetric water content, volumetric water content, and degree of saturation) can be expressed as the stress independent quantities (Matyas and Radhakrishna 1968). In other words, these properties can be expressed by the functions of net normal stress $(\sigma - u_a)$ and suction $(u_a - u_w)$ (Fredlund and Morgenstern 1976). Therefore, each of constitutive surfaces for the volume-mass properties can be represented as a three-dimensional surface. These constitutive surfaces can be obtained from a series of laboratory tests results.

Shuai and Fredlund (1998) measured the constitutive surfaces for the soil structure (void ratio) and water phase (i.e. gravimetric water content) of Regina clay under different loading conditions. For example, the void ratio and water content surfaces for the unsaturated soil under K_0 loading state are measured by conducting the one-dimensional swelling tests. These two surfaces are presented in Figure 3.3 and 3.4, respectively.

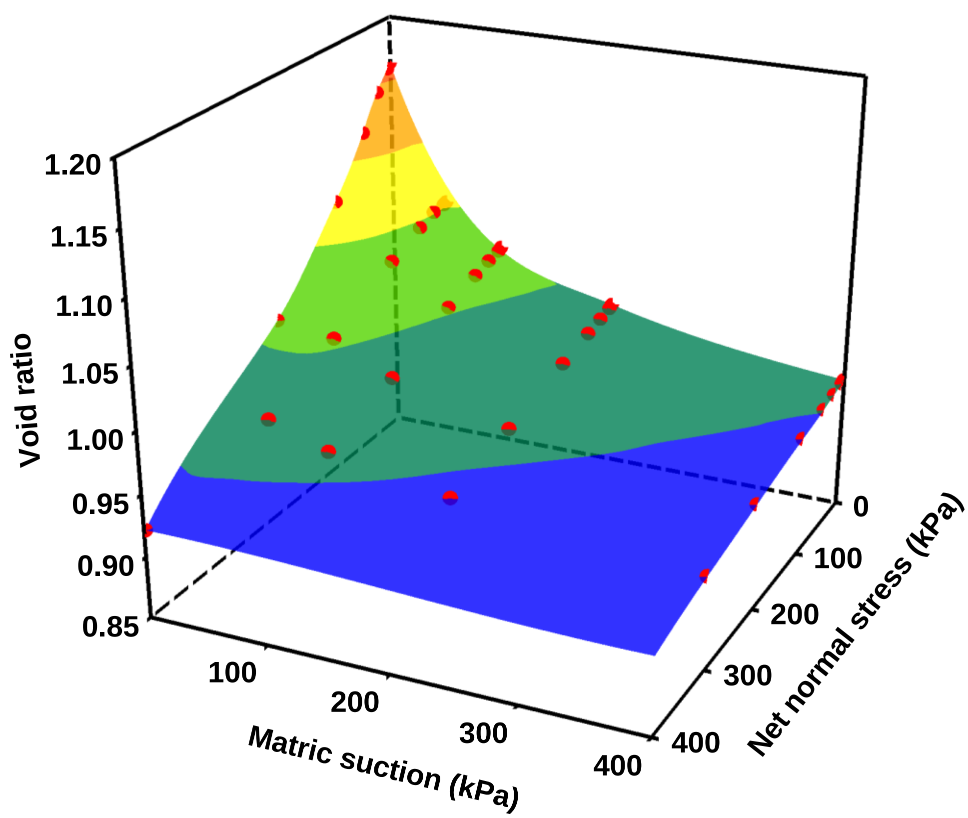

Figure 3.3 Measured soil structure constitutive surface for compacted Regina Clay (Shuai and Fredlund 1998).

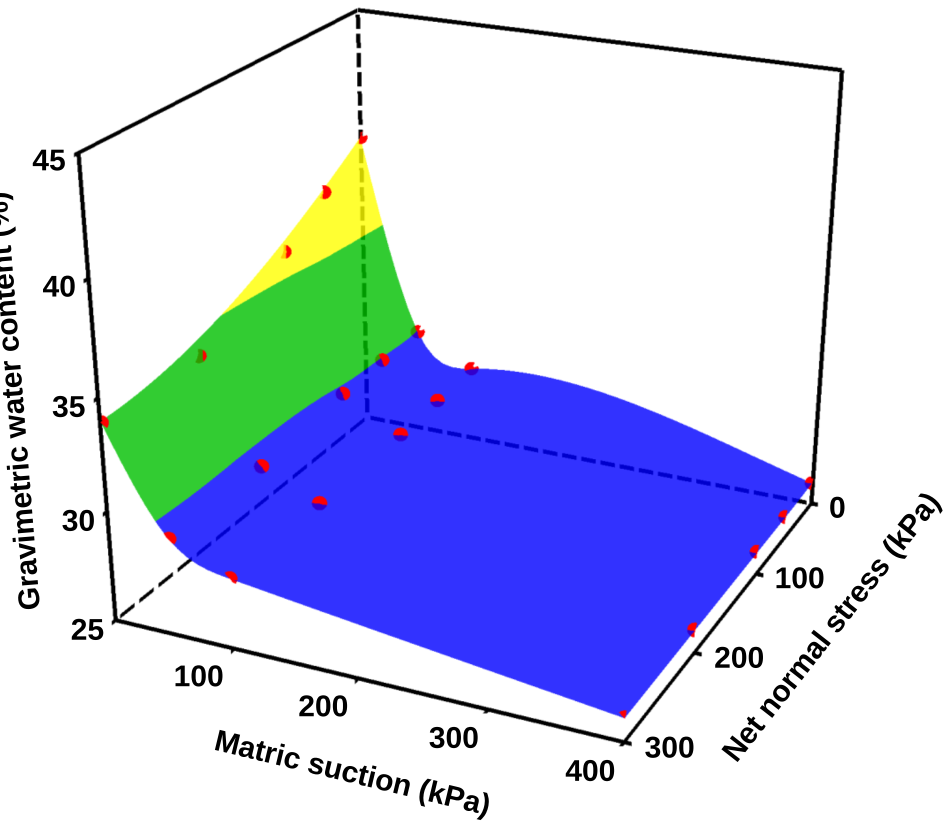

Figure 3.4 Measured water phase constitutive surface for compacted Regina Clay (Shuai and Fredlund 1998).

Many equations were proposed for the description of the void ratio and water content surfaces of the unsaturated soil (Fredlund 1979; Lloret and Alonso 1985). These equations can be determined for any soil under specific test conditions by choosing the best fitting parameters. They are flexible functions and can be used to determine the elastic parameters from the constitutive models for unsaturated soils, which are summarized in Table 3.2.

Table 3.2 Fitting equations for void ratio and water content surfaces.

References	Soil properties	Equations
Fredlund 1979	Void ratio, e	$e = e_0 - C_t \log \frac{(\sigma - u_a)}{(\sigma - u_a)_0} - C_m \log \frac{(u_a - u_w)}{(u_a - u_w)_0}$ or $e = a + b\log(\sigma - u_a) + c\log(u_a - u_w)$
	Gravimetric water content, w	$w = w_0 - D_t \log \frac{(\sigma - u_a)}{(\sigma - u_a)_0} - D_m \log \frac{(u_a - u_w)}{(u_a - u_w)_0}$ or $w = a + b\log(\sigma - u_a) + c\log(u_a - u_w)$
Lloret and Alonso 1985	Void ratio, e	$e = a + b(\sigma - u_a) + c\log(u_a - u_w)$ $+ d(\sigma - u_a)\log(u_a - u_w)$

However, there are limitations using these equations at low stresses and for suction values that are close to zero. The void ratio or water content tends to increase to infinity or very high values when the stress state variables approach zero. The calculated elastic modulus with respect to net normal stress and suction, E, and H, will become small. The small values of elastic modulus, E, and H, will result in the difficulty of the coverage in numerical modeling (Vu 2003). To solve the low stress and zero suction problem, Vu (2003) proposed a new function with six fitting parameters to fit the constitutive surfaces of the volume-mass properties of the unsaturated soil. The function is given by Equation (3.45).

$$f(\sigma - u_a, u_a - u_w) = a + b\log\left(\frac{1 + c(\sigma - u_a) + d(u_a - u_w)}{1 + f(\sigma - u_a) + g(u_a - u_w)}\right) \tag{3.45}$$

where:

f is the volume-mass properties of the unsaturated soil (i.e. void ratio, gravimetric water content, volumetric water content, degree of saturation), for example, if Equation (3.45) is used to fit constitutive surface of void ratio, $e(\sigma - u_a, u_a - u_w) = a + b\log\left(\frac{1 + c(\sigma - u_a) + d(u_a - u_w)}{1 + f(\sigma - u_a) + g(u_a - u_w)}\right)$,

a, b, c, d, f, g are the fitting parameters.

The derivatives of Equation (3.45) can be calculated by Equation (3.46) and (3.47).

$$\frac{\partial}{\partial(\sigma-u_a)}f(\sigma-u_a,u_a-u_w)=\frac{b[c(1+f(\sigma-u_a)+g(u_a-u_w))-f(1+c(\sigma-u_a)+d(u_a-u_w))]}{(1+f(\sigma-u_a)+g(u_a-u_w))(1+c(\sigma-u_a)+d(u_a-u_w))\ln(10)} \quad (3.46)$$

$$\frac{\partial}{\partial(u_a-u_w)}f(\sigma-u_a,u_a-u_w)=\frac{b[d(1+f(\sigma-u_a)+g(u_a-u_w))-g(1+c(\sigma-u_a)+d(u_a-u_w))]}{(1+f(\sigma-u_a)+g(u_a-u_w))(1+c(\sigma-u_a)+d(u_a-u_w))\ln(10)} \quad (3.47)$$

Equation (3.46) and (3.47) can be used to calculate the elastic moduli for the soil structure and water phase of the unsaturated soil.

The change in volumetric strain can be calculated from the change in void ratio assuming a constant initial volume of the unsaturated soil, as given by Equation (3.48).

$$d\varepsilon_v=\frac{de}{1+e_0} \quad (3.48)$$

where:

e_0 is the initial void ratio of the unsaturated soil,

de is the change in void ratio.

The coefficient of volume change with respect to net normal stress, m_1^s, is defined as the ratio between the change in the volumetric strain and net normal stress. The coefficient of volume change with respect to suction, m_2^s, is defined as the ratio between the change in the volumetric strain and suction. Therefore, m_1^s and m_2^s can be calculated from the change in void ratio, as given by Equation (3.49) and (3.50).

$$m_1^s=\frac{\partial\varepsilon_v}{\partial(\sigma_{\text{mean}}-u_a)}=\frac{1}{1+e_0}\frac{\partial e}{\partial(\sigma_{\text{mean}}-u_a)} \quad (3.49)$$

$$m_2^s=\frac{\partial\varepsilon_v}{\partial(u_a-u_w)}=\frac{1}{1+e_0}\frac{\partial e}{\partial(u_a-u_w)} \quad (3.50)$$

The derivative of void ratio to net normal stress and suction can be calculated from Equation (3.46) and (3.47).

The coefficient of water volume change with respect to net normal stress, m_1^w, is defined as the ratio between the change in the volume of water and net normal stress. The coefficient of water volume change with respect to net normal stress, m_2^w, is defined as the ratio between the change in the volume of water and suction. These two parameters can be calculated by differentiating the function of volumetric content with respect to $\sigma_{\text{mean}} - u_a$ and $u_a - u_w$, as given by Equation (3.51) thru (3.52).

$$m_1^w = \frac{\partial \theta_w}{\partial(\sigma_{\text{mean}} - u_a)} \tag{3.51}$$

$$m_2^w = \frac{\partial \theta_w}{\partial(u_a - u_w)} \tag{3.52}$$

where:

θ_w is the volumetric water content of the unsaturated soil.

If the constitutive surface of the gravimetric water content of the unsaturated soil is obtained, the coefficients of water volume change, m_1^w, and m_2^w, can be obtained by differentiating the function of the constitutive surface of the gravimetric water content, as given by Equation (3.53) thru (3.54).

$$m_1^w = \frac{\partial \theta_w}{\partial(\sigma_{\text{mean}} - u_a)} = \frac{G_s}{1+e_0} \frac{\partial w}{\partial(\sigma_{\text{mean}} - u_a)} \tag{3.53}$$

$$m_2^w = \frac{\partial \theta_w}{\partial(u_a - u_w)} = \frac{G_s}{1+e_0} \frac{\partial w}{\partial(u_a - u_w)} \tag{3.54}$$

where:

w is the gravimetric water content of the unsaturated soil,

G_s is the specific gravity of the unsaturated soil.

The derivative of water content to net normal stress and suction can be calculated from Equation (3.46) and (3.47).

3.4.2 Hydraulic conductivity of the unsaturated expansive soil

The hydraulic conductivity of the unsaturated soil can be predicted from the saturated hydraulic conductivity and the soil-water characteristic curve. Shuai (1996) presented the hydraulic conductivity function for Regina clay using Gardner (1958) equation. The function is given by Equation (3.55).

$$k_w = \frac{k_{w0}e^B}{1+A[\frac{(u_a-u_w)}{\rho_w g}]^N} \tag{3.55}$$

where:

k_{w0} is the hydraulic conductivity of the unsaturated soil when the void ratio is equal to 1,

A, B, N are the fitting parameters.

3.5 Constitutive model for unsaturated soil-structure interface

The soil-structure interface is defined as the thin layer that can transfer the stress between the soil and structure. As the soil-structure interface has a lower strength compared with the structure and the surrounding soil, the interface will fail first (Hamid and Miller 2009). Therefore, the interface controls the design of the geotechnical structures such as the pile foundation, retaining walls, and tunnels. Hence, the behavior of the soil-structure interface should be rigorously investigated.

The soil-structure interface shear strength degradation has been investigated by some investigators (Fakharian and Evgin 2000; Hu and Pu 2004; Long et al. 2017; Shahrour and Rezaie 1997). The typical curve of the shear stress and relative displacement at the soil-structure interface is plotted in Figure 3.5. Figure 3.5 shows that the shear stress in the soil-structure interface increases with the increase in the relative displacement between soil and structure before the shear stress reaches the peak shear stress. When the shear strength reaches the peak shear strength, the shear stress will decrease with an increase in the relative displacement. The shear strength will reach residual stress when there is a relatively large displacement. After reaching the residual stress, the change in shear stress will be relatively small with the change in the relative displacement. Therefore, the shear stress can be considered as a constant after reaching the residual stress. The degradation of the shear stress with the relative displacement is referred to as the softening behavior of the soil-structure interface.

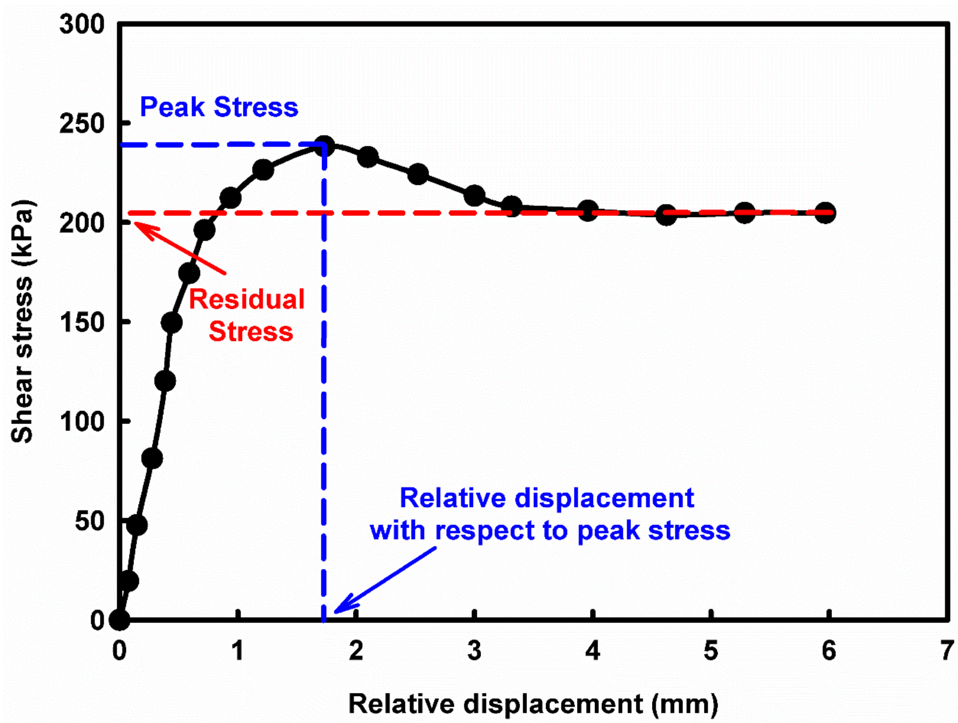

Figure 3.5 The curve of shear stress and relative displacement at the soil-structure interface (modified from Shahrour and Rezaie 1997).

Many models are proposed in the literature to formulate the softening behavior of the shear stress in the soil-structure interface (Boulon and Nova 1990; Desai and Ma 1992; Fakharian and Evgin 2000; Ghionna and Mortara 2002; Zhang and Zhang 2012; Cao et al. 2014; Soundara and Robinson 2017; Zhang et al. 2015; Cheng et al. 2018). One of the widely used models is the hyperbolic model because of the similarity of shear stress and the relative displacement in the soil-structure interface. The hyperbolic model proposed by Zhang and Zhang (2012) is capable of simulating the softening behavior of the soil-structure interface. This model is expressed by Equation (3.56) and (3.57). The various parameters in Equation (3.56) and (3.57) are presented in Figure 3.6.

$$\tau_s(z) = \frac{S_s(z)(a+cS_s(z))}{(a+bS_s(z))^2} \tag{3.56}$$

$$\begin{cases} a = \dfrac{\beta_s - 1 + \sqrt{1-\beta_s}}{2\beta_s}\dfrac{S_{su}}{\tau_{su}} \\ b = \dfrac{1 - \sqrt{1-\beta_s}}{2\beta_s}\dfrac{1}{\tau_{su}} \\ c = \dfrac{2 - \beta_s - 2\sqrt{1-\beta_s}}{4\beta_s}\dfrac{1}{\tau_{su}} \end{cases}$$

$$\beta_s = \frac{\tau_{sr}}{\tau_{su}} \tag{3.57}$$

where:

$\tau_s(z)$ is the interface shear stress (shaft friction) at a depth of z,

$S_s(z)$ is the relative displacement of pile and soil at a depth of z,

S_{su} is the relative displacement with respect to the peak shear strength,

τ_{su} is the peak shear strength,

β_s is the ratio between the residual shear strength and peak shear strength.

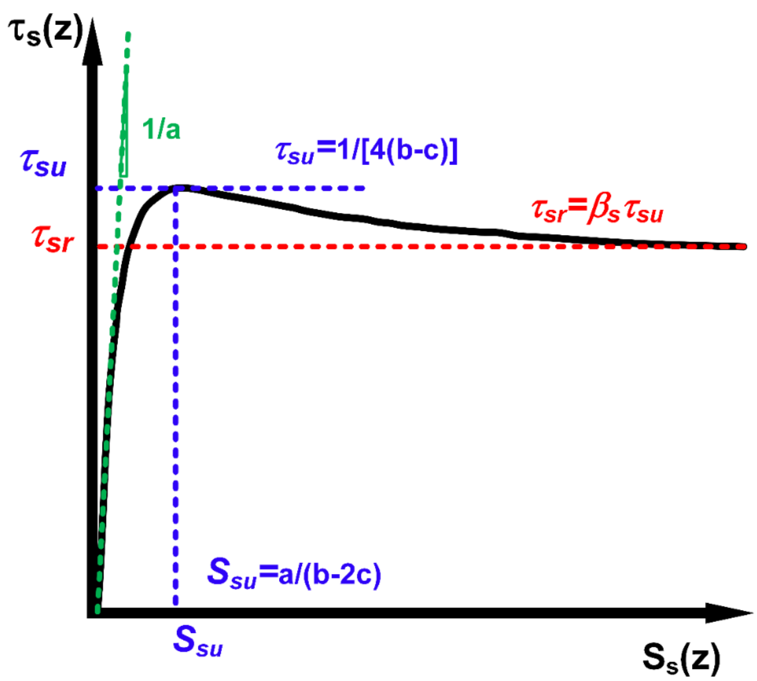

Figure 3.6 Assumed relationship between shear stress and relative displacement in the soil-structure interface (modified from Zhang and Zhang 2012).

For the unsaturated soil-structure interface, $(u_a - u_w)$, plays an important role in the mechanical behavior of the unsaturated soil-structure interface and should be considered in the unsaturated soil-structure interface models (Borana et al. 2016; Hamid and Miller 2009). Hamid and Miller used the modified direct shear apparatus to control matric suction and study the shear strength of unsaturated soil-structure interface (Hamid 2005; Hamid and Miller 2009; Miller and Hamid 2006). One set of results is plotted in Figure 3.7. The results suggest that the shear strength of unsaturated soil-structure interface can be calculated by Equation (3.58).

$$\tau_{su} = c_a' + (\sigma_{nf} - u_{af})\tan\ \delta' + (u_{af} - u_{wf})\tan\ \delta^b \tag{3.58}$$

where:

τ_{su} is the interface shear strength of the unsaturated soil-structure interface,

c_a' is the adhesion of the unsaturated soil-structure interface,

$\sigma_{nf} - u_{af}$ is the net normal stress of the unsaturated soil-structure interface,

δ' is the friction angle with respect to the net normal stress,

$u_{af} - u_{wf}$ is the suction of the unsaturated soil-structure interface,

δ^b is the friction angle with respect to suction.

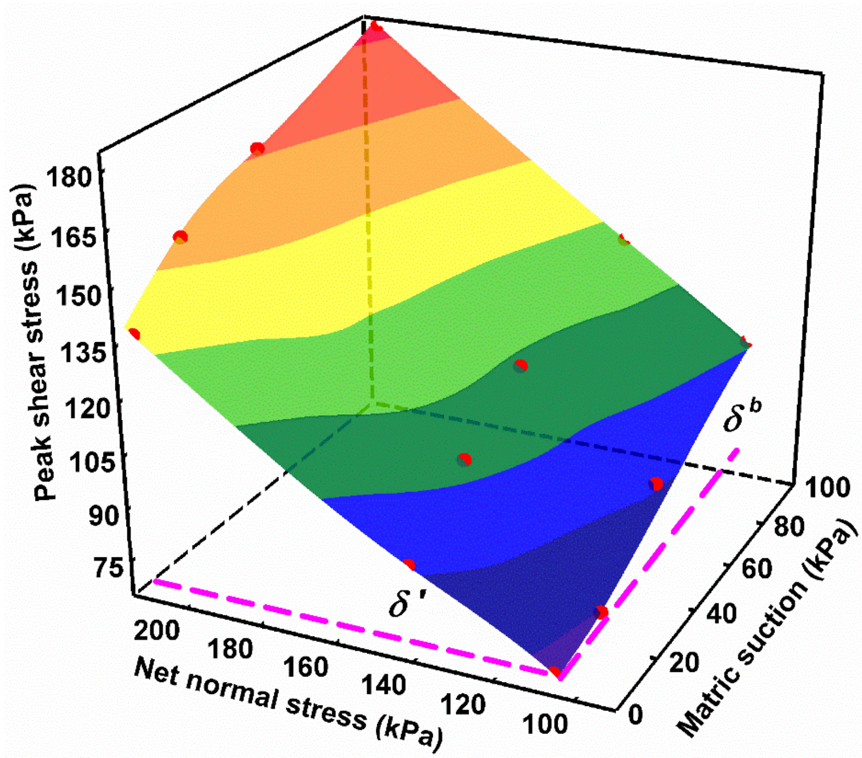

Figure 3.7 The peak shear stress of an unsaturated soil-structure interface (modified from Hamid and Miller 2009).

By conducting a series of direct shear tests, the strength parameters for the peak shear strength can be obtained and the peak shear strength for the unsaturated soil-structure interface, τ_{su}, can be calculated by Equation (3.58). By combining the peak shear strength for the unsaturated soil-structure interface and Zhang and Zhang model, the behavior of the shear stress in the unsaturated soil-structure interface can be described (Liu and Vanapalli 2019a).

The effect of suction on the relation between the shear stress and relative displacement is given in Figure 3.8. The parameters of the pile-soil interface were assumed. The assumed values are summarized in Table 3.3. A series of suctions (i.e. 0kPa, 10kPa, 20kPa, 30kPa, and 40kPa) are used to illustrate the different behavior of the pile-soil interface at the different suction. The results clearly show that the peak stress and the residual stress of the interface increase with the increase in the suction.

Table 3.3 Assumed values of the parameters of the constitutive model for the shear stress-relative displacement relationship.

Properties	Parameters	Values
the peak shear stress of the interface, τ_{su}	the friction angle with respect to the net normal stress, δ'	30°
	the friction angle with respect to suction, δ^b	30°
	the adhesion of the unsaturated soil-structure interface, c'_a	0 kPa
	the net normal stress of the unsaturated soil-structure interface, $\sigma_{nf} - u_{af}$	10 kPa
the hyperbolic model	the relative displacement with respect to the peak shear strength, S_{su}	1mm
	the ratio between the residual shear strength and peak shear strength, β_s	0.85

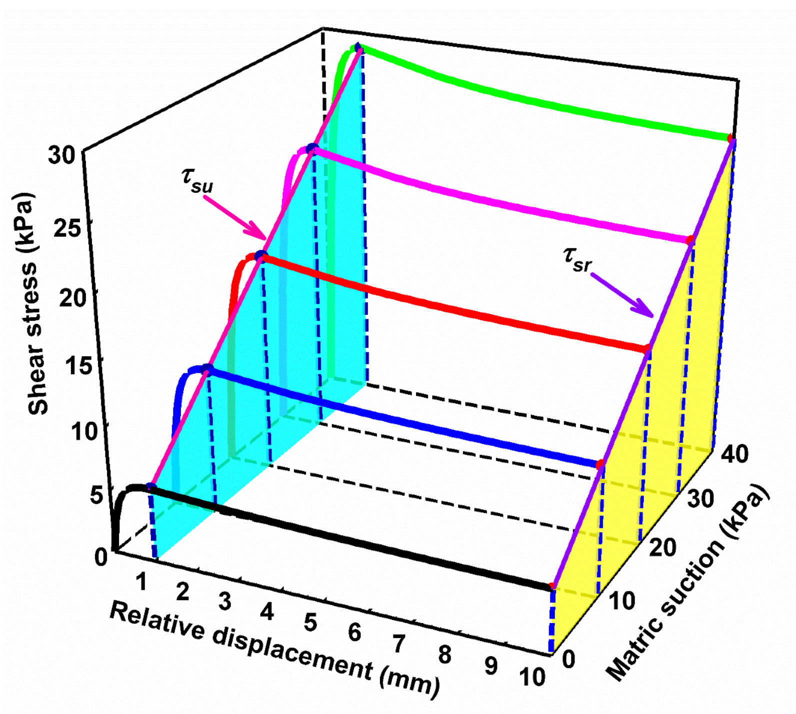

Figure 3.8 The behavior of the unsaturated pile-soil interface.

3.6 Summary and conclusion

In this chapter, the constitutive models and other equations used in the present study for performing the coupled hydro-mechanical analysis of the pile in the unsaturated expansive soils are briefly presented.

The constitutive relations for the soil structure and water phase of the unsaturated soil are formulated in terms of independent stress state variables; namely, net normal stress, $(\sigma_n - u_a)$, the suction, $(u_a - u_w)$. The incremental forms of the equations for the soil structure and water phase constitutive relations are briefly introduced. The flow law is also required in addition to the constitutive relations for the soil structure and water phase for a rational explanation of the flow behavior. By incorporating the balance equations and the constitutive relations for the soil structure and water phase, the differential governing equations for the coupled hydro-mechanical problems are established. When the boundary conditions are specified, the solutions for the coupled hydro-mechanical problems can be obtained by solving the governing equations. Except for the equations for the coupled hydro-mechanical problems, the constitutive relation for the unsaturated pile-soil interface is given in this chapter.

The equations for the coupled hydro-mechanical problems and constitutive model for the unsaturated pile-soil interface are developed in five subroutines of Abaqus. Abaqus is powerful numerical software, which offers a series of user-defined subroutines to define constitutive models for the material. Four user-defined subroutines are developed to simulate the coupled hydro-mechanical problem. The hydro-mechanical problem is transferred to the coupled thermo-mechanical problem to develop the subroutines. The user-defined field subroutine USDFILD is used to change and transfer parameters. Three subroutines including user-defined material subroutine UMAT, user-defined thermal material subroutine UMATHT, and user-defined thermal expansion subroutine UEXPAN are used to calculate the stress-deformation, the hydraulic behavior, and the expansion strain, respectively. The soil-structure interface model is implemented into user-defined friction behavior subroutine FRIC to calculate the friction between soil and pile. The theory for the development of the subroutines and the layout of the subroutines are available in Chapter 4.

CHAPTER 4

IMPLEMENTATION OF CONSTITUTIVE AND SOIL-STRUCTURE INTERFACE MODELS INTO ABAQUS FOR MODELING THE PILE BEHAVIOR IN UNSATURATED EXPANSIVE SOILS

4.1 Introduction

A coupled hydro-mechanical model for the unsaturated expansive soil is implemented into Abaqus software for analysis of the behavior of single piles in expansive soils during water infiltration. The features that are available in the Abaqus for solving thermo-mechanical problems are exploited for modeling the pile behavior in unsaturated expansive soils.

In the coupled hydro-mechanical problems, the water flow follows Darcy's law. In the coupled thermo-mechanical problems, the heat transfer can be described by Fourier's law. Darcy's law is similar to Fourier's law in principle and form (Groenevelt 2003; Rose 2000). The downward flow is directly proportional to the gradient of the hydraulic head as per Darcy's law. It is well known that as per Fourier's law the heat flow is directly proportional to the gradient of the temperature. This argument suggests that both Darcy and Fourier equations relate the driving forces (i.e. the gradient of pressure head, the gradient of temperature) to their conjugated flux (i.e. water flux, heat flux) (Groenevelt 2003). Therefore, Fourier's law can be used as a tool to simulate water flow behavior. In the coupled hydro-mechanical problems for the unsaturated soils, the strain is induced by the variations in the external stress and the suction. In the coupled thermo-mechanical problems, the strain is induced by the variations in the external stress and the temperature. Therefore, the constitutive relations for the mechanical behavior of the unsaturated soil in the coupled hydro-mechanical problems are similar to the constitutive relations for the mechanical behavior in the coupled thermo-mechanical problems. In other words, the equations for the coupled hydro-mechanical problems are similar to the equations for the coupled thermo-mechanical problems. Therefore, the coupled hydro-mechanical problems can be simulated by extending the approaches used for analyzing coupled thermo-mechanical problems.

In this chapter, the constitutive relations, heat transfer law, and the differential governing equations for the coupled thermo-mechanical problems are introduced. The equations for the coupled hydro-mechanical problems are compared with the equations for the coupled thermo-mechanical problems. The comparison clearly shows the similarity between the equations for the hydro-mechanical problems and that for the thermo-mechanical problems. By comparing these equations, the parameters associated with the coupled hydro-mechanical problems are transferred to the parameters in the coupled thermo-mechanical problems. The commercial numerical software Abaqus is used to perform the coupled thermo-mechanical analysis. Four user-defined subroutines including the user-defined field subroutine (USDFLD), the user-defined material subroutine (UMAT), the user-defined thermal material subroutine (UMATHT), and the user-defined thermal expansion subroutine (UEXPAN) are developed in this study to process the thermo-mechanical analysis. Except for the equations for the hydro-mechanical problems, the constitutive model for the unsaturated pile-soil interface is developed into the fifth subroutine, the user-defined friction behavior subroutine (FRIC). The theoretical development of the subroutines is summarized in this chapter.

4.2 Constitutive relation and heat transfer law for the coupled thermo-mechanical problems

In the coupled thermo-mechanical problems, the mechanical and thermal behaviors are included in soil and these two behaviors interact with each other. Therefore, to solve the coupled thermo-mechanical problems, the constitutive relations for each physical behavior are required (Zienkiewicz and Chan 1989). The stress-strain relation is modeled by the constitutive relations for mechanical behavior. The constitutive relation for thermal behavior is used to describe the variation of internal energy. Apart from the constitutive relations for mechanical and thermal behaviors, Fourier's law is introduced to calculate the heat transfer.

4.2.1 The constitutive relationship for the mechanical system

To construct the constitutive relation for the mechanical behavior of soil in the coupled thermo-mechanical problems, typically some assumptions are made. The soil is assumed as homogenous, elastic and isotropic. In addition, the soil particles are incompressible and the soil is dry.

The change in strain in the coupled thermo-mechanical problems can be considered as the summary of the strain induced by the external stress and the strain induced by the temperature (Cui et al. 2018), as given by Equation (4.1).

$$d\varepsilon = d\varepsilon_s + d\varepsilon_T \tag{4.1}$$

where:

$d\varepsilon_s$ is the change in the strain induced by the change in external stress,

$d\varepsilon_T$ is the change in the strain induced by the change in temperature.

The soil is assumed as the ideal elastic. Therefore, the strain induced by external stress can be calculated by Hooke's law. The incremental form is shown in Equation (4.2) thru (4.7).

$$(d\varepsilon_x)_s = \frac{d\sigma_x}{E} - \frac{\mu}{E} d(\sigma_y + \sigma_z) \tag{4.2}$$

$$(d\varepsilon_y)_s = \frac{d\sigma_y}{E} - \frac{\mu}{E} d(\sigma_x + \sigma_z) \tag{4.3}$$

$$(d\varepsilon_z)_s = \frac{d\sigma_z}{E} - \frac{\mu}{E} d(\sigma_x + \sigma_y) \tag{4.4}$$

$$d\gamma_{xy} = \frac{d\tau_{xy}}{G} \tag{4.5}$$

$$d\gamma_{yz} = \frac{d\tau_{yz}}{G} \tag{4.6}$$

$$d\gamma_{zx} = \frac{d\tau_{zx}}{G} \tag{4.7}$$

where:

$d\sigma_x$ is the change in the normal stress in x −direction,

$d\sigma_y$ is the change in the normal stress in y −direction,

$d\sigma_z$ is the change in the normal stress in z −direction,

$(d\varepsilon_x)_s$ is the change in the normal strain in x −direction due to the change in normal stress,

$(d\varepsilon_y)_s$ is the change in the normal strain in y −direction due to the change in normal stress,

$(d\varepsilon_z)_s$ is the change in the normal strain in z −direction due to the change in normal stress,

$d\tau_{xy}$ is the change in the shear stress on the x −plane in y −direction,

$d\tau_{yz}$ is the change in the shear stress on the y −plane in z −direction,

$d\tau_{zx}$ is the change in the shear stress on the z −plane in x −direction,

$d\gamma_{xy}$ is the change in the shear strain on the x −plane in y −direction,

$d\gamma_{yz}$ is the change in the shear strain on the y −plane in z −direction,

$\mathrm{d}\gamma_{zx}$ is the change in the shear strain on the z −plane in x −direction,

μ is the Poisson's ratio,

E is the elasticity modulus for the soil structure,

G is the shear modulus that can be calculated by $G = \frac{E}{2(1+\mu)}$.

The soil is assumed to an isotropic material. Therefore, the strains induced by the temperature are the same in x −, y −, and z − directions. The increment in strain in three directions induced by temperature can be calculated by Equation (4.8) thru (4.10).

$$(d\varepsilon_x)_T = \alpha dT \tag{4.8}$$

$$(d\varepsilon_y)_T = \alpha dT \tag{4.9}$$

$$(d\varepsilon_z)_T = \alpha dT \tag{4.10}$$

where:

$(d\varepsilon_x)_T$ is the change in the normal strain in x −direction due to the change in temperature,

$(d\varepsilon_y)_T$ is the change in the normal strain in y −direction due to the change in temperature,

$(d\varepsilon_z)_T$ is the change in the normal strain in z −direction due to the change in temperature,

dT is the change in the temperature,

α is the coefficient of heat expansion.

The temperature will not induce the change in shear strain. Therefore, the change in shear strain induced by temperature is equal to zero, as shown in Equation (4.11).

$$(d\gamma_{xy})_T = (d\gamma_{yz})_T = (d\gamma_{zx})_T = 0 \tag{4.11}$$

By substituting Equation (4.2) thru (4.11) to Equation (4.1), the incremental form of the constitutive relation for the soil structure of the soil can be given by Equation from (4.12) thru (4.17).

$$d\varepsilon_x = \frac{d\sigma_x}{E} - \frac{\mu}{E} d(\sigma_y + \sigma_z) + \alpha dT \tag{4.12}$$

$$d\varepsilon_y = \frac{d\sigma_y}{E} - \frac{\mu}{E} d(\sigma_x + \sigma_z) + \alpha dT \tag{4.13}$$

$$d\varepsilon_z = \frac{d\sigma_z}{E} - \frac{\mu}{E} d(\sigma_x + \sigma_y) + \alpha dT \tag{4.14}$$

$$d\gamma_{xy} = \frac{d\tau_{xy}}{G} \tag{4.15}$$

$$d\gamma_{yz} = \frac{d\tau_{yz}}{G} \tag{4.16}$$

$$d\gamma_{zx} = \frac{d\tau_{zx}}{G} \tag{4.17}$$

where:

$d\sigma_x$ is the change in the normal stress in x −direction,

$d\sigma_y$ is the change in the normal stress in y −direction,

$d\sigma_z$ is the change in the normal stress in z −direction,

$d\varepsilon_x$ is the change in the total normal strain in x −direction,

$d\varepsilon_y$ is the change in the total normal strain in y −direction,

$d\varepsilon_z$ is the change in the total normal strain in z −direction,

dT is the change in the temperature,

α is the coefficient of heat expansion,

$d\tau_{xy}$ is the change in the shear stress on the x −plane in y −direction,

$d\tau_{yz}$ is the change in the shear stress on the y −plane in z −direction,

$d\tau_{zx}$ is the change in the shear stress on the z −plane in x −direction,

$d\gamma_{xy}$ is the change in the shear strain on the x −plane in y −direction,

$d\gamma_{yz}$ is the change in the shear strain on the y −plane in z −direction,

$d\gamma_{zx}$ is the change in the shear strain on the z −plane in x −direction,

μ is the Poisson's ratio,

E is the elasticity modulus for the soil structure,

G is the shear modulus that can be calculated by $G = \frac{E}{2(1+\mu)}$.

The volumetric strain for the coupled thermo-mechanical problems can be obtained by Equation (4.18).

$$d\varepsilon_v = 3(\frac{1-2\mu}{E})d\sigma_{\text{mean}} + 3\alpha dT \tag{4.18}$$

where:

σ_{mean} is the mean normal stress, $\sigma_{\text{mean}} = \frac{(\sigma_x+\sigma_y+\sigma_z)}{3}$.

Equation (4.18) can be used to calculate the volumetric strain for the soil under a three-dimensional stress state. The volumetric strain for the soil under K_0 loading state can be obtained by Equation (4.19).

$$d\varepsilon_v = \frac{1-\mu-2\mu^2}{E(1-\mu)} d\sigma_y + \frac{1+\mu}{1-\mu} \alpha dT \tag{4.19}$$

4.2.2 The constitutive relationship for energy variation

The constitutive relation for energy variation is required in the coupled thermo-mechanical problems because the temperature is related to the volumetric energy. In the coupled thermo-mechanical problems, the variation of the volumetric energy is induced both by the change in temperature and change in the stress. Therefore, constitutive relation for the volumetric energy defines the relation of volumetric energy and temperature and stress.

The temperature will typically increase with an increase in energy in a matter. The change in energy induced by the temperature can be calculated by the change in temperature, as shown in Equation (4.20) (Bowers and Hanks 1962). The change in the volumetric energy is given by Equation (4.21).

$$dQ_T = mCdT \tag{4.20}$$

$$dE = \frac{dQ_T}{V} = \frac{mCdT}{V} = \rho CdT \tag{4.21}$$

where:

dQ_T is the change in the energy restored in a matter,

dE is the change in the volumetric energy,

m is the mass of the matter,

ρ is the density of the matter,

C is the specific heat capacity.

The specific heat capacity is defined as the required energy per unit mass of the matter when the temperature of the matter is increased by one degree.

Whenever a load is applied on the soil, the load is doing work on the soil. Part of work can be converted to heat energy in soil (Zhang 2004). The variation of volumetric energy induced by the change in the stress can be calculated by Equation (4.22).

$$dE = m_1^E d\sigma \tag{4.22}$$

where:

dE is the change in the volumetric energy,

$d\sigma$ is the change in stress,

m_1^E is the coefficient of volumetric energy with respect to the change in stress.

In the coupled thermo-mechanical problems, the variation of volumetric energy is induced by the change in temperature and stress. Therefore, the variation of volumetric energy can be calculated by adding Equation (4.22) to (4.21), as given by Equation (4.23).

$$dE = m_1^E d\sigma + \rho C dT \tag{4.23}$$

4.2.3 The flow law for the heat conduction

The heat conduction typically follows Fourier's law, as given by Equation (4.24). Fourier's law relates the heat flux to the gradient of the temperature.

$$q_i = -\lambda_i \frac{\partial}{\partial x_i} T \tag{4.24}$$

where:

q_i is the heat flux in i direction,

λ_i is the thermal conductivity of the matter in i direction,

T is the value of temperature.

4.3 Differential equations for the coupled thermo-mechanical problems

The governing differential equations for each physical phenomenon (i.e. mechanical behavior, heat transfer) are required for solving the coupled problems (Zienkiewicz et al. 2005). In this section, the differential equations for the mechanical static equilibrium and the heat transfer are summarized.

4.3.1 Differential equations for the stress-deformation relation

The equations of equilibrium state for mechanical stresses can be written as Equation (4.25).

$$\frac{\partial \sigma_{ij}}{\partial x_j} + b_i = 0 \tag{4.25}$$

where:

σ_{ij} are the components of the total stress tensor,

b_i are the components of the body force vector.

Solve Equation (4.12)-Equation (4.17) to get the expressions of the normal stress σ_{ij} in terms of ε_{ij}, and T, as shown in Equation (4.26)-Equation (4.31).

$$d\sigma_x = \lambda d\varepsilon_v + 2Gd\varepsilon_x - (3\lambda + 2G)\alpha \mathrm{d}T \tag{4.26}$$

$$d\sigma_y = \lambda d\varepsilon_v + 2Gd\varepsilon_y - (3\lambda + 2G)\alpha \mathrm{d}T \tag{4.27}$$

$$d\sigma_z = \lambda d\varepsilon_v + 2Gd\varepsilon_z - (3\lambda + 2G)\alpha \mathrm{d}T \tag{4.28}$$

$$d\tau_{xy} = Gd\gamma_{xy} \tag{4.29}$$

$$d\tau_{yz} = Gd\gamma_{yz} \tag{4.30}$$

$$d\tau_{zx} = Gd\gamma_{zx} \tag{4.31}$$

where:

λ is Lamé constant, $\lambda = \frac{E\mu}{1-\mu-2\mu^2}$.

The strain-displacement relation for the soil structure of unsaturated soil can be given by Equation (4.32) thru (4.34).

$$\varepsilon_x = \frac{\partial u}{\partial x}, \gamma_{yz} = \frac{\partial w}{\partial y} + \frac{\partial v}{\partial z} \tag{4.32}$$

$$\varepsilon_y = \frac{\partial v}{\partial y}, \gamma_{xz} = \frac{\partial w}{\partial x} + \frac{\partial u}{\partial z} \tag{4.33}$$

$$\varepsilon_z = \frac{\partial w}{\partial z}, \gamma_{xy} = \frac{\partial v}{\partial x} + \frac{\partial u}{\partial y} \tag{4.34}$$

where:

u, v, w are the displacement in $x-$, $y-$, and $z-$ direction, respectively.

By substituting Equation (4.26)-(4.34) to Equation (4.25), the differential equations for the soil structure of the unsaturated soil can be given by Equation (4.35)-(4.37).

$$(\lambda + G)\frac{\partial \varepsilon_v}{\partial x} + G\nabla^2 u - (3\lambda + 2G)\alpha\frac{\partial}{\partial x}T + X = 0 \tag{4.35}$$

$$(\lambda + G)\frac{\partial \varepsilon_v}{\partial y} + G\nabla^2 v - (3\lambda + 2G)\alpha\frac{\partial}{\partial y}T + Y = 0 \tag{4.36}$$

$$(\lambda + G)\frac{\partial \varepsilon_v}{\partial z} + G\nabla^2 w - (3\lambda + 2G)\alpha\frac{\partial}{\partial z}T + Z = 0 \tag{4.37}$$

where:

X, Y, Z are the components of body force in $x-$, $y-$, and $z-$ direction, respectively,

∇^2 is the Laplace operator, $\nabla^2 = \frac{\partial^2}{\partial x^2} + \frac{\partial^2}{\partial y^2} + \frac{\partial^2}{\partial z^2}$.

4.3.2 Differential equations for the heat flow

The differential equation for the heat flow can be given by Equation (4.38).

$$\frac{\partial q_x}{\partial x} + \frac{\partial q_y}{\partial y} + \frac{\partial q_z}{\partial z} + \frac{\partial E}{\partial t} = 0 \tag{4.38}$$

where:

q_x, q_y, q_z are the flux in $x-$, $y-$, and $z-$ direction, respectively,

E is the volumetric energy of the matter,

t is the time.

By substituting Equation (4.23) and Equation (4.24) into Equation (4.38), the differential equation for the water phase of the unsaturated soil can be given by Equation (4.39).

$$\frac{\partial}{\partial x}(\lambda_x(\frac{\partial}{\partial x}T)) + \frac{\partial}{\partial y}(\lambda_y(\frac{\partial}{\partial y}T)) + \frac{\partial}{\partial z}(\lambda_z(\frac{\partial}{\partial z}T)) = \rho C\frac{dT}{dt} + m_1^E\frac{d\sigma}{dt} \tag{4.39}$$

4.4 Similarity of the coupled hydro-mechanical problems and the coupled thermo-mechanical problems

The similarity between coupled thermo-mechanical and the hydro-mechanical problems can be found by comparing respective differential equations. Zhang (2005) studied the behavior of the residential buildings on expansive soil by using the similarity of these two problems.

Equation (3.39) thru (3.41) and Equation (3.44) are the differential equations for the coupled hydro-mechanical problems of the unsaturated soils. If the gravity is the only body force, Equation (3.39)-(3.41) and Equation (3.44) can be modified into Equation (4.40) thru (4.43).

$$(\lambda + G)\frac{\partial \varepsilon_v}{\partial x} + G\nabla^2 u + \frac{3\lambda+2G}{H}\frac{\partial u_w}{\partial x} = 0 \tag{4.40}$$

$$(\lambda + G)\frac{\partial \varepsilon_v}{\partial y} + G\nabla^2 v + \frac{3\lambda+2G}{H}\frac{\partial u_w}{\partial y} = 0 \tag{4.41}$$

$$(\lambda + G)\frac{\partial \varepsilon_v}{\partial z} + G\nabla^2 w + \frac{3\lambda+2G}{H}\frac{\partial u_w}{\partial z} + \rho g = 0 \tag{4.42}$$

$$\frac{\partial}{\partial x}(k_x\frac{\partial}{\partial x}(\frac{u_w}{\rho_w g})) + \frac{\partial}{\partial y}(k_y\frac{\partial}{\partial y}(\frac{u_w}{\rho_w g})) + \frac{\partial}{\partial z}(k_z(\frac{\partial}{\partial z}\frac{u_w}{\rho_w g} + 1))) = m_1^w\frac{\partial(\sigma_{\text{mean}} - u_a)}{\partial t} - m_2^w\frac{\partial u_w}{\partial t} \tag{4.43}$$

Equation (4.35) thru (4.37) and Equation (4.39) are the differential equations for the coupled thermo-mechanical problems. If gravity is the only body force, Equation (4.35) thru (4.37) and Equation (4.39) can be modified into Equation (4.44) thru (4.47).

$$(\lambda + G)\frac{\partial \varepsilon_v}{\partial x} + G\nabla^2 u - (3\lambda + 2G)\alpha\frac{\partial}{\partial x}T = 0 \tag{4.44}$$

$$(\lambda + G)\frac{\partial \varepsilon_v}{\partial y} + G\nabla^2 v - (3\lambda + 2G)\alpha\frac{\partial}{\partial y}T = 0 \tag{4.45}$$

$$(\lambda + G)\frac{\partial \varepsilon_v}{\partial z} + G\nabla^2 w - (3\lambda + 2G)\alpha\frac{\partial}{\partial z}T + \rho g = 0 \tag{4.46}$$

$$\frac{\partial}{\partial x}(\lambda_x(\frac{\partial}{\partial x}T)) + \frac{\partial}{\partial y}(\lambda_y(\frac{\partial}{\partial y}T)) + \frac{\partial}{\partial z}(\lambda_z(\frac{\partial}{\partial z}T)) = \rho C\frac{dT}{dt} + m_1^E\frac{d\sigma}{dt} \tag{4.47}$$

For the differential equations for the soil structure of the unsaturated soil (i.e. Equation (4.42)), the units of λ, G, and H are kPa. The unit of pore water pressure is kPa. The units of z and w are m. If the unit of the density ρ is kg/m^3 and the unit of the gravity acceleration g is 1000 m/s^2, the unit of ρg will be kPa/m. Therefore, the dimension analysis of the left side of Equation (4.42) can be given by Equation (4.48).

$$kPa \times \frac{1}{m} + kPa \times \frac{m}{m^2} + \frac{kPa}{kPa} \times \frac{kPa}{m} + \frac{kPa}{m} = \frac{kPa}{m} \tag{4.48}$$

For the differential equations for the stress-strain relation of the coupled thermo-mechanical problems (i.e. Equation (4.46)), the units of λ, G, and H are kPa. The unit of temperature is K. The units of z and w are m. The unit of the coefficient of heat expansion, α, is K^{-1}. If the unit of the density ρ is kg/m^3 and the unit of the gravity acceleration g is $1000\,m/s^2$, the unit of ρg will be kPa/m^3. Therefore, the dimension analysis of the left side of Equation (4.46) can be given by Equation (4.49).

$$kPa \times \frac{1}{m} + kPa \times \frac{m}{m^2} + kPa \times \frac{1}{K} \times \frac{K}{m} + \frac{kPa}{m} = \frac{kPa}{m} \tag{4.49}$$

Comparing with Equation (4.48) and (4.49), the transfer of the parameters used in the coupled hydro-mechanical problems and the parameters used in the coupled thermo-mechanical problems can be found. The pore water pressure, u_w, is corresponding with the temperature, T. The coefficient of the heat expansion, α, is corresponding with the reciprocal of the elasticity modulus for the soil structure with respect to the suction, $\frac{1}{H}$.

For the differential equation for the water phase of the unsaturated soil (Equation (4.43)), the equation can be modified into Equation (4.50) and (4.51).

$$\frac{1}{\rho_w}\frac{\partial}{\partial x}\left(\frac{k_x}{g}\frac{\partial}{\partial x}u_w\right) + \frac{1}{\rho_w}\frac{\partial}{\partial y}\left(\frac{k_y}{g}\frac{\partial}{\partial y}u_w\right) + \frac{1}{\rho_w}\frac{\partial}{\partial z}\left(\frac{k_z}{g}\left(\frac{\partial}{\partial z}u_w + \rho_w g\right)\right) = m_1^w\frac{\partial(\sigma_{\text{mean}} - u_a)}{\partial t} - m_2^w\frac{\partial u_w}{\partial t} \tag{4.50}$$

$$\frac{\partial}{\partial x}\left(\frac{k_x}{g}\frac{\partial}{\partial x}u_w\right) + \frac{\partial}{\partial y}\left(\frac{k_y}{g}\frac{\partial}{\partial y}u_w\right) + \frac{\partial}{\partial z}\left(\frac{k_z}{g}\left(\frac{\partial}{\partial z}u_w + \rho_w g\right)\right) = \rho_w m_1^w\frac{\partial(\sigma_{\text{mean}} - u_a)}{\partial t} - \rho_w m_2^w\frac{\partial u_w}{\partial t} \tag{4.51}$$

As given by Equation (3.53) and (3.54), the coefficients of water volume change can be calculated by differentiating the function of the constitutive surface of the gravimetric water content. Therefore, Equation (4.51) can be modified into Equation (4.52).

$$\frac{\partial}{\partial x}\left(\frac{k_x}{g}\frac{\partial u_w}{\partial x}\right) + \frac{\partial}{\partial y}\left(\frac{k_y}{g}\frac{\partial u_w}{\partial y}\right) + \frac{\partial}{\partial z}\left(\frac{k_z}{g}\left(\frac{\partial u_w}{\partial z} + \rho_w g\right)\right)$$

$$= \rho_w \frac{G_s}{1+e_0} \frac{\partial w}{\partial(\sigma_{\text{mean}} - u_a)} \frac{\partial(\sigma_{\text{mean}} - u_a)}{\partial t} + \rho_w \frac{G_s}{1+e_0} \frac{\partial w}{\partial u_w} \frac{\partial u_w}{\partial t}$$

$$= \rho_d \frac{\partial w}{\partial(\sigma_{\text{mean}} - u_a)} \frac{\partial(\sigma_{\text{mean}} - u_a)}{\partial t} + \rho_d \frac{\partial w}{\partial u_w} \frac{\partial u_w}{\partial t} \tag{4.52}$$

For Equation (4.52), the unit of the hydraulic conductivity, k_i, is m/s. The unit of the gravity acceleration g is $1000\ m/s^2$. The unit of pore water pressure is kPa. The units of z and w are m. If the unit of the density ρ is kg/m^3 and the unit of the gravity acceleration g is $1000\,m/s^2$, the unit of ρg will be kPa/m. Therefore, the dimension analysis of Equation (4.52) can be given by Equation (4.53) and (4.54).

$$\text{Left side: } \frac{1}{m} \times \frac{m}{s} \times \frac{1}{1000} \times \frac{s^2}{m} \times \frac{1}{m} \times kPa = \frac{1}{1000} \times \frac{s}{m^2} \times kPa = \frac{kg}{m^3 \times s} \tag{4.53}$$

$$\text{Right side: } \frac{kg}{m^3} \times \frac{1}{kPa} \times \frac{kPa}{s} = \frac{kg}{m^3 \times s} \tag{4.54}$$

For the differential equation for the heat conduction (Equation (4.47)), the unit of the thermal conductivity, λ_i, is $\frac{J}{s \times m \times K}$. The unit of the specific heat capacity, C, is $\frac{J}{kg \times K}$. The unit of coefficient of volumetric energy with respect to stress, m_1^E, is $\frac{J}{m^3 \times kPa}$. Therefore, the dimension analysis of Equation (4.47) can be given by Equation (4.55) and (4.56).

$$\text{Left side: } \frac{1}{m} \times \frac{J}{s \times m \times K} \times \frac{1}{m} \times K = \frac{J}{s \times m^3} \tag{4.55}$$

$$\text{Right side: } \frac{kg}{m^3} \times \frac{J}{kg \times K} \times \frac{K}{s} + \frac{J}{m^3 \times kPa} \times \frac{kPa}{s} = \frac{J}{m^3 \times s} \tag{4.56}$$

By comparing Equation (4.53) and (4.55), it is found that the mass of water is corresponding to the energy of the matter.

As a conclusion, the pore water pressure, u_w, is corresponding with the temperature, T. The coefficient of the heat expansion, α, is corresponding with the reciprocal of the elasticity modulus for the soil structure with respect to the suction, $\frac{1}{H}$. The mass of water is corresponding to the energy of the matter. By using these relations, the parameters of the coupled hydro-mechanical problems can be transferred into the parameters of the coupled thermo-mechanical problems.

A new hydraulic conductivity is defined as $K = \frac{k_i}{g}$. The new hydraulic conductivity is corresponding to the thermal conductivity, λ_i. The transformation can be given by Equation (4.57).

$$K = \frac{k_i}{g} = \frac{m}{s} \times \frac{1}{1000} \times \frac{s^2}{m} = \frac{m}{s} \times \frac{1}{1000} \times \frac{s^2}{m} \times \frac{kg}{kg} \times \frac{m^2}{m^2} = \frac{kg}{s \times m \times kPa} = \frac{J}{s \times m \times K} = \lambda_i \quad (4.57)$$

The gravimetric water content is corresponding with the energy per unit mass. The transformation can be given by Equation (4.58).

$$w = \frac{m_w}{m_s} = \frac{kg}{kg} = \frac{J}{kg} \quad (4.58)$$

The coefficient of the water volume change with respect to suction, m_2^w, is corresponding to the product of the density, ρ, and the specific heat capacity, C. The transformation can be given by Equation (4.59).

$$m_2^w = \rho_d \frac{\partial w}{\partial (u_a - u_w)} = \frac{kg}{m^3} \times \frac{kg}{kg} \times \frac{1}{kPa} = \frac{kg}{m^3} \times \frac{kg}{kg \times kPa} = \frac{kg}{m^3} \times \frac{J}{kg \times K} = \rho C \quad (4.59)$$

The coefficient of the water volume change with respect to stress, m_1^w, is corresponding to the coefficient of volumetric energy with respect to stress, m_1^E. The transformation can be given by Equation (4.60).

$$m_1^w = \rho_d \frac{\partial w}{\partial (\sigma_{\text{mean}} - u_a)} = \frac{kg}{m^3} \times \frac{kg}{kg} \times \frac{1}{kPa} = \frac{kg}{m^3 \times kPa} = \frac{J}{m^3 \times kPa} = m_1^E \quad (4.60)$$

The water flux can be calculated by Equation (3.28). Equation (3.28) can be modified into Equation (4.61).

$$\rho_w q_{wi} = -\frac{k_i}{g}\left(\frac{\partial u_w}{\partial z} + \rho_w g\right) \quad (4.61)$$

where:

q_{wi} is the water flux in i direction,

k_i is the hydraulic conductivity of the unsaturated soil in i direction,

u_w is the value of pore water pressure,

ρ_w is the density of water,

g is the density of water.

The dimension analysis for Equation (4.61) can be given by Equation (4.62) and (4.63).

$$\text{Left side: } \frac{kg}{m^3} \times \frac{m}{s} = \frac{kg}{m^2 \times s} \tag{4.62}$$

$$\text{Right side: } \frac{m}{s} \times \frac{1}{1000} \times \frac{s^2}{m} \times \frac{1}{m} \times kPa = \frac{1}{1000} \times \frac{s}{m} \times kPa = \frac{kg}{m^2 \times s} \tag{4.63}$$

The heat flux can be calculated by Equation (4.64).

$$q_{Ti} = -\lambda_i \frac{\partial}{\partial x_i} T \tag{4.64}$$

where:

q_{Ti} is the heat flux in i direction,

λ_i is the thermal conductivity of the matter in i direction,

T is the value of temperature.

The dimension analysis for Equation (4.64) can be given by Equation (4.65) and (4.66).

$$\text{Left side: } \frac{J}{m^2 \times s} \tag{4.65}$$

$$\text{Right side: } \frac{J}{s \times m \times K} \times \frac{1}{m} \times K = \frac{J}{s \times m^2} \tag{4.66}$$

By comparing Equation (4.62), (4.63) and Equation (4.65), (4.66), it can be found that $\rho_w q_{wi}$ is corresponding to the heat flux, q_{Ti}.

The comparison of the parameters of the coupled hydro-mechanical problems and the coupled thermo-mechanical problems is given in Table 4.1.

Table 4.1 The comparison of parameters used in the coupled hydro-mechanical (HM) problems and the coupled thermo-mechanical (TM) problems.

	Coupled HM problems			Coupled TM problems		
	Parameter	**Symbol**	**Unit**	**Parameter**	**Symbol**	**Unit**
Physical parameters	Mass of water	m_w	kg	Energy	E	J
	Density	ρ	kg/m^3	Density	ρ	kg/m^3
	Length	x, y, and z	m	Length	x, y, and z	m
	Time	t	s	Time	t	s
	Gravimetric acceleration	g	$1000\,m/s^2$	Gravimetric acceleration	g	$1000\,m/s^2$
Equilibrium equation	Stress	σ_{ij}	kPa	Stress	σ_{ij}	kPa
	Elastic modulus	E	kPa	Elastic modulus	E	kPa
Continuity Equation	Pore water pressure	u_w	kPa	Temperature	T	K
	Water volume change coefficient	$\frac{\partial w}{\partial(u_a - u_w)}$	$\frac{kg}{kg \times kPa}$	Specific heat capacity	C	$\frac{J}{kg \times K}$
	Elasticity modulus	$\frac{1}{H}$	kPa^{-1}	Heat expansion coefficient	α	K^{-1}
	Hydraulic conductivity	$\frac{k_i}{g}$	$\frac{kg}{s \times m \times kPa}$	Thermal conductivity	λ_i	$\frac{J}{s \times m \times K}$
	Water flux	$\rho_w q_{wi}$	$\frac{kg}{m^2 \times s}$	Heat flux	q_{Ti}	$\frac{J}{m^2 \times s}$

4.5 Programming

4.5.1 Introduction

ABAQUS/Standard is a software program used to perform the simulation of the coupled thermo-mechanical problems. The main program and five user-defined material subroutines are typically used to perform the simulations. ABAQUS/CAE is used to perform the main program. The main program is used to define the size of the model, the material properties, type of the elements and size of the meshes, soil-pile interface, initial conditions, boundary conditions, and analysis steps to simulate. The properties of soil and soil-pile interface are transferred into user-defined subroutines to perform the coupled thermo-mechanical problems. Four user-defined subroutines including USDFLD, UMAT, UEXPAN, and UMATHT are used to perform thermo-mechanical problems. One subroutine, FRIC, is used to calculate the shaft friction between pile and soil. USDFLD is used to get the temperature and stress state of the previous step for the elements and transferred the values of these parameters to user-defined subroutines UEXPAN, and UMATHT. UMAT is used to calculate the strain induced by external stress. UEXPAN is used to calculate the expansion induced by the increase in the temperature. UMATHT is used to define the constitutive relation of the thermal conduction. FRIC is used to define the constitutive relationship of the soil-pile interface. The framework of the user-defined subroutines is plotted in Figure 4.1.

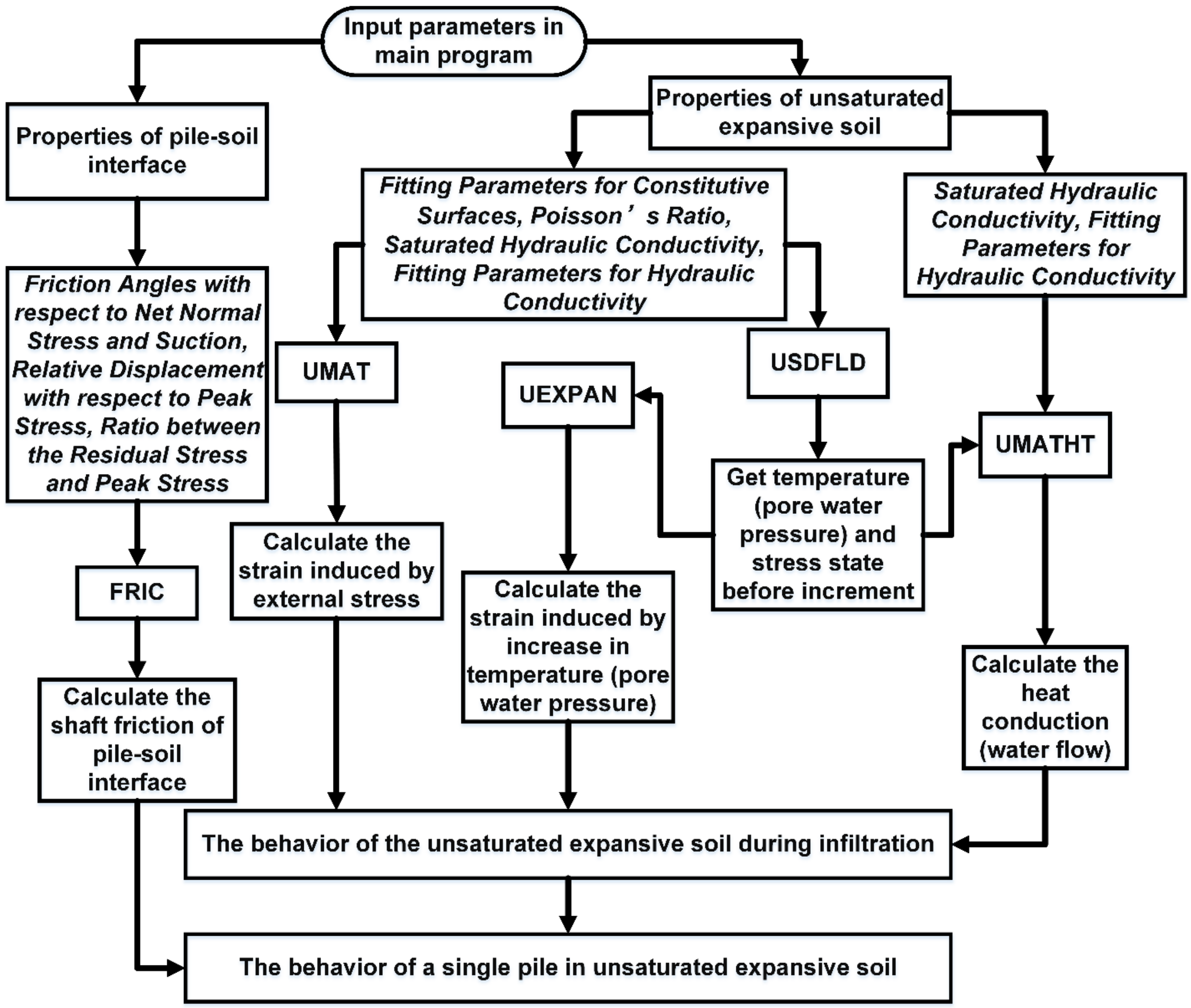

Figure 4.1 The framework for the user-defined subroutines.

4.5.2 Programs

4.5.2.1 Main program

Abaqus/CAE (Computer Aided Engineering) is used to perform the main program. Abaqus/CAE is an Abaqus environment that provides a simple interface to create, calculate, and evaluate the results from Abaqus/Standard simulation. In Abaqus/CAE, defining the geometry, material properties, mesh, analysis steps, boundary conditions, and initial conditions are performed. The material properties are transferred into user-defined subroutines. The flow chart of the main program is given in Figure 4.2.

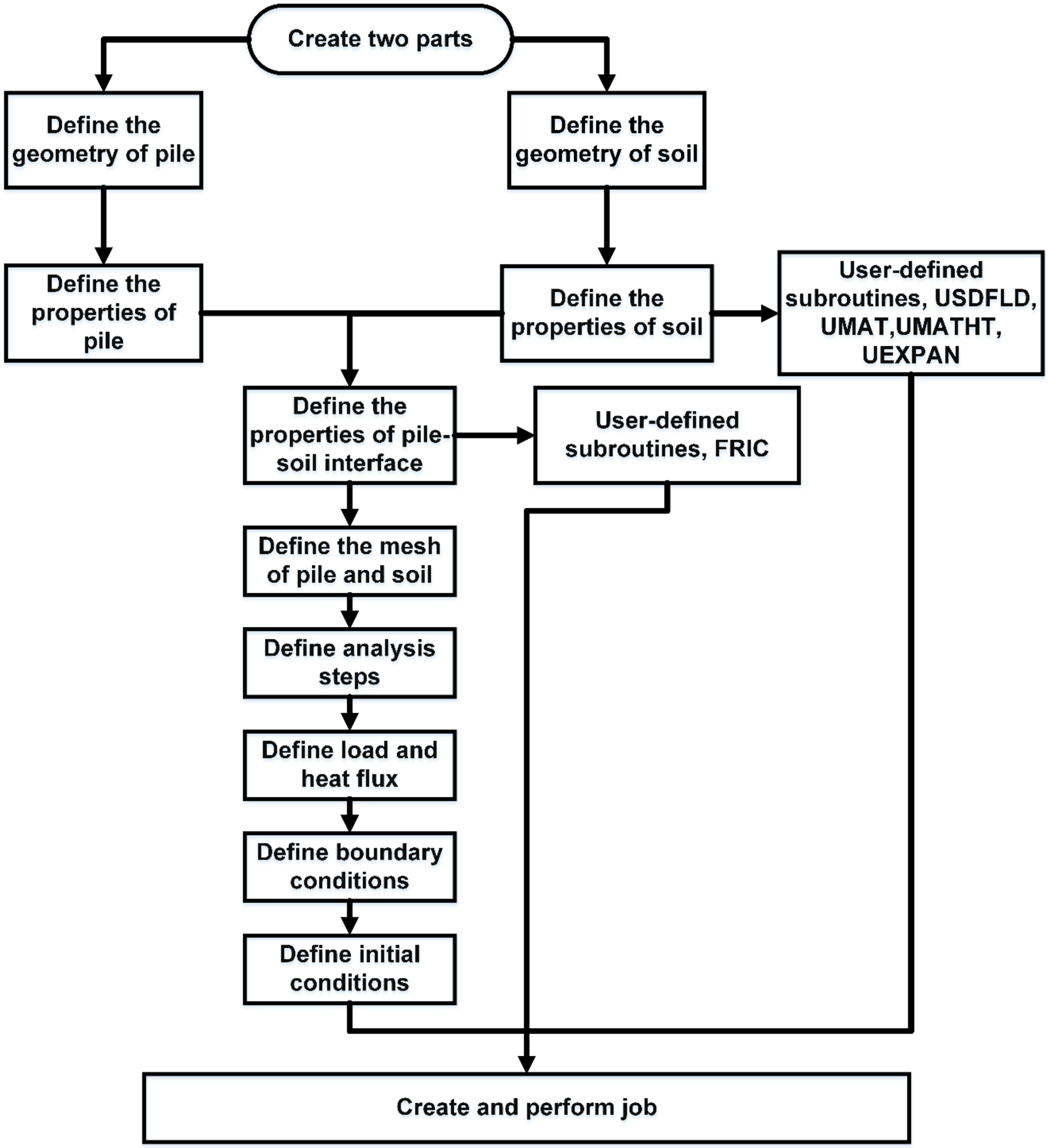

Figure 4.2 The flow chart for the main program.

4.5.2.2 User-defined field subroutine (USDFLD)

USDFLD processes access to material point data such as stress state, strain, and temperature (pore-water pressure). These data are transferred into other user-defined subroutines.

The coefficients of volume change and water content (the coefficient of the volume change with respect to net normal stress m_{1-1}^{s}, the coefficient of the volume change with respect to suction m_{1-2}^{s}, the coefficient of the water volume change with respect to net normal stress m_{1-1}^{w}, and the coefficient of the water volume change with respect to suction m_{1-2}^{w}) are functions of net normal stress and pore water pressure (suction). The hydraulic conductivity of unsaturated soil, k_i, is a function of the void ratio. Therefore, to calculate these coefficients, the stress state, strain, and temperature (pore water pressure) are required. However, user-defined subroutine UMATHT cannot access the stress state and strain. Therefore, USDFLD is used to obtain the stress state and strain before UMATHT. USDFLD is also used to access the temperature and transfer it into UEXPAN to calculate the strain induced by the variation of temperature. The utility routine GETVRM is used to get the values of stress, strain, and temperature. The flow chart of USDFLD is plotted in Figure 4.3.

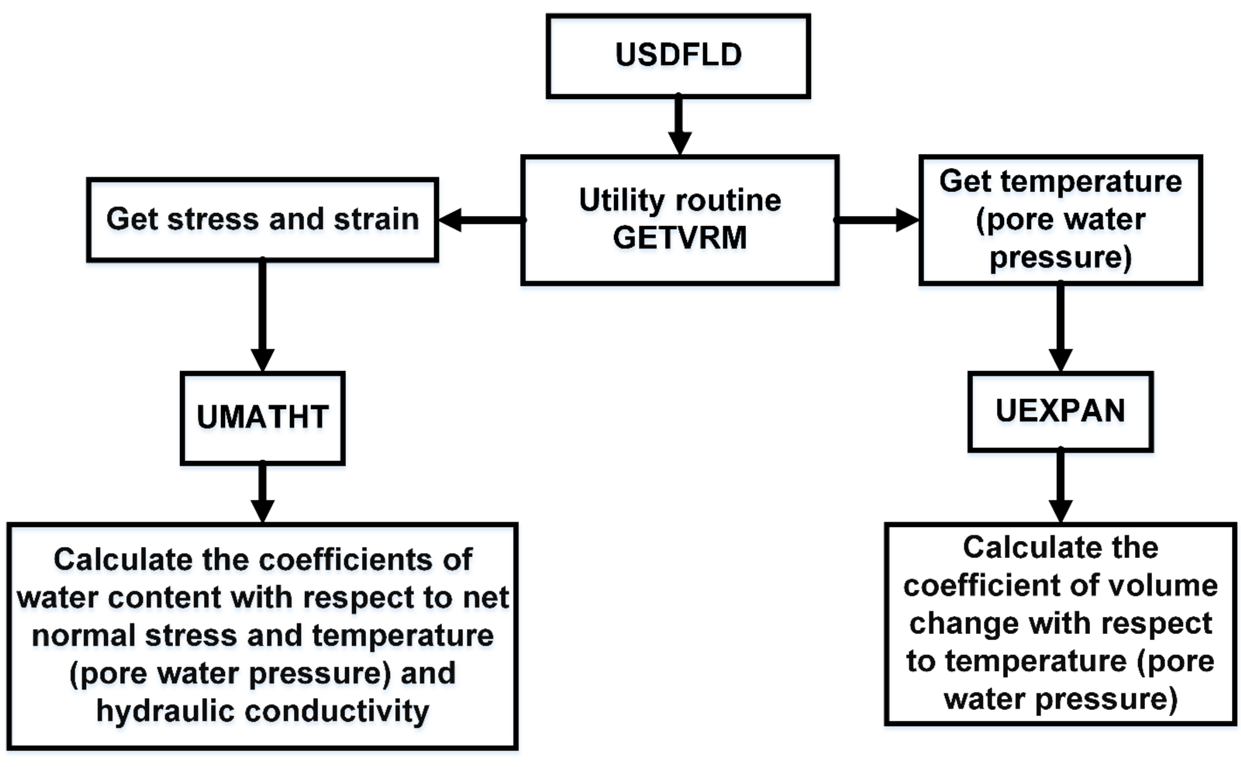

Figure 4.3 The flow chart of USDFLD.

4.5.2.3 User-defined material subroutine (UMAT)

UMAT is the user-defined subroutine to define a material's mechanical behavior. It can be used to define the mechanical constitutive relationship. It can be used to update the stresses induced by the strain at the end of the increment.

The mechanical properties of soil are transferred from the main program to UMAT. The mechanical properties of soil include the fitting parameters for the constitutive surface of the void ratio, initial void ratio, and Poisson's ratio. The elastic modulus with respect to net normal stress, E, can be calculated from the mechanical properties. For example, the elastic modulus, E, for the soil under K_0 loading state can be given by Equation (4.67).

$$E = \frac{1-\mu-2\mu^2}{m_{1-1}^s(1-\mu)} = (1+e_0) \times \frac{1-\mu-2\mu^2}{1-\mu} \times \frac{1}{\frac{\partial e}{\partial(\sigma_y - u_a)}} \tag{4.67}$$

where:

e is the function of net normal stress and suction, $e = a + b\log(\frac{1+c(\sigma-u_a)+d(u_a-u_w)}{1+f(\sigma-u_a)+g(u_a-u_w)})$.

In UMAT, to update the stress, the Jacobian matrix of the constitutive model, $\frac{\partial\Delta\sigma}{\partial\Delta\varepsilon}$, should be defined. The Jacobian matrix is the function of elastic modulus, E. The Jacobian matrix can be given by Equation (4.68).

$$\frac{\partial\Delta\sigma}{\partial\Delta\varepsilon} = \frac{E(1-\mu)}{(1+\mu)(1-2\mu)} \begin{Bmatrix} 1 & \frac{\mu}{1-\mu} & \frac{\mu}{1-\mu} & 0 & 0 & 0 \\ & 1 & \frac{\mu}{1-\mu} & 0 & 0 & 0 \\ & & 1 & 0 & 0 & 0 \\ & & & \frac{1-2\mu}{2(1-\mu)} & 0 & 0 \\ & SYM & & & \frac{1-2\mu}{2(1-\mu)} & 0 \\ & & & & & \frac{1-2\mu}{2(1-\mu)} \end{Bmatrix} \tag{4.68}$$

The increment of strain is given by Abaqus and transferred into UMAT. The increment of stress is updated by the product of the Jacobian matrix and the increment of strain, as given by Equation (4.69).

$$\Delta\sigma = \frac{\partial \Delta\sigma}{\partial \Delta\varepsilon}\Delta\varepsilon \tag{4.69}$$

The stress at the end of this increment can be calculated by adding the increment in stress to the stress before this increment, as given by Equation (4.70).

$$\sigma_i = \sigma_{i-1} + \Delta\sigma_i \tag{4.70}$$

where:

σ_{i-1} is the stress before this increment,

$\Delta\sigma_i$ is the increment in stress in this increment,

σ_i is the stress after this increment.

As the increment in stress can induce the change in energy and temperature, the increment in stress calculated by UMAT is also transferred into UMATHT to calculate the heat conduction induced by the increment in stress. The flow chart of the UMAT is given in Figure 4.4.

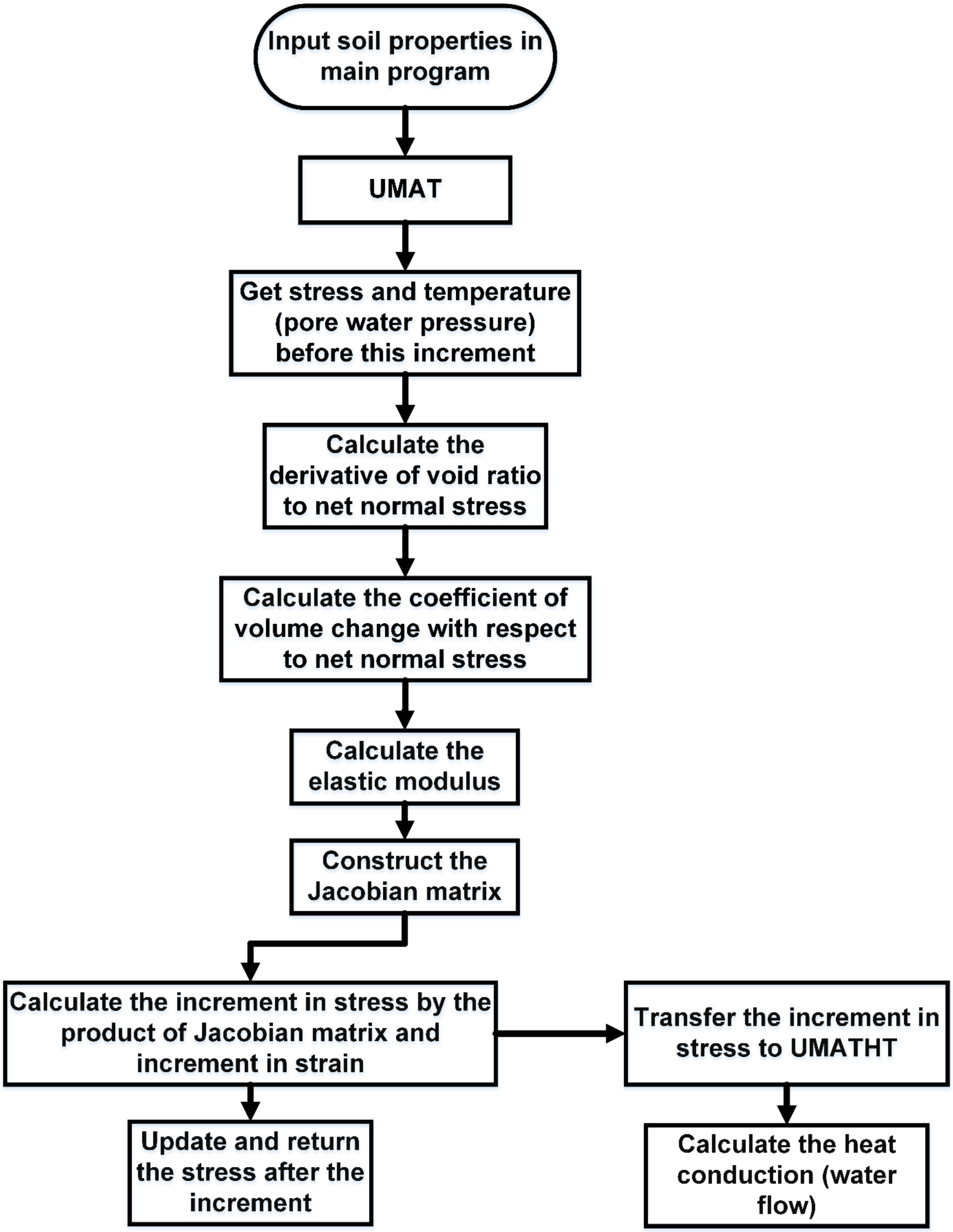

Figure 4.4 The flow chart of UMAT.

4.5.2.4 User-defined thermal expansion subroutine (UEXPAN)

UEXPAN is used to define the incremental thermal strains as the function of temperature. In this model, the expansion induced by the increment in temperature is assumed as isotropic. In other words, the expansion strains are the same in three directions. Therefore, the incremental thermal strains can be calculated by Equation (4.71).

$$d\varepsilon_T = \alpha dT \tag{4.71}$$

where:

dT is the change in the temperature,

α is the coefficient of heat expansion.

As mentioned above, the coefficient of heat expansion, α, is corresponding with the reciprocal of the elasticity modulus for the soil structure with respect to the suction, $\frac{1}{H}$. Therefore, the coefficient of heat expansion, α, can be determined by the elasticity modulus for the soil structure, H. For example, the coefficient of heat expansion for the soil under K_0 loading state can be given by Equation (4.72).

$$\alpha = -\frac{1}{H} = m_{1-2}^{s}\frac{\mu-1}{1+\mu} = \frac{\mu-1}{1+\mu}\frac{\partial\varepsilon_v}{\partial(u_a-u_w)} = \frac{\mu-1}{1+\mu}\frac{1}{1+e_0}\frac{\partial e}{\partial(u_a-u_w)} \tag{4.72}$$

where:

e is the function of net normal stress and suction, $e = a + b\log(\frac{1+c(\sigma-u_a)+d(u_a-u_w)}{1+f(\sigma-u_a)+g(u_a-u_w)})$.

Before UEXPAN is used, USDFLD is used to obtain the temperature before the increment and transfer the value of the temperature to UEXPAN. The flow chart of UEXPAN is given in Figure 4.5.

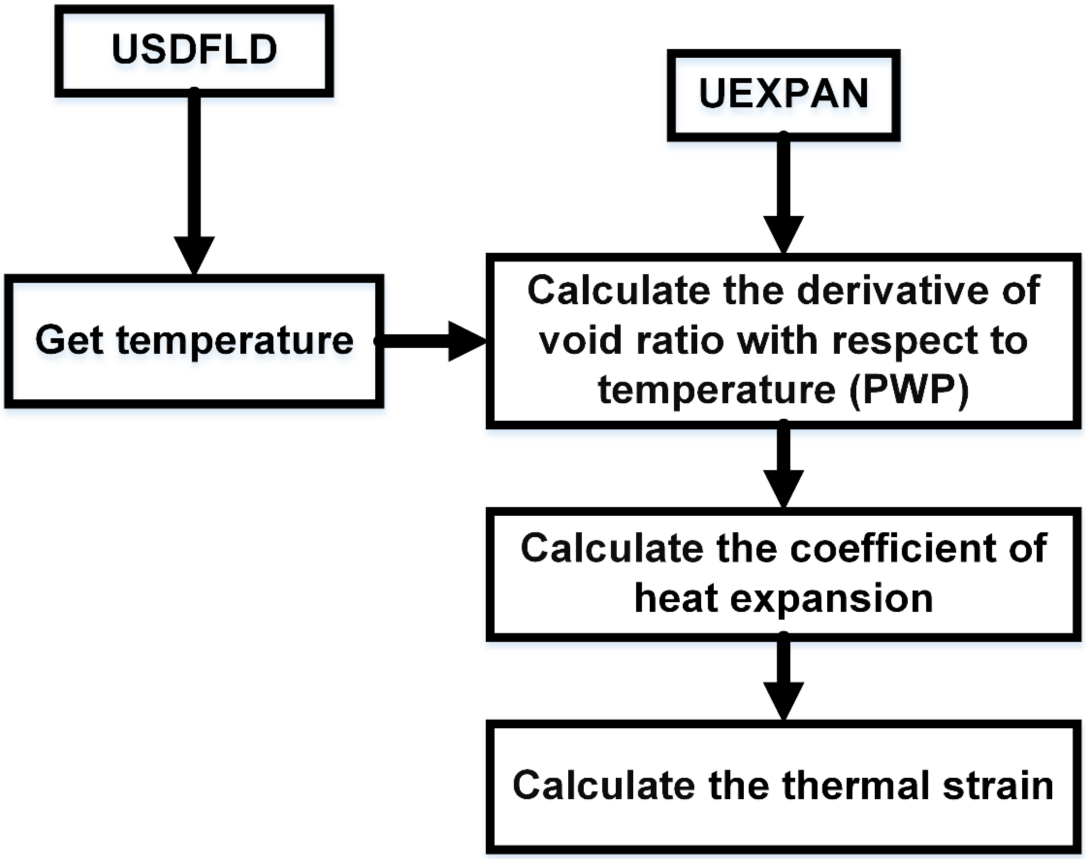

Figure 4.5 The flow chart of UEXPAN.

4.5.2.5 User-defined thermal material subroutine (UMATHT)

UMATHT can be used to define the thermal constitutive model of the material. In UMATHT, the internal energy per unit mass and the heat flux must be defined.

The first parameter that should be updated in UMATHT is the internal energy per unit mass, U. The internal energy per unit mass, U, can be defined by Equation (4.73).

$$U = \frac{E}{m} \tag{4.73}$$

where:

E is the internal energy in the material,

m is the mass of the material.

In the coupled thermo-mechanical problems for the soil, the soil is assumed as dry. Therefore, the mass of soil, m, is equal to the mass of soil particles, m_s. As discussed in Section 4.4, the internal energy, E, is corresponding to the mass of water of the unsaturated soil in the coupled hydro-mechanical problems. Therefore, the inter energy per unit mass, U, can be transferred to the gravimetric water content of the unsaturated soil, as given by Equation (4.74).

$$U = \frac{E}{m} = \frac{E}{m_s} \rightarrow \frac{m_w}{m_s} = w \tag{4.74}$$

In the coupled thermo-mechanical problems, the increment in the internal energy per unit mass can be induced by the increase in temperature and the variation of the stress, as given by Equation (4.75).

$$dU = \frac{\partial U}{\partial \sigma} d\sigma + \frac{\partial U}{\partial T} dT \tag{4.75}$$

As the internal energy per unit mass, U, is corresponding to the gravimetric water content, w and the temperature, T, is corresponding to the pore water pressure, u_w, the increment in the internal energy per unit mass, dU, can be calculated from the increment in the gravimetric water content, dw, as given by Equation (4.76).

$$dU = dw = \frac{\partial w}{\partial \sigma_y} \partial \sigma_y + \frac{\partial w}{\partial u_w} \partial u_w \tag{4.76}$$

where:

w is the function of net normal stress and suction, $w = a + b \log(\frac{1+c(\sigma-u_a)+d(u_a-u_w)}{1+f(\sigma-u_a)+g(u_a-u_w)})$.

The derivatives of gravimetric water content with respect to stress and pore water pressure can be calculated by differentiating the function for the constitutive surface of gravimetric water content. The increment in stress, $\partial \sigma_y$, is calculated and transferred from UMAT.

The second parameter that should be updated in UMATHT is the heat flux, q_{Ti}. The heat flux is calculated by the product of the thermal conductivity and the spatial gradients of temperature.

To simulate the influence of gravity on the water flow, the gravity is added to the spatial gradients of temperature in the vertical direction. The heat flux in three directions is given by Equation (4.77).

$$\begin{aligned} q_{Tx} &= -\lambda_x \frac{\partial}{\partial x} T \\ q_{Ty} &= -\lambda_y \left(\frac{\partial}{\partial y} T + 10\right) \\ q_{Tz} &= -\lambda_z \frac{\partial}{\partial z} T \end{aligned} \tag{4.77}$$

As discussed in Section 4.4, the thermal conductivity, λ_i, is corresponding to the new hydraulic conductivity, $K = \frac{k_i}{g}$. The hydraulic conductivity, k_i, can be calculated by Equation (3.55). As the hydraulic conductivity of the unsaturated expansive soil is affected by the void ratio, the total strain before the increment is obtained by USDFLD before UMATHT and is transferred into UMATHT. The flow chart of UMATHT is given in Figure 4.6.

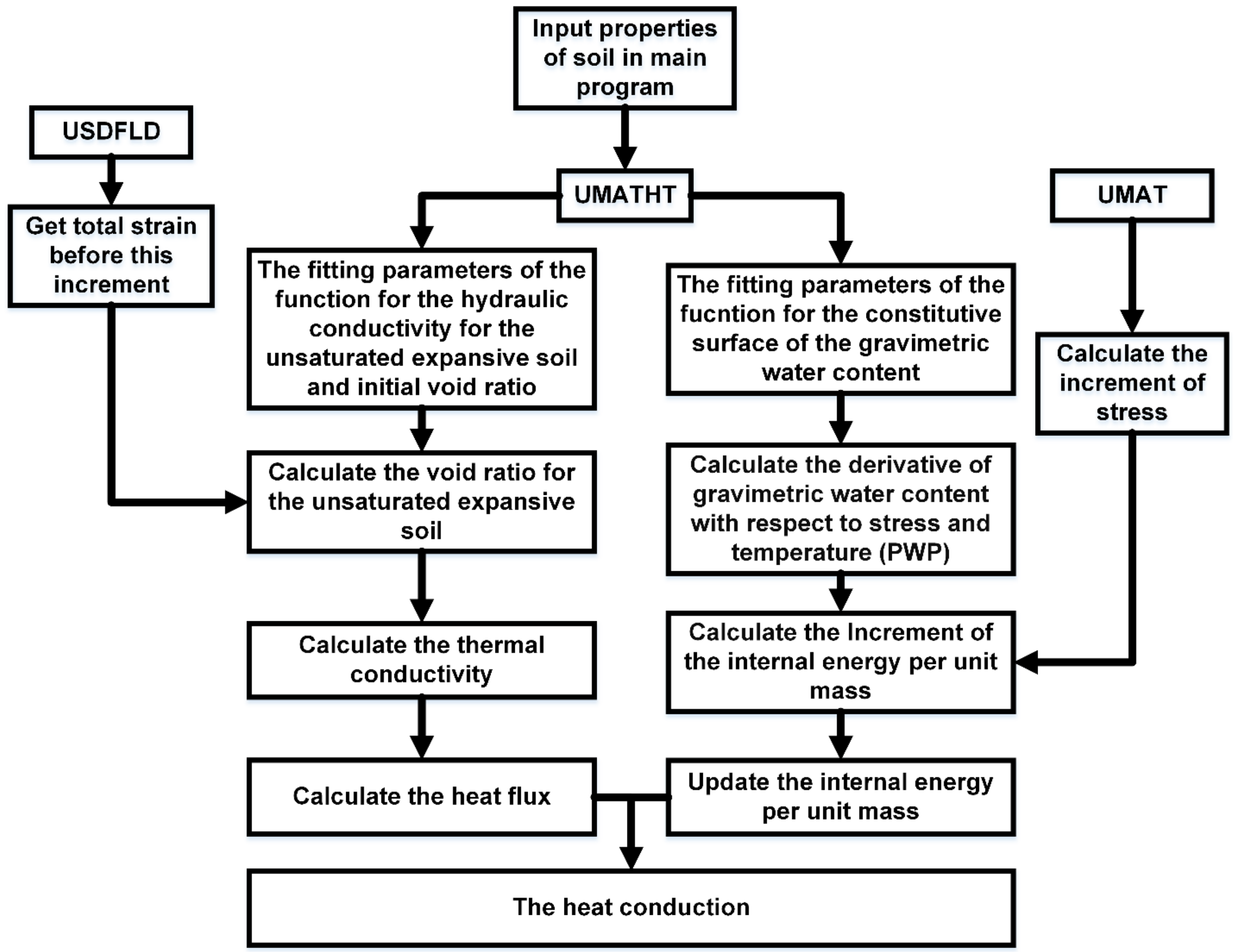

Figure 4.6 The flow chart of UMATHT.

4.5.2.6 User-defined friction behavior subroutine (FRIC)

FRIC is used to define the frictional behavior between contact surfaces. In FRIC, the friction stress between contact surfaces, τ, should be updated at the end of the increment.

In Abaqus, the increment in the friction stress can be calculated by the product of the derivative of the friction stress with respect to the relative motion, as given by Equation (4.78). The friction stress can be updated by Equation (4.79).

$$d\tau_i = \frac{d\tau}{dS} dS_i \tag{4.78}$$

$$\tau_i = \tau_{i-1} + d\tau_i \tag{4.79}$$

where:

dS_i is the relative motion in this increment,

τ_{i-1} is the friction stress before this increment,

$d\tau_i$ is the increment in the friction stress in this increment,

τ_i is the friction stress after this increment.

The hyperbolic soil-structure interface model is used to simulate the mechanical behavior of the pile-soil interface, as given by Equation (4.80) thru (4.83).

$$\tau_s(z) = \frac{S_s(z)(a+cS_s(z))}{(a+bS_s(z))^2} \tag{4.80}$$

$$\begin{cases} a = \frac{\beta_s - 1 + \sqrt{1-\beta_s}}{2\beta_s}\frac{S_{su}}{\tau_{su}} \\ b = \frac{1-\sqrt{1-\beta_s}}{2\beta_s}\frac{1}{\tau_{su}} \\ c = \frac{2-\beta_s-2\sqrt{1-\beta_s}}{4\beta_s}\frac{1}{\tau_{su}} \end{cases} \tag{4.81}$$

$$\beta_s = \frac{\tau_{sr}}{\tau_{su}} \tag{4.82}$$

$$\tau_{su} = c'_a + (\sigma_{nf} - u_a)\tan\ \delta' + (u_{af} - u_{wf})\tan\ \delta^b \tag{4.83}$$

where:

S is the relative motion,

τ is the friction stress,

τ_{su} is the peak friction stress,

S_{su} is the relative motion with respect to the peak stress,

τ_{sr} is the residual friction stress,

c'_a is the adhesion of the unsaturated soil-structure interface,

$\sigma_{nf} - u_{af}$ is the net normal stress of the unsaturated soil-structure interface,

δ' is the friction angle with respect to the net normal stress,

$u_{af} - u_{wf}$ is the suction of the unsaturated soil-structure interface,

δ^b is the friction angle with respect to suction.

The derivative of the friction stress with respect to the relative motion can be calculated by differentiating Equation (4.80), as given by Equation (4.84).

$$\frac{d\tau}{dS} = \frac{a(2cS_s(z) - bS_s(z) + a)}{(a + bS_s(z))^3} \tag{4.84}$$

The parameters for the pile-soil interface are inputted into the main program. The input parameters include the relative motion with respect to the peak stress, S_{su}, the adhesion of the unsaturated soil-structure interface, c'_a, the friction angle with respect to the net normal stress, δ', the friction angle with respect to suction, δ^b, and the ratio between the residual strength and the peak strength, β_s. The flow chart of FRIC is given in Figure 4.7.

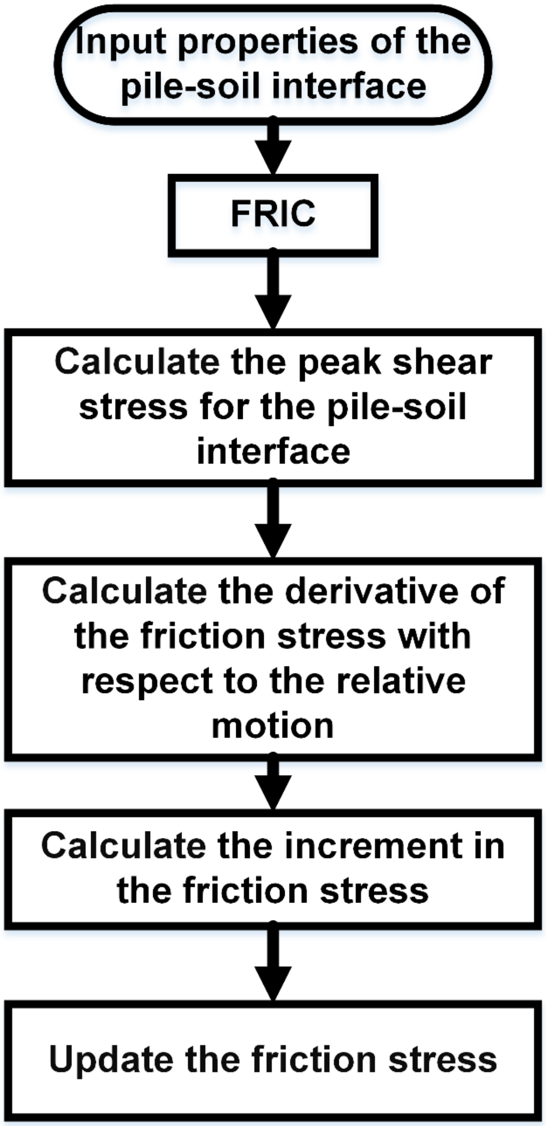

Figure 4.7 The flow chart of FRIC.

4.6 Summary and conclusion

In this chapter, the theoretical development of the subroutines is introduced.

The similarity between the coupled hydro-mechanical problems and the coupled thermo-mechanical problems is highlighted. The constitutive relations and the heat transfer law for the coupled thermo-mechanical problems are introduced in this chapter. The constitutive relations include the constitutive relation for the mechanical system and the internal energy. By comparing the equations for the coupled thermo-mechanical problems and the coupled hydro-mechanical problems, the similarity between these equations is explained. Due to the similarity, it is possible to transfer the parameters in the coupled hydro-mechanical problems to the parameters in the coupled thermo-mechanical problems. For example, the pore water pressure, u_w, in the coupled hydro-mechanical problems is corresponding to the temperature, T in the coupled thermo-mechanical problems.

The equations for the coupled hydro-mechanical problems are developed by employing the similarity between the equations for the coupled hydro-mechanical problems and the thermo-mechanical problems. Four subroutines including USDFLD, UMAT, UEXPAN, and UMATHT are developed. USDFLD processes access to material point data such as stress state, strain, and temperature. These data are transferred into other user-defined subroutines. UMAT is the user-defined subroutine to define a material's mechanical behavior. It can be used to define the mechanical constitutive relationship. UEXPAN is used to define the incremental thermal strains as the function of temperature. UMATHT can be used to define the thermal constitutive model of the material.

In addition, the constitutive model for the unsaturated pile-soil interface is also developed in this study. This is achieved by using a hyperbolic pile-soil interface that is developed and introduced into the subroutine FRIC. The subroutine, FRIC, is used the frictional behavior between pile and soil.

CHAPTER 5

MODELING THE EXPERIMENTAL STUDY RESULTS OF A SINGLE MODEL PILE IN UNSATURATED EXPANSIVE SOIL

5.1 Introduction

Liu (2019) conducted a comprehensive model pile test in expansive soil from Regina, Canada, in the Geotechnical laboratory at the University of Ottawa. The index, hydraulic and mechanical properties of Regina clay were measured. Some of the key properties measured include the saturated shear strength parameters, pile-soil interface strength at different net normal stress and suction, and the soil-water characteristic curve. The load versus deformation behavior of the model pile model was measured subjecting it to water infiltration. In this chapter, the pile model test is briefly introduced. The test results were simulated to verify the program developed in this study. The size of the model and mesh, boundary conditions, input parameters are introduced. There is a reasonably good comparison between the numerical simulation results and the experimental results obtained from the pile model test. The results illustrate that the developed program is effective to perform numerical simulations. The results clearly showed that the increase in the water content induced a decrease in shaft friction. The decrease in the shaft friction contributed pile to carry more load axially contributing to a pile head displacement.

5.2 Experimental study of a single pile in Regina clay

Liu (2019) conducted a model pile test to study the mechanical behavior of a single pile in unsaturated expansive soil during infiltration. Several tests, which include the soil properties tests, soil, and pile-soil interface shear strength test, and infiltration tests were conducted in this comprehensive experimental study.

5.2.1 The properties of Regina clay

The expansive soil used in the tests is collected from a site in Regina, Saskatchewan, Canada. The physical soil properties are determined by following different ASTM standards. The measured physical soil properties include liquid limit, plastic limit, specific gravity, optimum water content, the maximum dry unit weight, vertical swelling pressure, and the free swell index. The values of these soil properties are summarized in Table 5.1. The physical soil properties clearly show that Regina clay is highly expansive soil.

Table 5.1 The physical soil properties for Regina Clay (Liu 2019).

Liquid limit, LL (%)	89
Plastic limit, PL (%)	32
Plastic index, PI	57
Specific gravity, G_s	2.85
Maximum dry unit weight, $\gamma_{d,max}$ (kN/m^3)	13.82
Optimum water content, w (%)	29
Vertical swelling pressure under constant volume condition, (kPa)	136
Free swell index	100.6

The soil-water characteristic curve (SWCC) of Regina Clay is measured. Four methods including the chilled mirror hygrometer (WP4) method, pressure plate method, filter paper method, and desiccator method are employed for the measurement of the SWCC. The soil used in the measurement of SWCC was compacted at a gravimetric water content of 27% and a dry density of 1367kg/m^3. The large-scale model pile test was also conducted at the same gravimetric water content and the same dry density to achieve the same soil structure. Therefore, the measured SWCC can be used to explain the hydraulic behavior of Regina clay in the large-scale model pile tests. The measured SWCC is given in Figure 5.1.

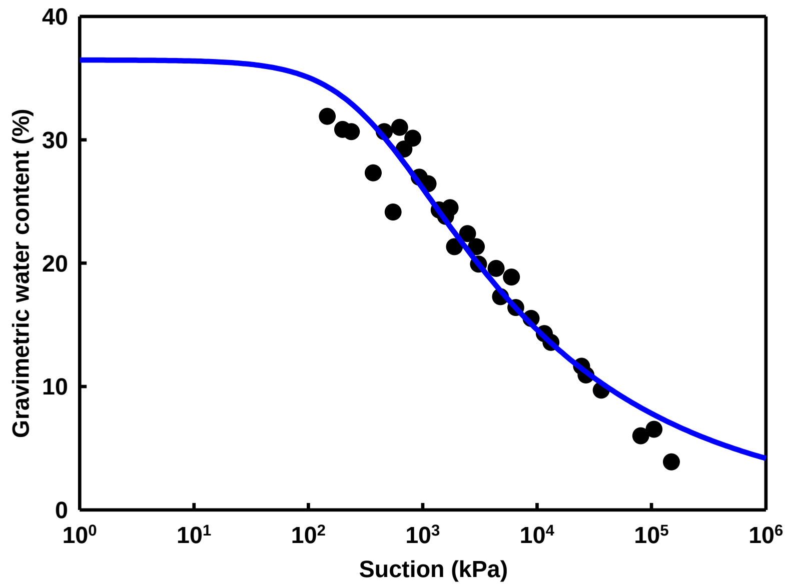

Figure 5.1 The measured SWCC (Liu 2019).

5.2.2 Direct shear test on soil and pile-soil interface

A series of direct shear tests were conducted on unsaturated soil specimens and on unsaturated pile-soil interface to study the shear strength of soil specimens and unsaturated pile-soil interface. The used soil specimens in the shear tests were compacted with different initial gravimetric water content values (i.e. 24%, 27%, 30%). The applied normal stresses in the direct shear tests are summarized in Table 5.2. The formats for the direct shear of soil specimens and pile-soil interface are given in Figure 5.2.

Table 5.2 The stress and initial conditions of direct shear tests (Liu 2019).

	Unsaturated soil specimens			**Saturated soil specimens**
Gravimetric water content	24%	27%	30%	
Dry density (kg/m^3)	1.37	1.37	1.37	1.37
Normal Stress (kPa)	50 100 150	50 100 150	50 100 150	50 100 150

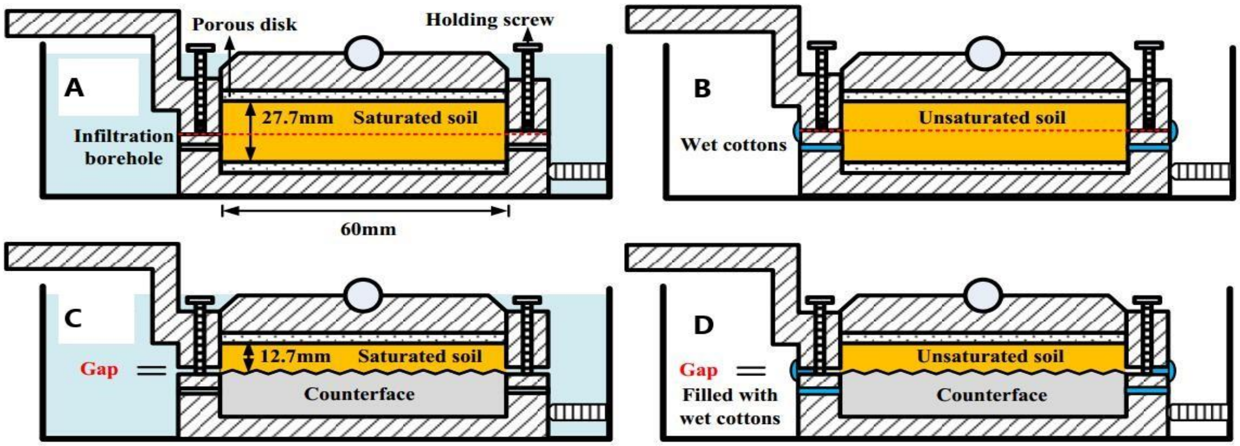

Figure 5.2 The formats of soil and pile-soil interface (A) direct shear test on saturated soil; (B) direct shear test on unsaturated soil; (C) direct shear test on saturated pile-soil interface; (D) direct shear test on unsaturated pile-soil interface (Liu 2019).

The results of the direct shear test on soil and pile-soil interface are given in Figure 5.3. The peak shear strength of saturated soil and saturated pile-soil interface can be formulated by Mohr-Coulomb failure criteria as given by Equation (5.1) and (5.2). Fredlund et al. (1978) proposed an equation for unsaturated soil considering suction as the second stress state variable, as given by Equation (5.3). Hamid and Miller (2009) modified Equation (5.3) to interpret the peak shear strength of the unsaturated pile-soil interface. The equation of the peak shear strength for the unsaturated pile-soil interface is given by Equation (3.58).

$$\tau_{ss} = c' + \sigma_{nf} \tan\ \phi' \tag{5.1}$$

$$\tau_{si} = c'_a + \sigma_{nf} \tan\ \delta' \tag{5.2}$$

where:

τ_{ss}, τ_{si} are the shear strength of the saturated soil and the saturated pile-soil interface, respectively,

c', c'_a are the cohesion of saturated soil and the adhesion of the saturated pile-soil interface, respectively,

σ_{nf} is the normal stress,

ϕ', δ' are the friction angle with respect to normal stress for the saturated soil and the saturated pile-soil interface, respectively.

$$\tau = c' + (\sigma_n - u_a)\tan\ \phi' + (u_a - u_w)\tan\ \phi^b \tag{5.3}$$

where:

τ is the shear strength of the unsaturated soil,

c' is the cohesion of the unsaturated soil,

$\sigma_n - u_a$ is the net normal stress,

$(u_a - u_w)$ is the suction,

ϕ', ϕ^b are the friction angle with respect to net normal stress and suction, respectively.

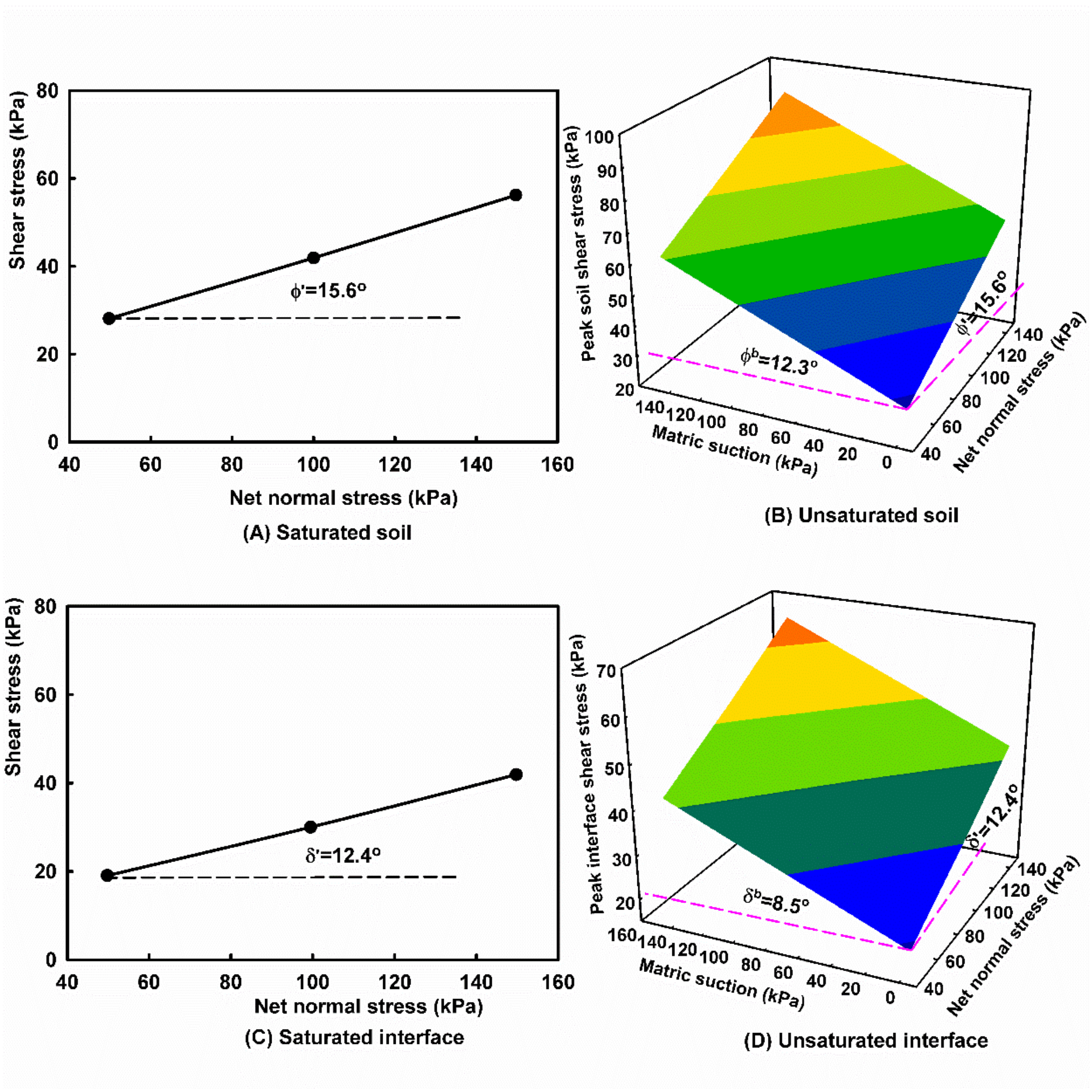

Figure 5.3 The direct shear test results (A) saturated soil; (B) unsaturated soil; (C) saturated pile-soil interface; (D) unsaturated pile-soil interface.

The parameters for the shear strength of soil and pile-soil interface are summarized in Table 5.3.

Table 5.3 The parameters for the shear strength of the unsaturated soil and the unsaturated pile-soil interface (Liu 2019).

Friction angle for the unsaturated soil with respect to net normal stress, ϕ'	15.6°
Friction angle for the unsaturated soil with respect to suction, ϕ^b	12.3°
Friction angle for the unsaturated pile-soil interface with respect to net normal stress, δ'	12.4°
Friction angle for the unsaturated pile-soil interface with respect to suction, δ^b	8.5°
Cohesion for the unsaturated soil, c', kPa	14
Adhesion for the unsaturated pile-soil interface, c_a', kPa	8

5.2.3 Model pile infiltration test

A model pile test was conducted to study the mechanical behavior of a single pile in unsaturated Regina expansive clay during infiltration. This experiment simulates the scenario that infiltration happens during the service stage of the single pile. The parameters required for the interpretation of the hydro-mechanical are collected during the test. In this section, the format of the test and the testing procedures are introduced.

Figure 5.4 shows the aluminum model pile used in the test. The height of the pile is 600mm. The outer diameter is 25.4mm and the wall thickness is 3mm. A rough surface is achieved on the pile shaft by pasting a thin layer of fine sand using epoxy. Five strain sensors were pasted inside to measure the strain of the single pile during the test. Two aluminum columns were used to block the hollow model at the pile top and bottom. Therefore, the pile was closed at the top and bottom. The infiltration test is conducted in a cylindrical aluminum tank. The height of the cylindrical aluminum tank is 700mm. The internal diameter is 300mm. The ratio of the diameter of the model pile and diameter of the tank is 12. The diameter can reduce the effect of the boundary conditions on the mechanical behavior of the single pile (Fan et al. 2007; Han et al. 2016).

The pile infiltration test is conducted by following four steps. The first step is to fix the model pile. The second step is to compact the soil to the predefined dry density. The third step is to apply the predefined vertical load to the model pile. The fourth step is to add the water into the soil manually to simulate the infiltration.

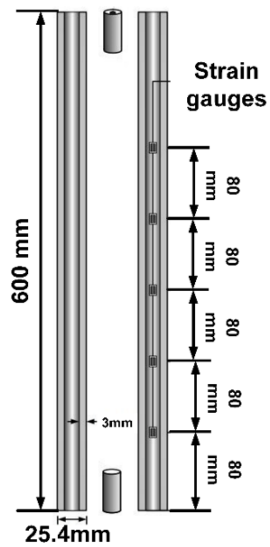

Figure 5.4 The size of the model pile (Liu 2019).

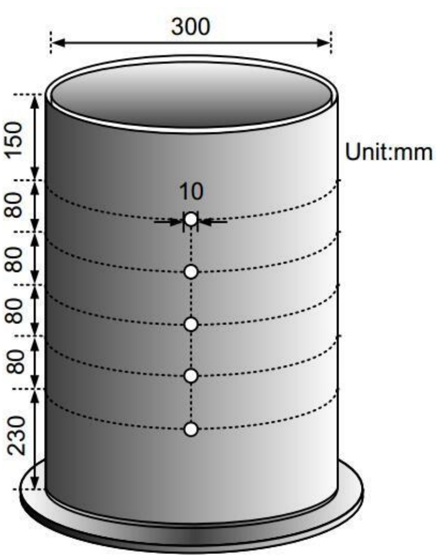

Figure 5.5 The size of the cylindrical aluminum tank (Liu 2019).

In the first step, the pile is fixed to the loading machine using a bolt to keep its position during the compaction process.

In the second step, sand was poured into the tank until a height of 150mm was achieved. A load cell was placed at the bottom of the model pile to measure the ending bearing resistance. After the installation, the expansive soil that was mixed at the gravimetric water content of 27% was divided into 20 layers to compact to reach the wet density of 1.736×10^3 kg/m^3 (dry density of 1.367×10^3 kg/m^3). The height of each layer is 20mm. Therefore, after compaction, the height of the expansive soil is 400mm. GS-3 water content sensors and MPS-6 suction sensors were buried in each layer to measure the variation in water content and suction of Regina clay during the test. The test setup is shown in Figure 5.6.

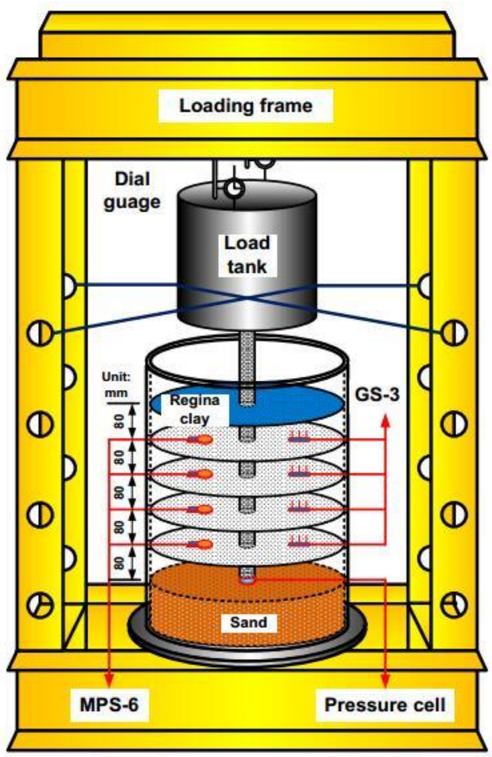

Figure 5.6 The test set up (Liu 2019).

In the third step, a total pile head load of 500N was applied to the model pile by the loading machine. The load of 500N was applied in three steps (150N, 150N, 200N). Initially, a load of 150N was applied to the head of the pile. The displacement of the pile was measured at hourly intervals. When the pile head displacement was observed to keep constant for 24 hours, the next load was applied to the pile head. The total pile head load of 500N was applied. The static loading process took 160 hours.

After a total pile head load of 500N was applied, the water was added manually to simulate the groundwater was always higher than the ground surface. The mechanical behavior of the single pile including the axis force distribution, the ending bearing resistance, the shaft friction, and the displacement of the pile head was detected during the test. The soil behaviors including the change in pore water pressure, and the displacement of the soil surface were monitored as well. The test was terminated when the displacement of the pile head was constant and all buried GS-3 water content sensors and MPS-6 suction sensors indicated that the soil has been fully saturated. The infiltration process took 240 hours.

5.3 Simulation of the behavior of a single model pile in Regina Clay upon infiltration

The large scale model pile infiltration test is stimulated by combing the ABAQUS/Standard and five user-defined subroutines. In this section, the size of the model and meshes, details of the soil parameters, pile, and pile-soil interface properties, boundary conditions, analysis steps, and the simulation results are discussed.

5.3.1 The size of the model and meshes

To increase the efficiency of the simulation, the size of the model pile infiltration test is simplified in the simulation.

As shown in Figure 5.4, the height of the model pile is 0.6m (600mm) and the diameter is 0.0254m (25.4mm). In the infiltration test, the height of 150mm (0.15m) fine sand was compacted at the bottom of the pile. The height of the compacted soil is 0.4m (400mm). The part of the pile above the surface of the expansive soil with a height of 0.2m (200mm) does not interact with the expansive soil. The function of this part of the pile is to transfer the pile head loading to the lower part. Liu (2019) measured the axial force distribution of the part of the model pile blow the surface of expansive soil. The surface of the expansive soil is set as the depth of 0 m. The distribution of the axial force after the loading process is shown in Figure 5.7. The results show that the axial force of the model pile at the depth of 0 m is 500N. The results illustrate that the total pile head load of 500N is transferred from the part of the pile above the surface of expansive soil to the part of the pile below the surface. Therefore, the part of the pile above the surface of the soil will not influence the mechanical behavior of the pile below the surface of the soil. Hence, part of the model pile above the surface of the expansive soil is ignored in the simulation. The height of the pile in simulation is 0.4m (400mm).

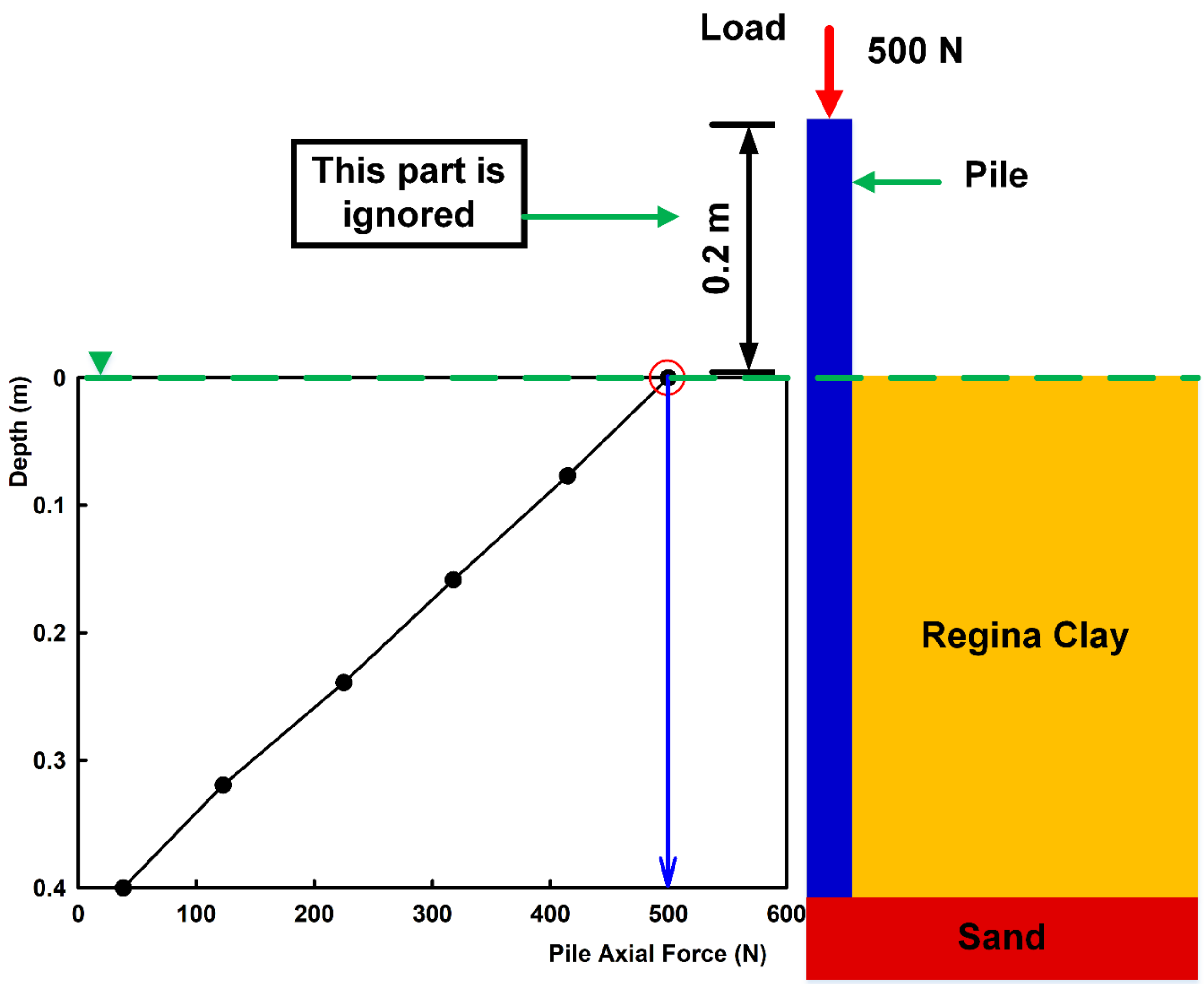

Figure 5.7 The distribution of the axial force after the loading process (modified from Liu 2019).

To reduce the simulation time and increase the efficiency of the simulation, the model should be simplified. One-fourth of the model pile is simulated in this simulation. The size of the model is plotted in Figure 5.8. As shown in Figure 5.8, the height of the pile is 0.4m. The radius of the pile is 0.0127m. The height of the expansive soil is 0.4m. The internal radius of the expansive soil is 0.0127m and the outer radius is 0.15m. The height of the sand is 0.15m and the radius is 0.15m. The size of the meshes is set as 0.06m. The pile and soil have the same size of meshes. The total number of meshes is 144. The mesh of the model is given in Figure 5.8.

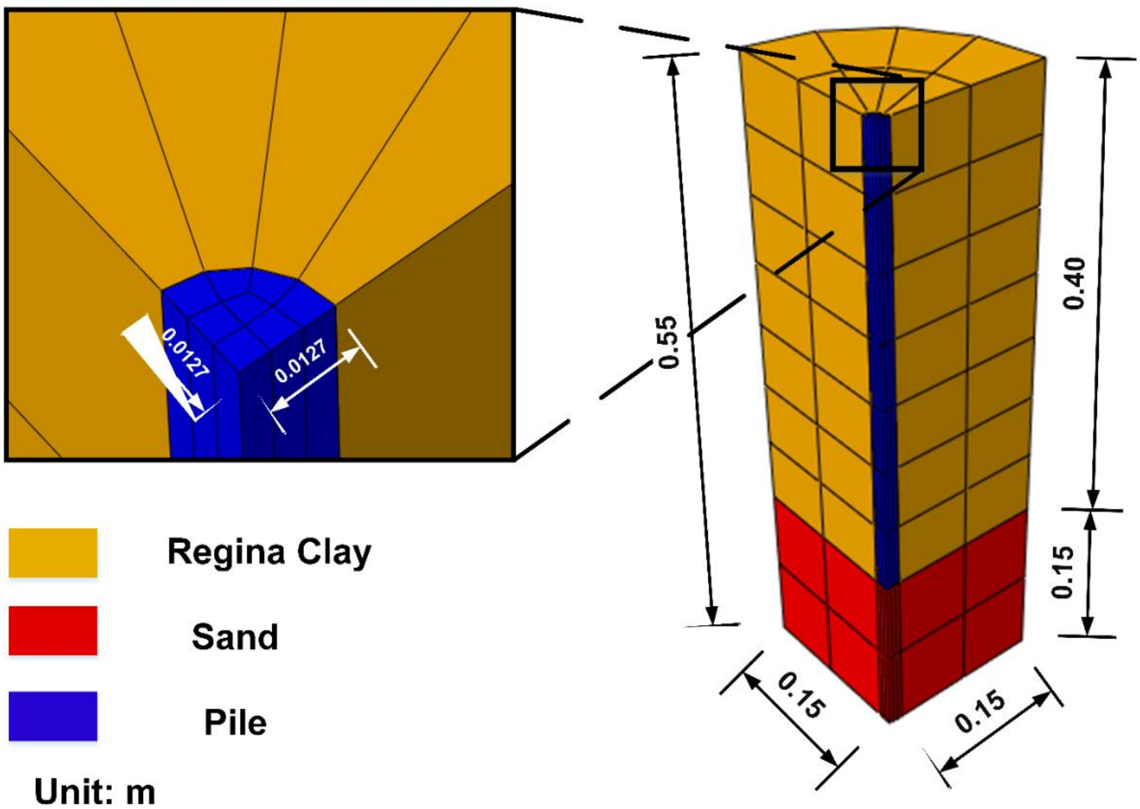

Figure 5.8 The size of the model and the distribution of the mesh.

5.3.2 Properties of the pile, soil, and pile-soil interface

To simulate the infiltration test, several input parameters which include soil, pile, and the pile-soil interface properties are required. Table 4.1 from the previous chapter, provides a summary of these properties.

In this simulation, the pile is assumed as the linear elastic material. The elastic modulus of the pile is 70GPa (Liu 2019). The Poisson's ratio is assumed as 0.3 (Curran 1963). The density of aluminum is 2.7×10^3kg/m^3. In the infiltration test, the model pile is hollow. In the simulation, however, the pile is solid. Therefore, the density of aluminum used in the simulation is modified to represent the model pile. The modification of the density of the pile is given in Equation (5.4). The input value of the density of the model pile is 1.125×10^{3}kg/m^3. The input values of the properties of the model pile in the simulation are summarized in Table 5.4.

$$\rho = \frac{m}{V} = \frac{2.7\times10^3\times\pi\times[0.0127^2-(0.0127-0.003)^2]\times0.6}{\pi\times0.0127^2\times0.6} kg/m^3 = 1.125\times10^3 kg/m^3 \quad (5.4)$$

where:

m is the mass of the pile,

V is the volume of the pile.

Table 5.4 The values of the properties of the model pile used in the simulation.

Parameters	Values	Reference
Elastic modulus, E(kPa)	7×10^7	Liu 2019
Poisson's ratio, μ	0.3	Curran 1963
Density (kg/m^3)	1.125×10^3	

Regina clay used in the pile infiltration test was compacted at the initial water content of 27% and reached the wetting density of 1.736×10^3 kg/m^3 (dry density of 1.367×10^3 kg/m^3). The specific gravity, G_s, is set as 2.85. Therefore, the initial void ratio can be calculated from the dry density and the specific gravity, as given by Equation (5.5). The value of the initial void ratio is 1.0849. The Poisson's ratio of Regina clay is 0.3 (Liu 2019). Poisson's ratio is assumed as constant in this model. In other words, Poisson's ratio will not vary with suction. Oh and Vanapalli (2016) studied the influence of Poisson's ratio on the stress vs. settlement behavior of shallow foundations in unsaturated fine-grained soil. Their results illustrated that the stress at the same settlement will increase with an increase in the Poisson's ratio. However, the increase in stress induced by Poisson's ratio was less than the increase induced by suction. Therefore, Poisson's ratio was assumed as a constant.

$$e_0 = G_s\frac{\rho_w}{\rho_d} - 1 = 2.85\times\frac{1000}{1367} - 1 = 1.0849 \quad (5.5)$$

where:

e_0 is the initial void ratio of the soil,

G_s is the specific gravity of the soil,

ρ_w is the density of free water (kg/m^3),

ρ_d is the dry density of the soil (kg/m^3).

To determine the elastic parameters used in the constitutive relation for the unsaturated expansive soils, the constitutive surfaces for the soil structure (void ratio) and water phase (water content) for Regina expansive soil should be determined. The soil structure constitutive surface can be constructed from the measured void ratio values at various suctions and applied net normal stress. Likewise, the constitutive surface for the water phase can be given by measuring the water content at the different suction and applied loads. These values were determined using a one-dimensional swelling test and a series of constant suction consolidation test. The soil was allowed to swell from the initial state and then it was consolidated at a constant value of suction. The void ratio and water content changes were measured at various equilibrium state. The stress paths followed in these tests are presented in Figure 5.9 (Vu 2003). Shuai (1996) measured the void ratio and water content surface of Regina clay under the K_0-loading state by conducting the constant suction consolidation. In the K_0-loading state, the soil is allowed to swell in one-dimension. In the numerical modeling, the expansive soil surrounding the pile was allowed to move in one direction (i.e. $z-$direction) and the displacement in the other two dimensions (i.e. $x-$direction and $y-$directiono) was constrained, which is similar to the volume change behavior of the soil in the K_0-loading state. Therefore, the soil in numerical modeling was assumed at K_0-loading state. Hence, the void ratio and water content surface measured under the K_0-loading state were used in the simulation to simulate the pile infiltration test. The measured surfaces for the void ratio and gravimetric water content are shown in Figure 5.10 and Figure 5.11.

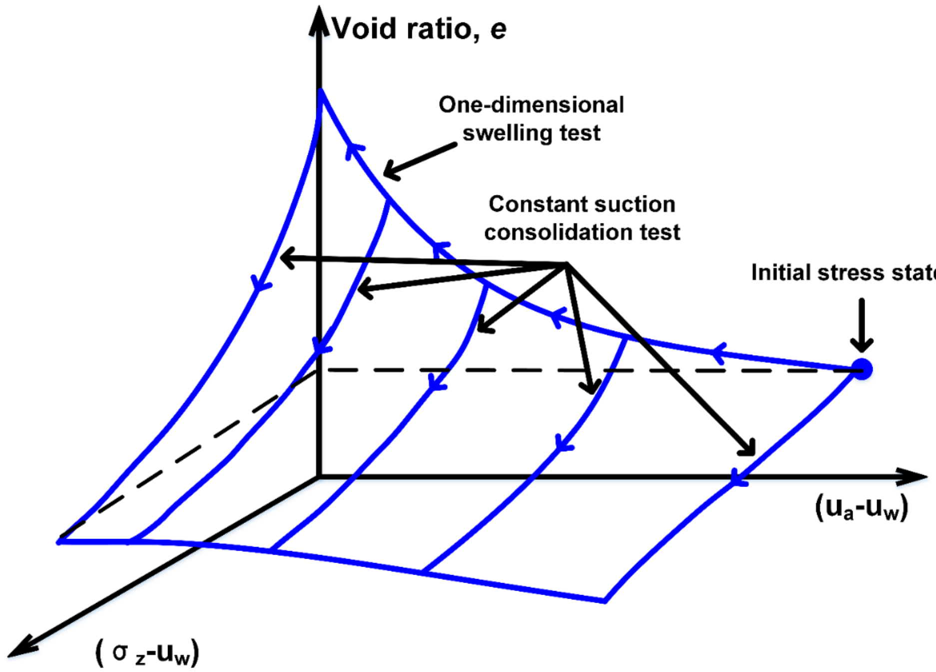

Figure 5.9 The stress path followed in the constant suction consolidation test (Modified from Vu 2003).

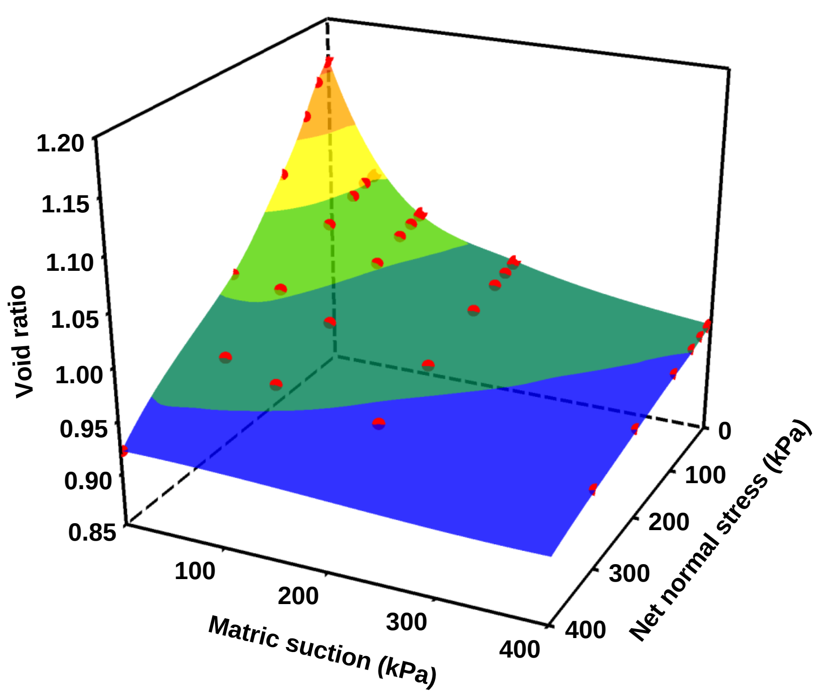

Figure 5.10 The measured constitutive surface for the void ratio of Regina clay under the K_0-loading state (from Shuai 1996).

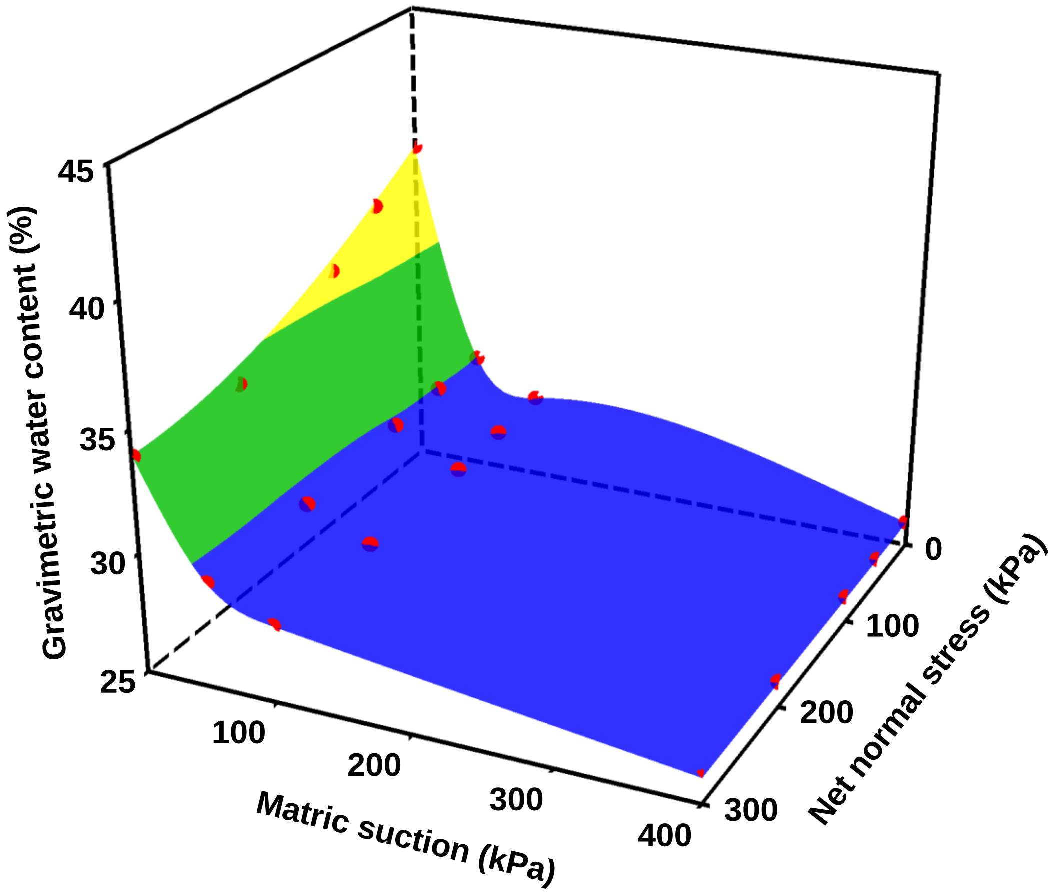

Figure 5.11 The measured constitutive surface for the gravimetric water content of Regina clay under the K_0-loading state (from Shuai 1996).

Vu (2003) proposed an equation with six fitting parameters to fit the surfaces, as given by Equation (5.6). The best-fitting parameters corresponding with Figure 5.10 and 5.11 are summarized in Table 5.5.

$$f(\sigma - u_a, u_a - u_w) = a + b\log\left(\frac{1 + c(\sigma - u_a) + d(u_a - u_w)}{1 + f(\sigma - u_a) + g(u_a - u_w)}\right) \qquad (5.6)$$

where:

f is the volume-mass properties of the unsaturated soil (i.e. void ratio, gravimetric water content, volumetric water content, degree of saturation),

a, b, c, d, f, g are the fitting parameters.

Table 5.5 Fitting parameter values for the constitutive surfaces of Regina clay (Vu 2003).

Surface	Fitting parameters						Figure
	a	***B***	***c***	***d***	***f***	***g***	
Void ratio	1.1828	-0.2832	0.0147	0.0454	0	0.00534	5.9
Gravimetric water content	0.4195	-0.1205	0.0129	0.2495	0.0000683	0.0102	5.10

The elastic modulus with respect to net normal stress, E, and the elastic modulus with respect to suction, H can be calculated by differential the fitting equation for the void ratio surface. The values of E and H are plotted in Figure 5.12 and 5.13.

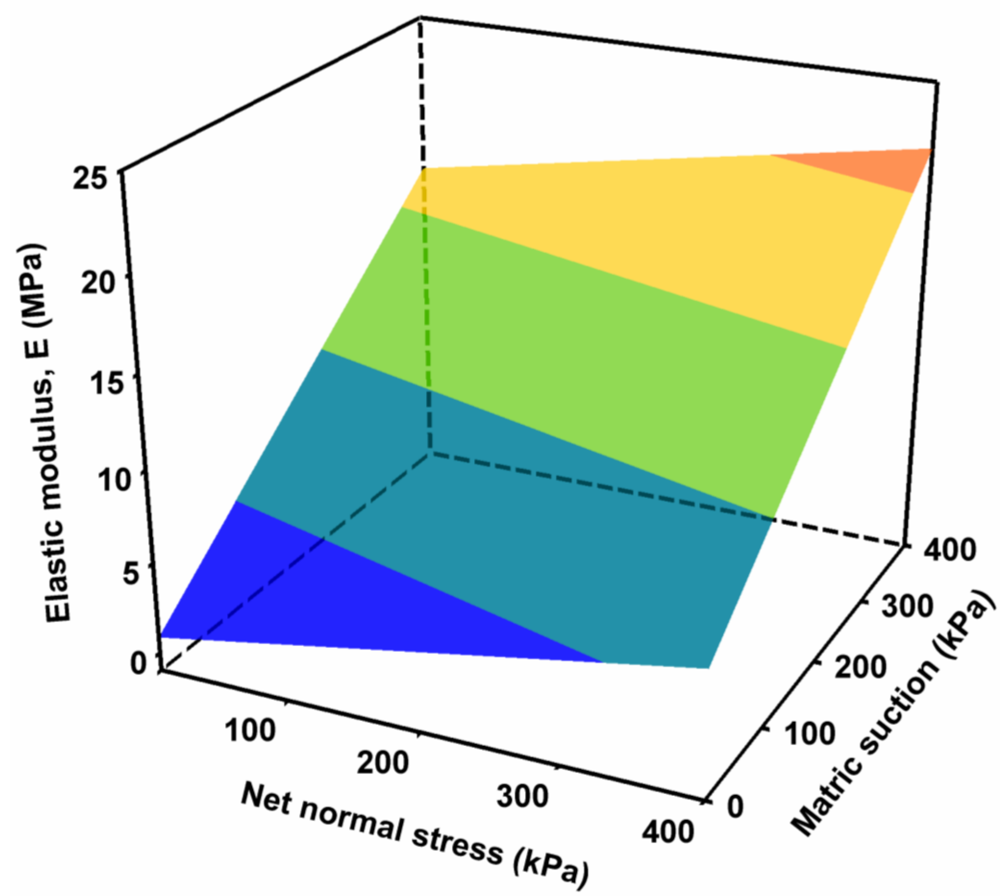

Figure 5.12 The elastic modulus with respect to net normal stress, *E*, used in the simulation.

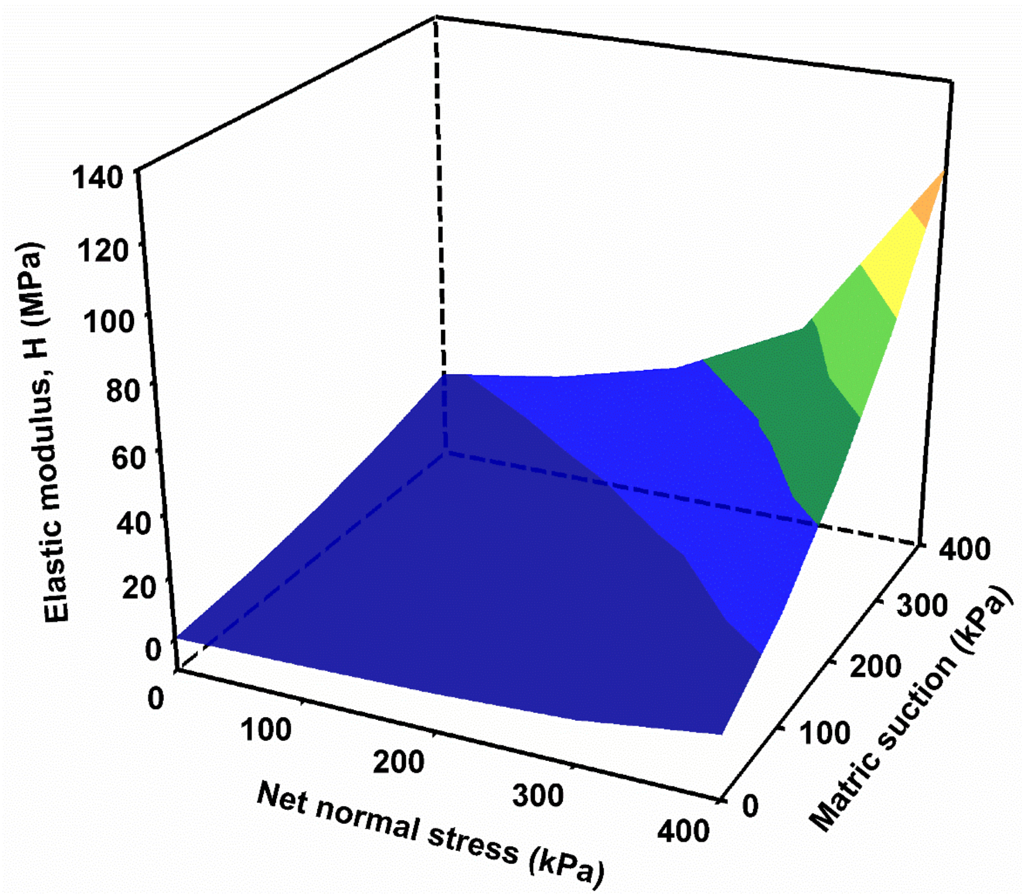

Figure 5.13 The elastic modulus with respect to suction, *H*, used in the simulation.

The derivatives of gravimetric water content with respect to stress and suction, $\frac{\partial w}{\partial(\sigma_{\text{mean}}-u_a)}$, and $\frac{\partial w}{\partial(u_{\text{a}}-u_w)}$, can be calculated by differentiating the function for the constitutive surface of gravimetric water content. The derivatives of gravimetric water content are plotted in Figure 5.14 and 5.15.

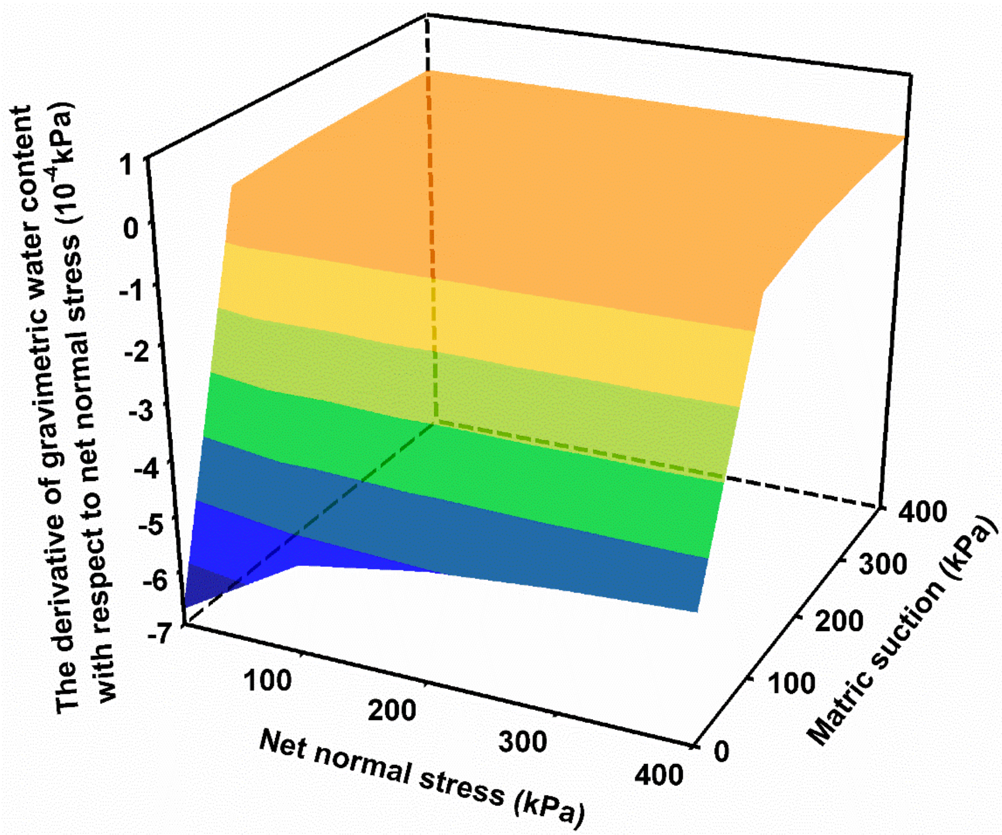

Figure 5.14 The surface of the derivative of gravimetric water content with respect to net normal stress, $\frac{\partial w}{\partial(\sigma_{\text{mean}}-u_a)}$.

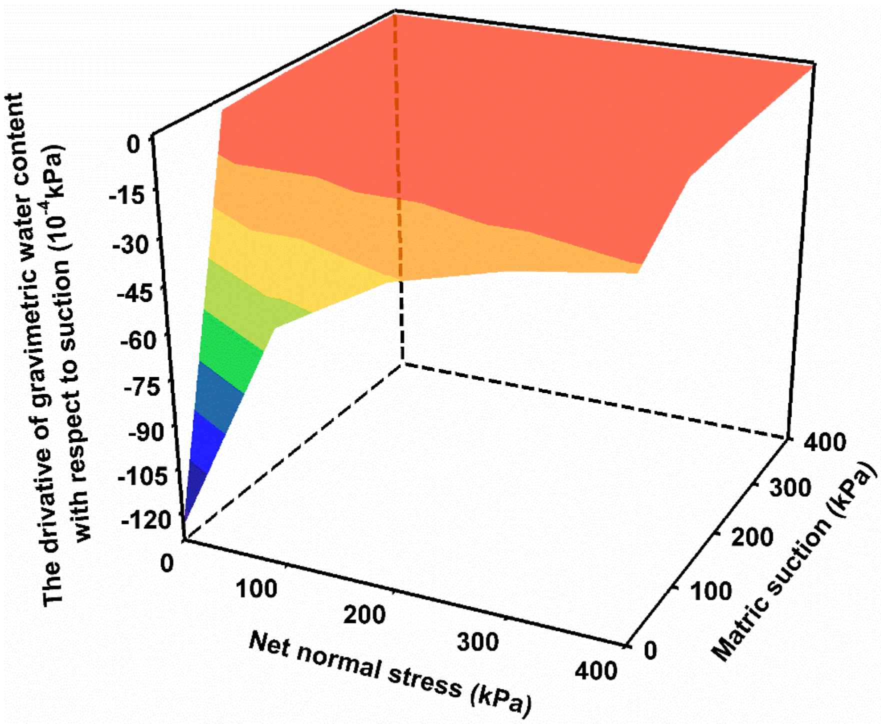

Figure 5.15 The surface of the derivative of gravimetric water content with respect to suction, $\frac{\partial w}{\partial(u_a - u_w)}$.

Shuai (1996) presented the function for the hydraulic conductivity of Regina clay as Equation (5.7). For Regina clay, the saturated hydraulic conductivity, k_{w0} for the void ratio value equal to 1 is 4×10^{-9}m/s. The values of the fitting parameter, A, B, N, are 0.01, 18.5, and 1.1, respectively (Shuai 1996).

$$k_w = \frac{k_{w0}e^B}{1 + A[\frac{(u_a - u_w)}{\rho_w g}]^N} \tag{5.7}$$

where:

k_{w0} is the hydraulic conductivity of the unsaturated soil when the void ratio is equal to 1,

A, B, N are the fitting parameters.

The values of parameters for the constitutive relation of Regina clay are summarized in Table 5.6.

Table 5.6 The values of the properties of the Regina clay used in the simulation.

	Parameters	Values	Reference
Physical properties	Specific gravity, G_s	2.85	Liu 2019
	Initial void ratio, e_0	1.0849	
	Dry density, ρ_d (kg/m^3)	1367	
	Poisson's ratio, μ	0.3	
Void ratio	Fitting parameter, b	-0.2832	Vu 2003
	Fitting parameter, c	0.0147	
	Fitting parameter, d	0.0454	
	Fitting parameter, f	0	
	Fitting parameter, g	0.00534	
Water content	Fitting parameter, b	-0.1205	Vu 2003
	Fitting parameter, c	0.0129	
	Fitting parameter, d	0.2495	
	Fitting parameter, f	0.0000683	
	Fitting parameter, g	0.0102	
Hydraulic conductivity	The saturated hydraulic conductivity, k_{w0} (m/s)	4×10^{-9}	Shuai 1996
	Fitting parameter, A	0.01	
	Fitting parameter, B	18.5	
	Fitting parameter, N	1.1	

The fine sand below the pile and the expansive soil is assumed linear elastic. The elastic modulus is 1000 kPa and Poisson's ratio is set as 0.3 (Liu 2019). To prevent the water flow between the expansive soil and fine sand, the hydraulic conductivity of sand is inputted as 0.

The constitutive relation of the pile-soil interface is formulated by the equation proposed by (Zhang and Zhang 2012). The peak shear strength parameters of the pile-soil interface are measured by (Liu 2019). The input values of the parameters for the pile-soil interface are summarized in Table 5.7.

Table 5.7 The values of the properties of the unsaturated pile-soil interface used in the simulation.

	Parameters	Values	Reference
The peak shear strength	Friction angle for unsaturated pile-soil interface with respect to net normal stress, δ'	12.4^{o}	Liu 2019
	Friction angle for unsaturated pile-soil interface with respect to suction, δ^b	8.5^{o}	
	Adhesion for the unsaturated pile-soil interface, c_a'	8 kPa	
The softening curve	The relative displacement with respect to the peak shear strength, S_{su}	1mm	Zhang and Zhang 2012
	The ratio between the residual shear strength and peak shear strength, β_s	0.85	

5.3.3 Boundary conditions and analysis steps

Boundary conditions including the displacement boundary conditions and the thermal boundary conditions are applied to the model. After the boundary conditions are applied, three analysis steps are set to simulate the pile infiltration test. The first step is the Geostatic step. The Geostatic step is used to simulate the initial stress state of the pile and soil. The second step is the static loading step. The static loading step is used to simulate the static loading process. The third step is the coupled thermo-mechanical analysis step. This step is used to simulate the infiltration process.

The boundary conditions including the displacement boundary conditions and the thermal boundary conditions (i.e. temperature (pore water pressure) boundary condition and heat flux (water flux) boundary condition) should be applied to the model for obtaining numerical simulation results. There is no displacement is allowed at the bottom of the model. Therefore, the displacement of the bottom surface of the model is restricted in $x-$, $y-$, and $z-$ direction. Only the vertical displacement can occur at the side surfaces in the pile model test. Therefore, in the simulation, the vertical displacement ($y-$direction) is allowed and the displacement in the other two directions ($x-$, and $z-$ direction) are not allowed at the side surface. For the pile, the vertical displacement is allowed and the displacements in other directions are restricted.

The expansive soil compacted at a gravimetric water content of 27% has a bulk density of 1.736×10^3 kg/m^3 (dry density of 1.367×10^3 kg/m^3). Liu (2019) measured the soil-water characteristic curve (SWCC) of Regina clay in an identical state. The suction of Regina clay can be determined from SWCC. As given in Figure 5.1, the value of suction is 1000 kPa when the gravimetric water content is 27%. During the pile model test, the pore water pressure at different depths (8cm, 16cm, 24cm, and 32cm) is measured, as given in Figure 5.16. The results showed that the initial pore water pressure is -1000 kPa and the distribution of the initial pore water pressure can be assumed uniform in Regina clay. Therefore, the initial suction of Regina clay is assumed as 1000kPa. As given in Table 4.1, the pore water pressure is corresponding to the temperature. Therefore, the initial temperature in Regina clay in the simulation is set as -1000K. The sand used in the large scale model test is dry (Liu 2019). The suction of the sand is assumed as 1000kPa. There are two reasons for this value. The first one is the hydraulic properties of sand. The SWCC of soil is typically divided into three zones, boundary zone, transition zone, and residual zone. Typically, the gravimetric water content is relatively small in the residual zone. The residual zone is at the relatively low suction for sands (i.e. generally between 0 and 200kPa suction range) (Vanapalli et al. 1996). Therefore, the sand with the suction of 1000kPa can be considered at the residual state and the sand has low water content. Hence, the suction of 1000kPa is chosen to represent the dry state of the sand. The second reason for the assumption of the suction of 1000kPa is to reduce the effect of the sand on Regina clay. The suction of 1000kPa is the same as the initial suction of Regina clay. The same suction between the sand and Regina clay can reduce the seepage between these two layers, which can reduce the effect of the sand on the hydraulic behavior of Regina clay. Therefore, the initial suction of sand is assumed as 1000kPa and accordingly the initial temperature of sand is set as -1000K in the simulation.

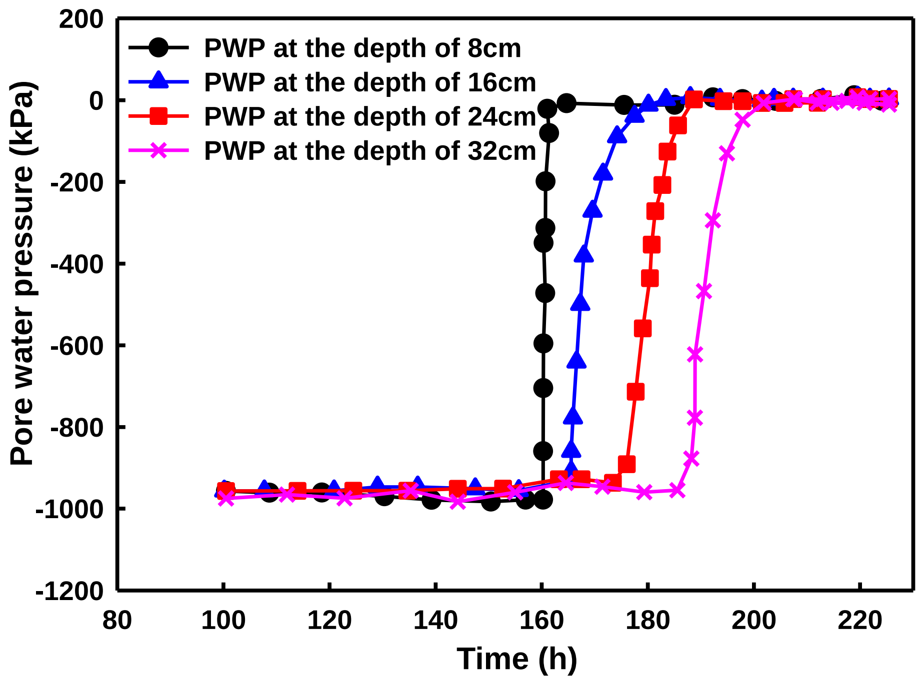

Figure 5.16 The variations of the pore water pressure at different depths (Liu 2019).

All of the surfaces except the top surface of Regina clay in the model are assumed as the no-flow boundary. The heat flux is applied on the top surface of Regina clay in the coupled thermo-mechanical analysis.

After applying the boundary conditions, three analysis steps including the Geostatic step, static loading step, and the coupled thermo-mechanical analysis step are set to simulate the behavior of the pile in unsaturated expansive soil. The first step is to use the Geostatic step to simulate the initial stress state. The expansive soil is compacted before the loading process and the infiltration process in this model pile test. Therefore, an initial stress state was induced by the compaction in the expansive soil. To reproduce the initial stress state, the Geostatic step is used (Said et al. 2009). The gravitational acceleration of $0.01 m/s^2$ is applied to the pile, expansive soil, and sand. The stress that was induced by gravity was calculated by the step of geostatic. The stress obtained in the Geostatic step was inputted as the initial stress state of the following steps (i.e. the static loading process and the infiltration process).

The second step is the static loading step. The total load of 0.5kN (500N) was applied in the model pile test. However, as one-fourth of the model is simulated, one-fourth of the load (0.125kN) is applied to the pile head in the simulation. The applied load in the first two steps is 0.0375kN. The load of 0.05kN is applied in the third step. In the pile model test, the next load was applied to the pile when the displacement was observed to be constant for 24 hours. However, the exact time for each load was not given. Therefore, the assumption of time is made on each step. The time of the first two steps is assumed as 172,800s (48 hours). The time of the third step is assumed as 230,400s (64 hours). The total time of three steps is 576,000s (160 hours), which coincides with the time of the loading process in the pile model test.

The third step involves coupled thermo-mechanical analysis. A heat flux is applied to the top surface of expansive soil in this step. The water flux of 2×10^{-8} m/s is typically used to simulate the infiltration in Regina clay (Adem and Vanapalli 2013; Qi and Vanapalli 2015; Vu 2003). As given in Table 4.1, the new water flux, $\rho_w q_{wi}$, is corresponding to the heat flux, q_{Ti}. Therefore, the water flux of 2×10^{-8} m/s is changed to 2×10^{-5} m/s by multiplying the density of water 1000 kg/m^3. Therefore, the heat flux of 2×10^{-5} J/(m^2×s) is used as the value of the input parameter. The infiltration test takes 240h in the pile model test (Liu 2019). The expansive soil reached the saturated state when the time of the infiltration test was 40 hours. The results of the pile model test show that the displacement of pile and soil surface and the mechanical behavior of the pile did not change. The time of the infiltration process set in the simulation should be long enough to simulate the time of the 40 hours of the infiltration test in the model pile test. Therefore, the time of the infiltration process is set as 50 hours (180,000s) in the simulation.

5.3.4 Simulation results

The hydro-mechanical behaviors of the expansive soil including the variation of pore water pressure and variation of the displacement of the expansive soil surface are obtained by the simulation. The mechanical behaviors of pile such as the distribution of the shaft friction, the distribution of the ending bearing resistance, and the distribution of the axial force are obtained.

The results are compared with the results obtained from the large-scale model test. The results obtained by simulation are compared with the experimental results.

The variations of the pore water pressure at different depths are simulated by numerical modeling. The pore-water pressures at the depth of 80 mm, 160 mm, 240 mm, and 300 mm are obtained and compared with the experimental results. The comparisons are plotted in Figure 5.17-5.20.

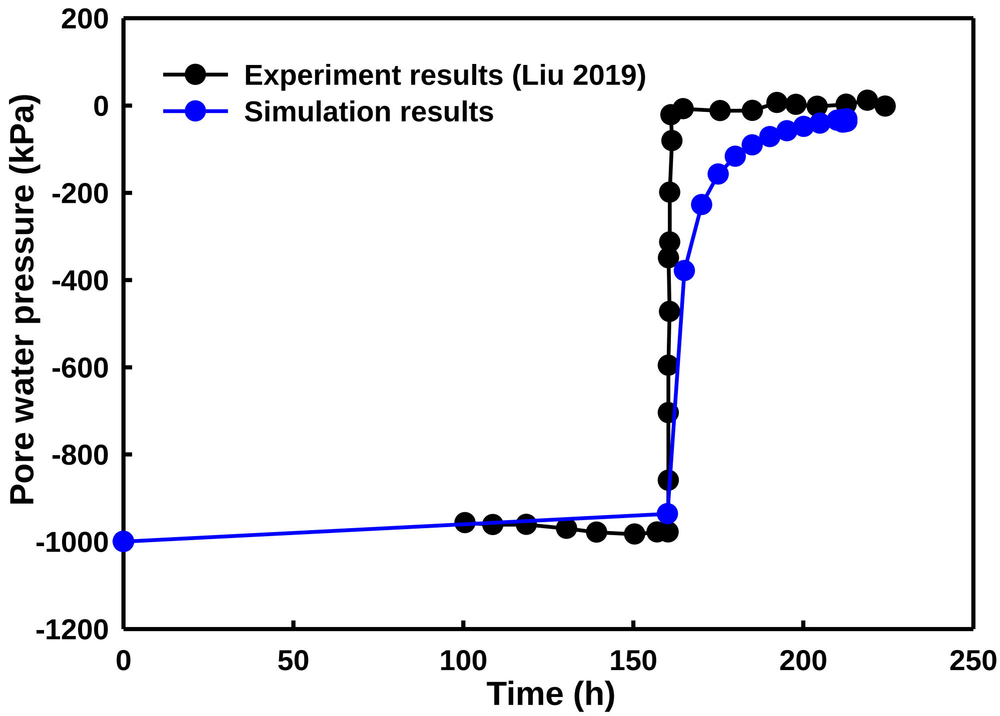

Figure 5.17 The comparison of the variation of the pore water pressure at the depth of 80 mm.

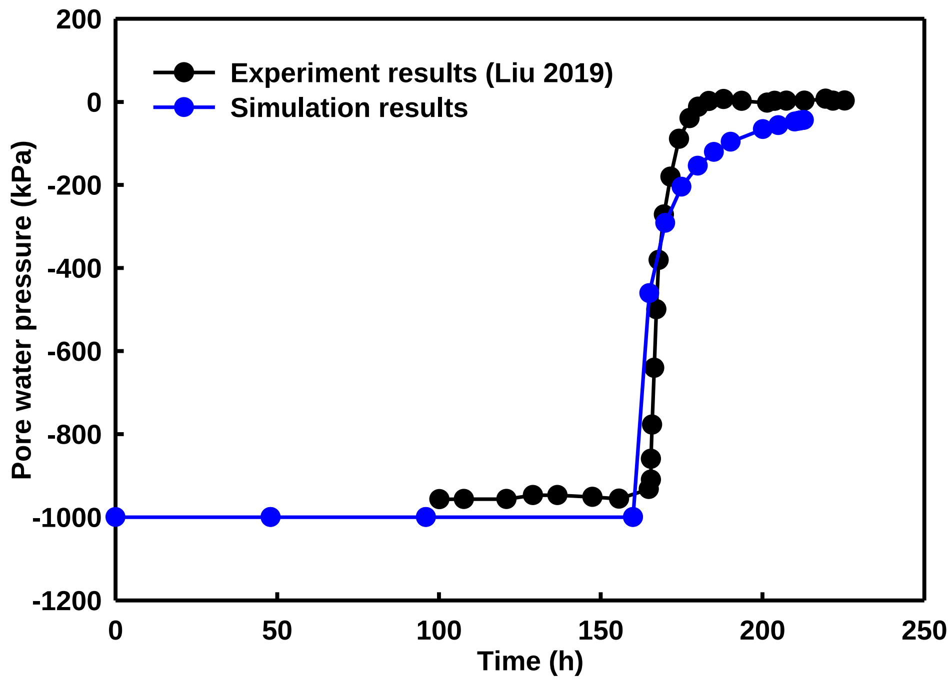

Figure 5.18 The comparison of the variation of the pore water pressure at the depth of 160 mm.

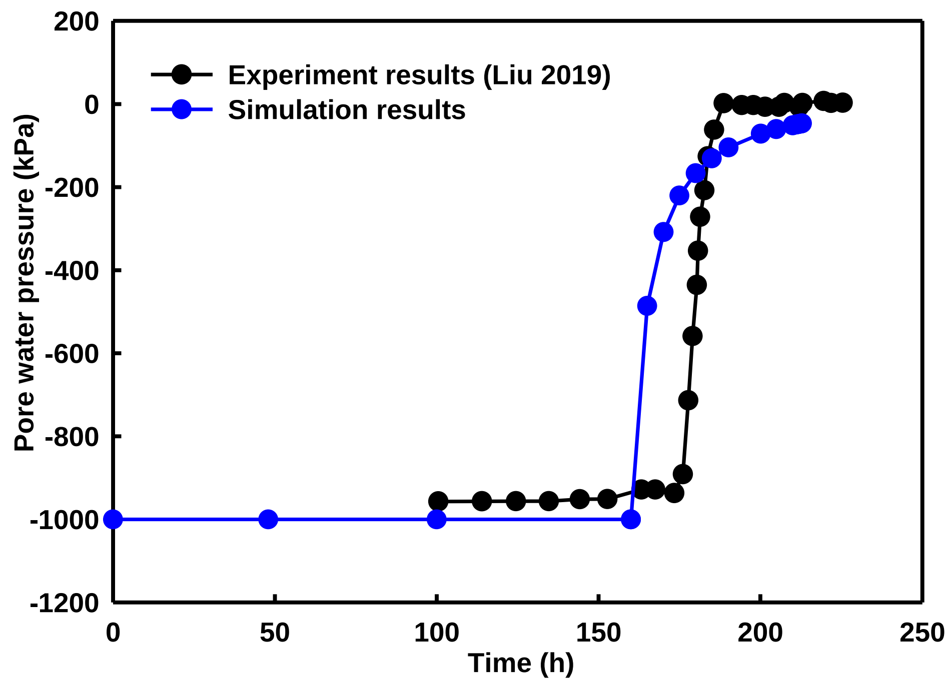

Figure 5.19 The comparison of the variation of the pore water pressure at the depth of 240 mm.

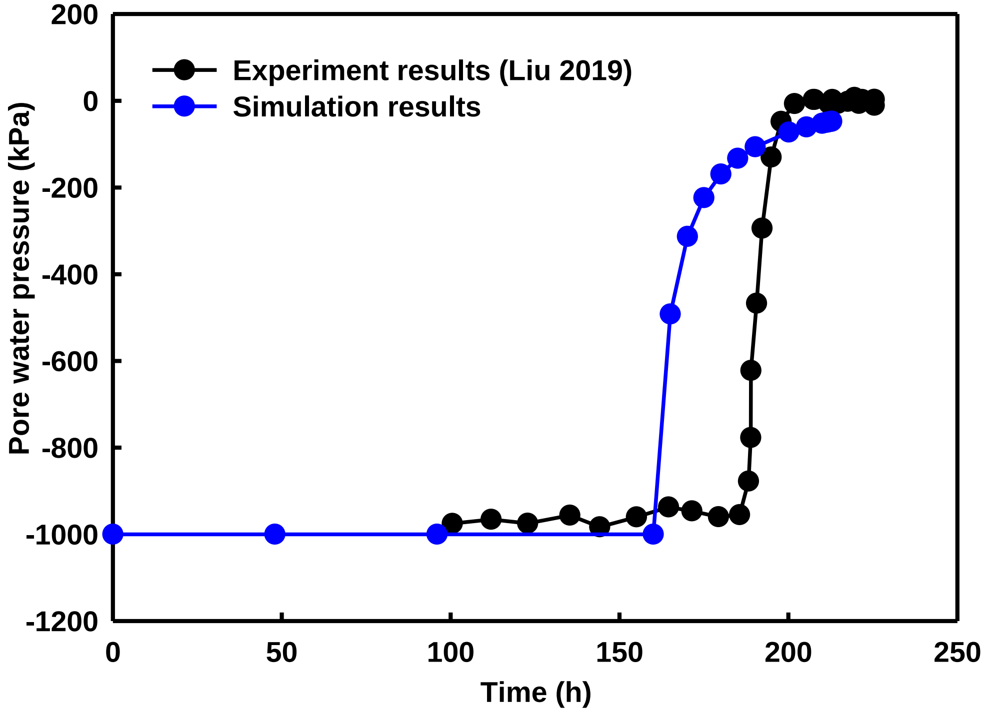

Figure 5.20 The comparison of the variation of the pore water pressure at the depth of 320 mm.

The displacements of the soil surface and the pile head are plotted in Figure 5.21. The experimental results suggest that there was no noticeable displacement of the soil surface during the static loading process. The displacement of the pile head after the static loading process was around 3mm. After the water was added manually for infiltration, the expansive soil showed an evident volume change in the vertical direction (i.e. ground heave). The ground heave however terminated after 200 hours. The ground heave of 25mm was detected when the ground heave was stable. The displacement of the pile head, however, increased from 3mm to 7mm during the infiltration process.

The simulation results trends were similar to the experimental results. In the static loading process, the displacement of the soil surface was zero. The displacement of the pile loading under the applied load of 0.5kN was around 1.7mm. In the infiltration process, the soil surface moved upward due to the expansion of the Regina clay. The displacement of the soil surface increased with time. After the infiltration, the displacement of the soil surface was around 24.2mm. The pile moved downward in the infiltration process. The displacement of the pile head was 5.3mm after the infiltration process. The simulation results are close to the experimental results.

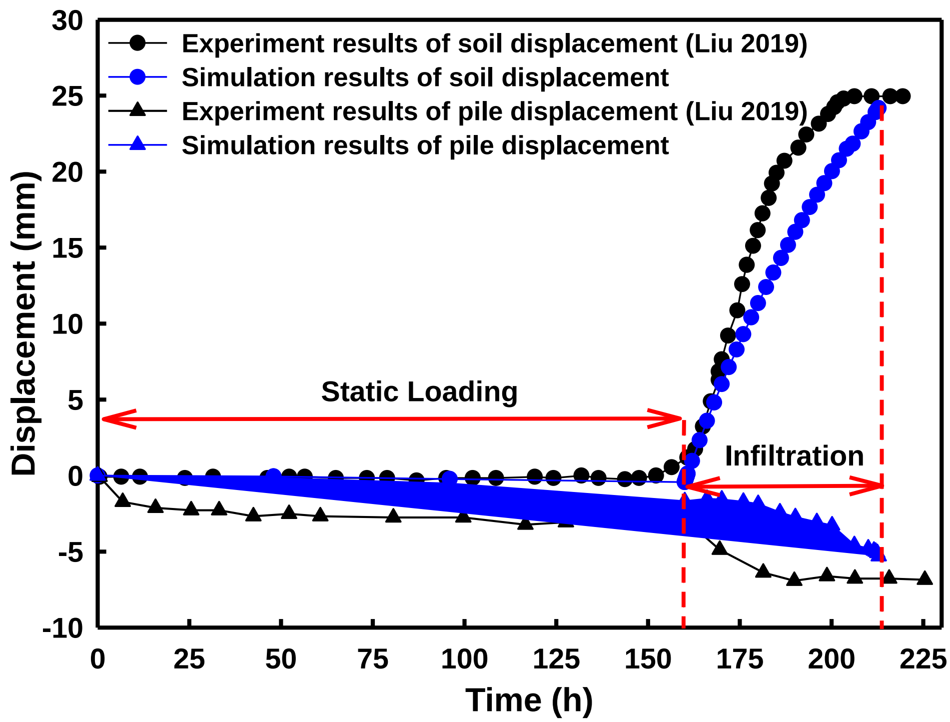

Figure 5.21 The comparison of the displacement of the soil surface and the pile head.

The shaft friction in the pile-soil interface is simulated by conducting numerical modeling. In Figure 5.22, the shaft friction distributions during the different stages of the test along the depth obtained from the simulations are compared with the distribution obtained from the pile infiltration test. Figure 5.22 (A) compared the shaft frictions obtained by the experiment and simulation after the static loading. Figure 5.22 (A) showed that the shaft frictions were around 15kPa. Figure 5.22 (B)-(D) compared the distribution of the shaft friction at the different stages of the infiltration test. The results showed that the distribution of the shaft friction from numerical simulations have similar trends as the experimental results. After 170 hours, the simulation results showed that the shaft friction increased from 9kPa to 17kPa with the depth. After 180 hours, the shaft friction increased from 7kPa to 19kPa. After the infiltration (200h), both the simulation results and the experimental results were kept as constants. The shaft friction obtained by the tests was around 10kPa. The shaft friction obtained by the simulation was around 7kPa. Figure 5.23 summarizes the simulation results at different stages. The results clearly show that the shaft friction decreases with an increase in the water infiltration process.

To study the effect of the suction (pore water pressure) on the shaft friction, the variations of the shaft friction and the suction (pore water pressure) at the depth of 80 mm with time are plotted in Figure 5.24. The shaft friction increased from 0 to 14.55kPa during the static loading process. In the static loading process, the suction was kept as 1000kPa. When the infiltration was applied manually, the suction began to decrease. After the infiltration process, the soil was saturated and the suction reached 0kPa. In this process, the shaft friction at the depth of 80 mm decreased with time. The shaft friction decreased from 14.55kPa to 6.44kPa. The rate of the decrease was 56%. In the interface model, the relative displacement between the pile and soil also can induce the softening of the shaft friction. In the simulation, the ratio between the residual stress and the peak stress, β, was set as 0.85. Therefore, the degradation of the shaft friction induced by the relative displacement was 15%. Hence, for the point at the depth of 80 mm, the degradation induced by the decrease in the suction was 41% (56% -15% = 41%). Therefore, the softening of the shaft friction induced by the decrease in the suction was higher than the degradation induced by the relative displacement. In other words, the decrease in suction significantly contributed to a decrease in shaft friction. The decrease in the shaft friction associated with water infiltration can be used to explain the hydro-mechanical behavior of the pile.

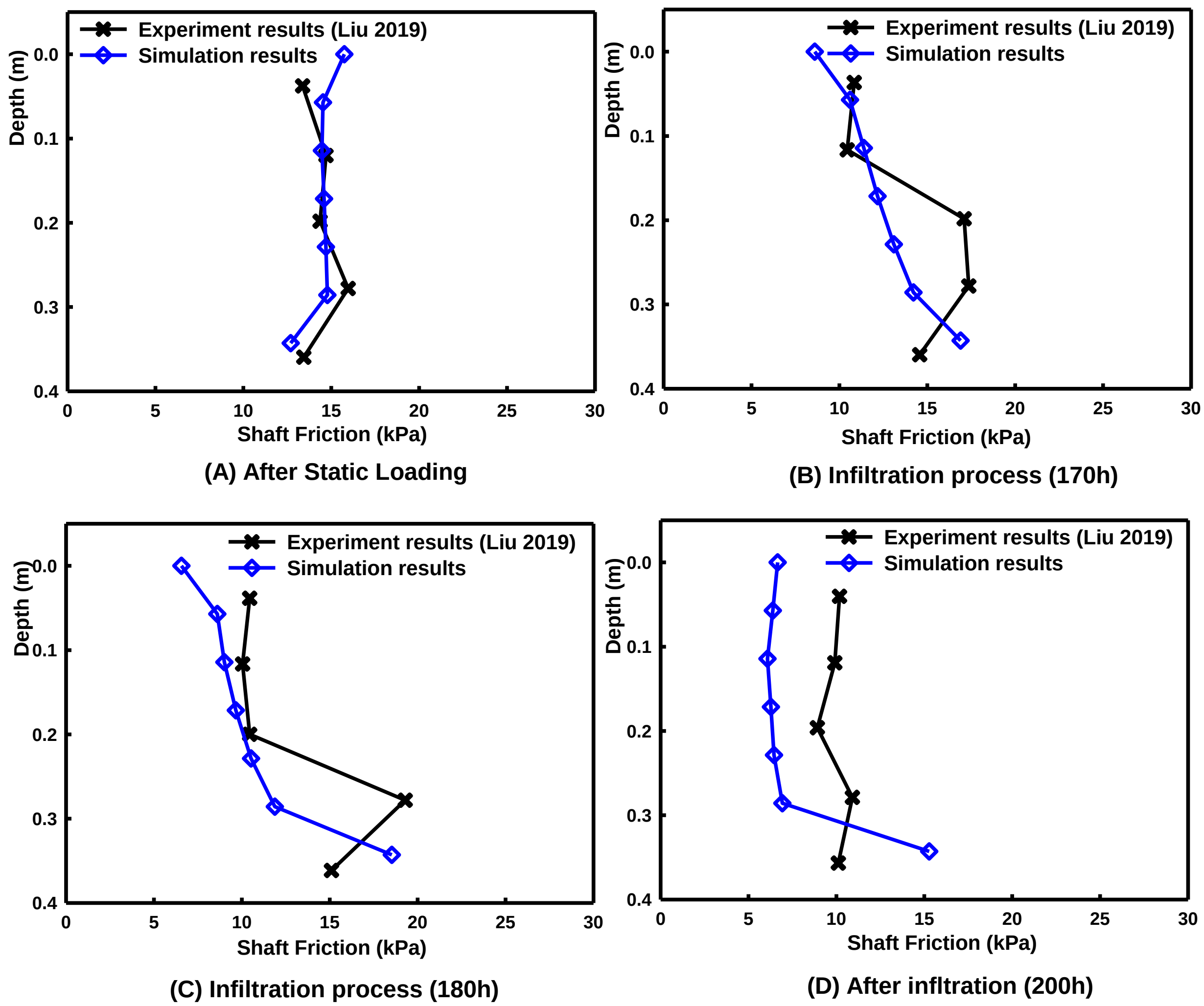

Figure 5.22 The comparison of the distribution of the shaft friction along with the depth at the different stage of the large scale test (A) the shaft friction distribution after static loading; (B) the shaft friction distribution in the infiltration process (170h); (C) the shaft friction distribution in the infiltration process (180h); (D) the shaft friction distribution after the infiltration process (200h).

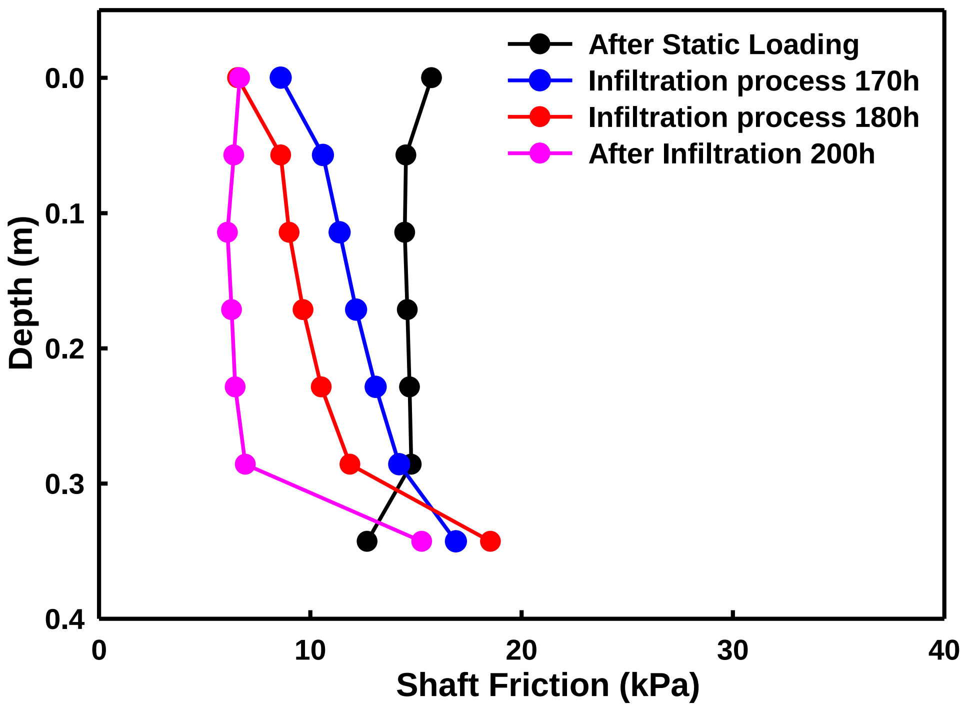

Figure 5.23 The distribution of the shaft friction at different stages of the test.

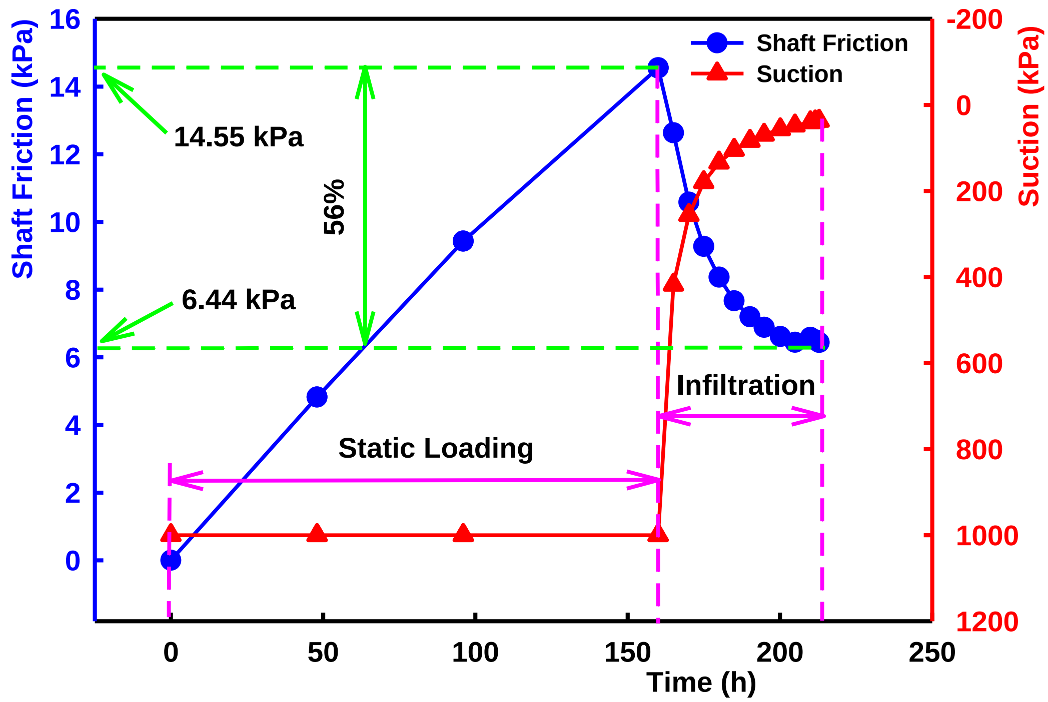

Figure 5.24 The variation of the shaft friction and suction with time at the depth of 80 mm.

The axial force acting on the pile at different stages of the pile model test was obtained from numerical modeling. The comparisons of the distribution of the axial force along with the depth obtained by the simulation and the test were plotted in Figure 5.25. Figure 5.25 shows that the results obtained from the numerical simulations had a good agreement with the experimental results of the model pile test.

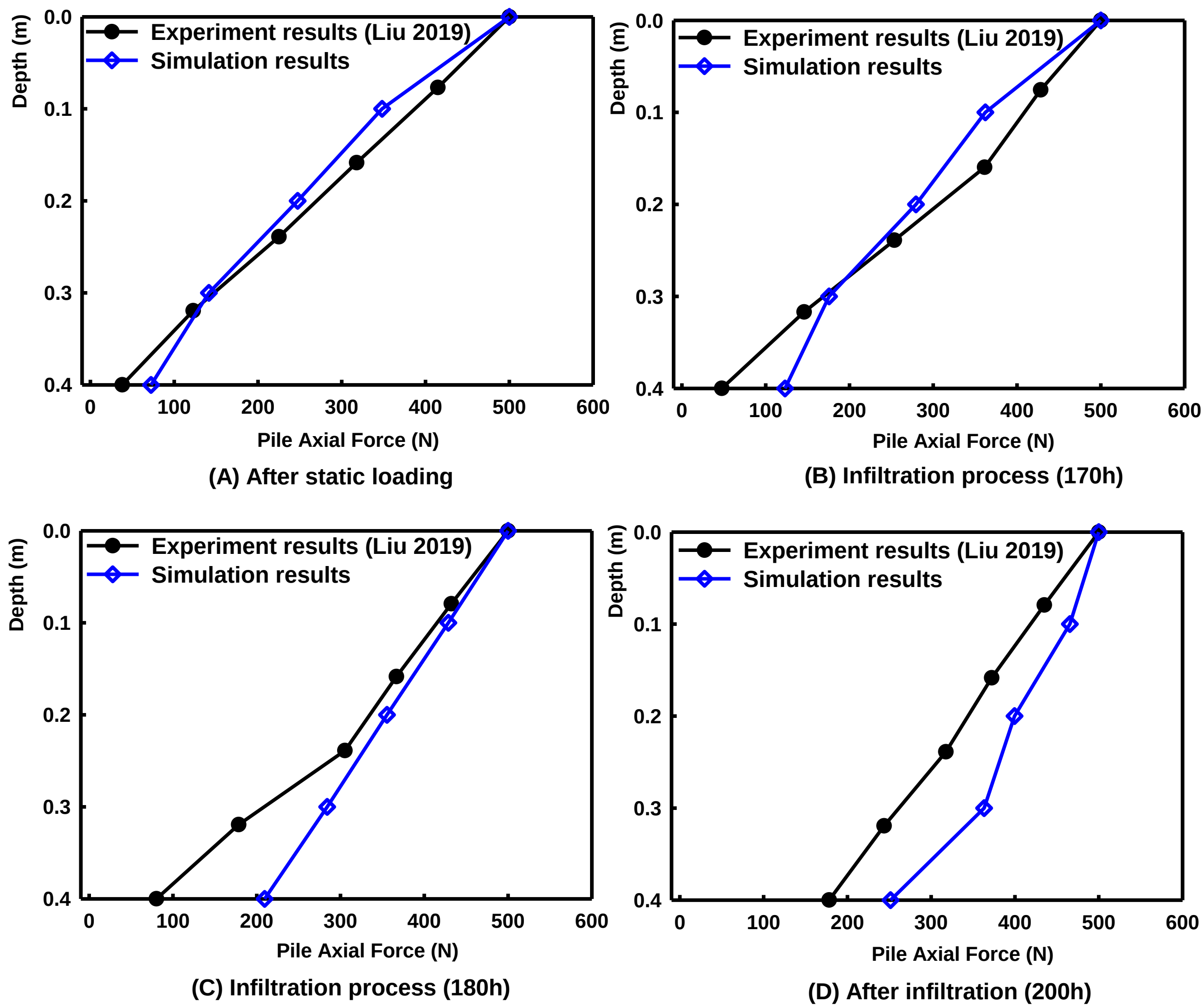

Figure 5.25 The comparison of the distribution of the axial force along with the depth at the different stage of the large scale test (A) the axial force distribution after static loading; (B) the axial force distribution in the infiltration process (170h); (C) the axial force distribution in the infiltration process (180h); (D) the axial force distribution after the infiltration process (200h).

The distributions of the axial force at different stages were summarized in Figure 5.26. The results in Figure 5.26 showed that the axial load acting on the pile increased during the water infiltration process. As discussed earlier, the shaft friction decreases with a decrease in the suction associated with water infiltration.

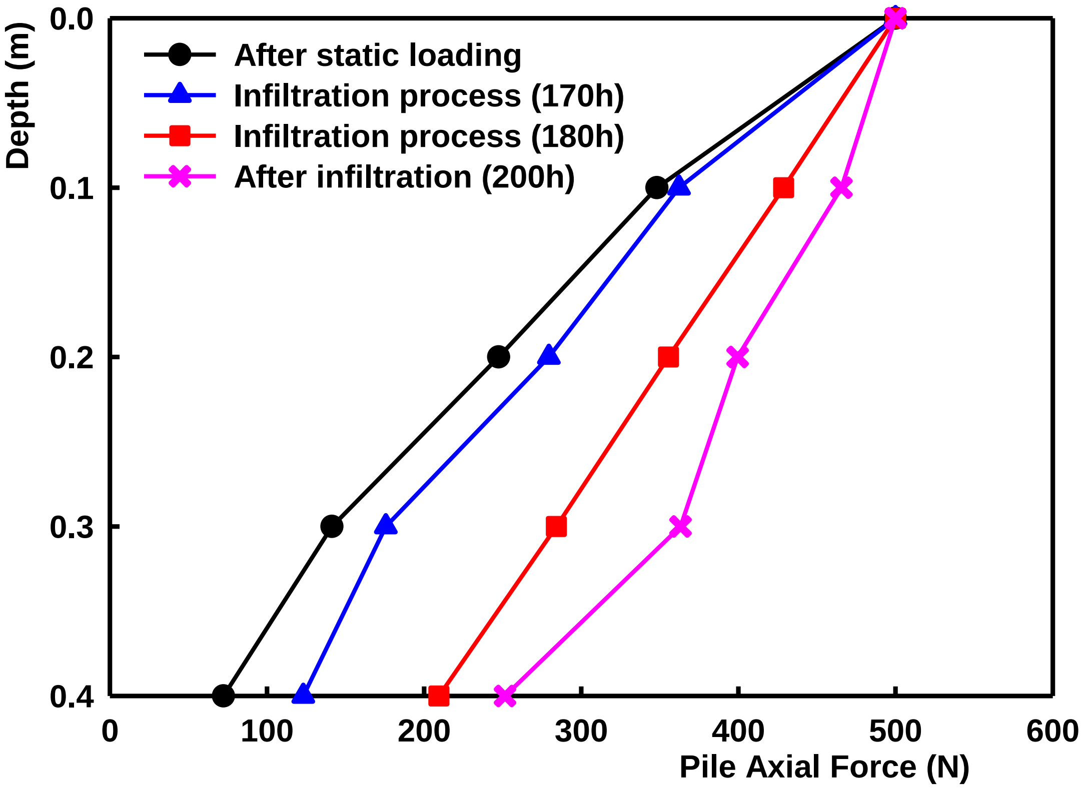

Figure 5.26 The distribution of the axial force at different stages of the test.

The comparisons between the end bearing resistance obtained from numerical simulations and experimental results are plotted in Figure 5.27. The simulation results had a similar trend as the experiment results. After the static loading process, the end bearing resistance obtained by the simulation was 45N, which is in good agreement with the measured value, 34N. When the infiltration was applied manually, both the simulation and the experimental results increased with time. After the infiltration process, both the simulation and the experiment results were 181N. The variation of the end bearing resistance agrees well with the variation of the shaft friction and axial force of the pile. In the infiltration process, the shaft friction was reduced due to the decrease in the suction. More load was transferred into the axial force; this load was resisted as end bearing resistance of the pile. Therefore, both the axial force and the end bearing resistance increased with time in the infiltration process. The increase in the end bearing resistance and the decrease in the shaft friction resulted in the pile moved downward and the increase in the displacement.

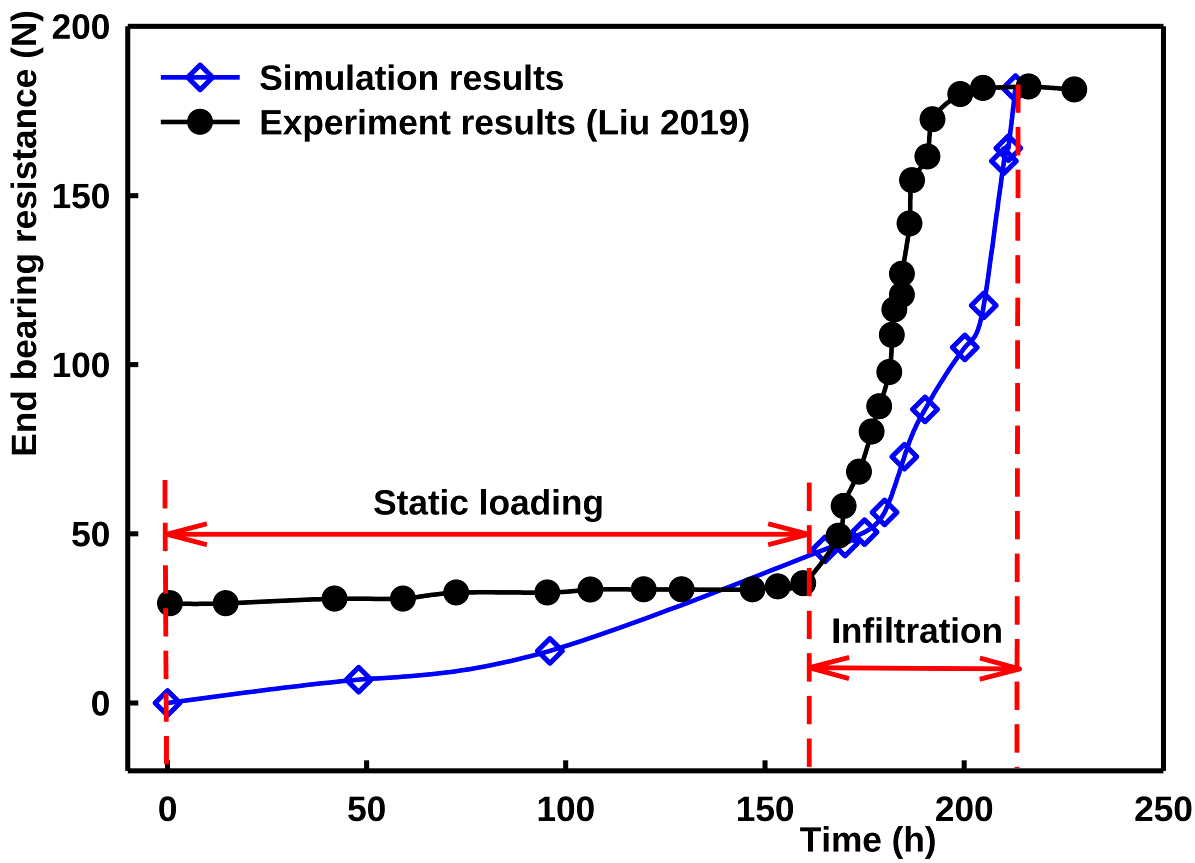

Figure 5.27 The comparison of the variation of the end bearing resistance with time.

Therefore, it can be summarized that during the infiltration process there will be a decrease in the suction or the increase in the pore water pressure, which can result in a reduction in the shaft friction in the pile-soil interface. Due to the decrease in the shaft friction, more load was transferred to the pile and soil below the pile, which contributed to an increase in the axial force and the end bearing resistance of the pile. The variation of the shaft friction, axial force, and the end bearing resistance can result in a downward displacement of the pile.

The simulation results illustrated that the suction may play a more important role in the mechanical behavior of single piles in unsaturated expansive soils. The decrease in suction can result in more degradation in shaft friction in the pile-soil interface than an increase in the relative displacement. The effect of suction or pore water pressure, however, is normally ignored in the engineering practice, which may result in the estimated shaft friction to be higher than the shaft friction in the real conditions. In other words, the neglect of suction may cause the overestimation of the bearing capacity of the pile foundation. Therefore, considering the effect of suction in the pile foundation design is necessary.

5.3.5 Limitations Discussion

The good agreement between the simulation results and experiment results illustrate that the developed subroutines are capable of simulating the mechanical behavior of a single pile in unsaturated expansive soils. However, there are some limitations in this model, which are discussed in this section.

The first limitation is that a simple stress path was simulated in this study. Constitutive surfaces for soil structure (void ratio) and water phase (water phase) were used to determine the elastic parameters. As discussed in Section 5.3.2, the constitutive surfaces were determined by conducting constant suction consolidation tests. In constant suction consolidation tests, suction decreased and net normal stress increased. In other words, suction followed the wetting path and the net normal stress followed the loading path. Therefore, the model used in this study is limited in its capability of simulating the behavior of expansive soil following the wetting and loading path.

The second limitation is that the elasticity assumption does not fully account the real behavior of unsaturated expansive soils. The expansive soil is typically a highly plastic soil. Both the suction and external stress can result in the evident plastic strain of expansive soils. The model used in this thesis, however, is assumed as non-elastic, therefore, the plastic strain of expansive soils cannot be simulated by this model. Therefore, more investigations are necessary for simulating different scenarios that are typically encountered in practice.

5.4 Summary and conclusion

A model pile test performed by Liu (2019) was used as an example to verify the developed subroutines (i.e. USDFLD, UMAT, UMATHT, UEXPAN, and FRIC) for modeling the load-deformation behavior of pile in unsaturated Regina expansive clay that was subjected to water infiltration. This chapter briefly introduces the model pile test and the properties of Regina clay, the property test of the pile-soil interface, and the load-deformation behavior of model pile. In addition, information of the numerical modeling including the size of the model and mesh, the properties of the pile and soils, and the boundary conditions and analysis steps, was introduced. Finally, the simulation results were presented and compared with the results obtained from the model pile test.

The model pile test was carried out at the University of Ottawa by Liu (2019). The physical properties and the soil-water characteristic curve of Regina clay were measured. The saturated and unsaturated shear strength of Regina clay and the soil-pile interface were measured by using direct shear tests. After obtaining the properties of Regina clay and the soil-pile interface, the large-scale pile model test was conducted. In the large-scale model test, two steps including the static loading process and the infiltration process were conducted. In the static loading process, a total load with a value of 500N was applied to the pile head. After the displacement of the pile head was stable, the water was added manually to the soil and the soil was allowed to swell. During the test, the mechanical properties of the pile and the expansive soil including the pore water pressure, the displacement of the pile head and the soil surface, the shaft friction, the axial force of the pile, and the end bearing resistance were detected.

The pile model test was simulated by the developed subroutines and Abaqus. One-fourth of the model pile was simulated. 144 meshes were applied to the model. The pile was assumed as elastic and the values of the parameters were obtained from Liu (2019). The elastic modulus of the pile was input as 7×10^7kPa. The input value of Poisson's ratio was set as 0.3. Shuai (1996) measured the constitutive surfaces for the soil structure (void ratio) and water content (gravimetric water content) of Regina clay under the K_0-loading state by conducting the constant suction consolidation tests. Vu (2003) proposed a mathematical equation to fit these constitutive surfaces and presented the values of the fitting parameters. These values were used as the input parameters to simulate the mechanical behavior of Regina clay. Shuai (1996) measured the unsaturated hydraulic conductivity for Regina clay and proposed an equation to fit it. The values of these fitting parameters were used to simulate the hydraulic behavior of Regina clay. The sand below the Regina clay was assumed as elastic and the values of properties of the sand were available in Liu (2019) and were input in the numerical modeling. The shear strength parameters of the pile-soil interface were measured by Liu (2019) and these values were used to simulate the behavior of the pile-soil interface in simulation. The boundary conditions including the displacement conditions and thermal conditions were applied to the model at the initial state. The pile and soil (i.e. expansive soil and sand) are allowed to move in the vertical direction and the other two directions are constrained. The initial temperature (pore water pressure) is set as -1000K (-1000kPa). Two analysis steps were set in the simulation according to the pile model test. The first step is the static loading process. The applied total loading in the static loading process is 0.125kN and the time is 576,000s (160 hours). The second step is the infiltration process. The heat flux of 2×10^{-5} J/($m^2\times s$) was applied to the top surface of the expansive soil in simulation. The time of this process is set as 180,000s (50 hours).

Finally, the simulation results are presented and compared with the experiment results. The results obtained by the simulation were compared with the experiment results. The results showed that the simulation results had a reasonably good agreement with the experimental results. The results illustrated that during the infiltration process there will be a decrease in the suction or the increase in the pore water pressure, which can result in a reduction in the shaft friction in the pile-soil interface. Due to the decrease in the shaft friction, more load was transferred to the pile and soil below the pile, which contributed to an increase in the axial force and the end bearing resistance of the pile. The variation of the shaft friction, axial force, and the end bearing resistance can result in a downward displacement of the pile.

The good agreement between the simulation results and experiment results showed that the developed subroutines have a good ability to simulate the pile behavior in unsaturated expansive soils. More advanced programming is expected in the future, which will make this model possible to simulate more complex stress and hydraulic conditions, for example, loading-unloading, and wetting-drying conditions.

CHAPTER 6
SUMMARY AND CONCLUSIONS

6.1 Summary

Geotechnical engineers consider expansive soils as a nightmare because of several problems associated with the construction of civil infrastructure with or within these soils. The volume change behavior associated with water content changes contributes to these major problems. For example, losses associated with these soils in the USA is several billions of dollars annually. Similar trends in losses are also reported in various regions of the world. To limit the problems associated with expansive soils, piles are widely used as foundations to safely carry the loads from the superstructure and reduce the damages associated with settlement problems. To achieve this objective, there is an urgent need to understand the hydromechanical behavior of the pile foundations in unsaturated expansive soils. Such studies will be valuable to propose rational methods for the design of pile foundations in unsaturated expansive soils. In this thesis, finite element methods were employed using commercial software Abaqus to study the variation in the behavior of a single pile in unsaturated expansive soil that was subjected to water infiltration.

Abaqus is a powerful software to conduct numerical analysis in geotechnical engineering. This software provides various options for coupling several non-linear problems with the aid of a number of user-defined subroutines for users to define different material behavior. For this reason, Abaqus was used to study the behavior of the pile foundation in expansive soils. However, Abaqus does not have tools to directly use them for modeling the coupled hydro-mechanical behavior of unsaturated expansive soils. In addition, Abaqus does not have a constitutive relationship that can be used for modeling the unsaturated pile-soil interface which is required for the analysis. To simulate the pile foundation behavior of load carrying capacity and settlement behavior associated with water infiltration, a coupled hydro-mechanical model for the unsaturated expansive soil and a model for the unsaturated pile-soil interface were developed into subroutines. A state surface model for the unsaturated expansive soils was used in this study to simulate the mechanical behavior of the expansive soil. The water flow in the unsaturated expansive soil was described by Darcy's law. Combining equations for the constitutive relations and Darcy's law made it possible to conduct the coupled hydro-mechanical analysis. A modified hyperbolic model for the pile-soil interface was used to describe the frictional behavior of the unsaturated pile-soil interface. To develop the equations for the constitutive models for the unsaturated expansive soil and unsaturated pile-soil interface into user-defined subroutines, the similarity between the coupled hydro-mechanical analysis and the coupled thermo-mechanical analysis was exploited. The equations coupled available for modeling the thermo-mechanical problems in Abaqus were transferred into user-defined subroutines for modeling the coupled hydro-mechanical problems. Five subroutines were developed, which included User-defined field subroutine (USDFLD), User-defined material subroutine (UMAT), User-defined thermal expansion subroutine (UEXPAN), User-defined thermal material subroutine (UMATHT), and User-defined friction behavior subroutine (FRIC). USDFLD processes access to material point data such as stress state, strain, and temperature and transfers these values into other user-defined subroutines. UMAT is used to define the mechanical constitutive relationship. UEXPAN is used to define the incremental thermal strains as the function of temperature. UMATHT is used to define the thermal constitutive model of the material. FRIC is used to define the constitutive model for the pile-soil interface. The finite element analysis was conducted by combining the developed subroutines and a commercial software Abaqus.

A large scale model test conducted at the University of Ottawa by Liu (2019) was used as an example to verify the developed programs within Abaqus. The results showed that the developed programs proved to be a valuable tool to simulate the behavior of pile foundation behavior in expansive soils associated with water infiltration. The results also illustrated that the variation of the pore water pressure (suction) had a great influence on the behavior of the pile foundation. The decrease in the suction resulted in a decrease in the shaft friction between the pile and soil. As the decrease in the shaft friction, more load was transferred to the axial force and the end bearing resistance of the pile, which resulted to carry more pile head load which contributed to a more downward displacement.

6.2 Conclusions

This thesis is summarized in six Chapters and each of the chapters independently focuses on summarizing information that contributes towards understanding the hydro-mechanical behavior of expansive soils. The key conclusions arrived from each of the Chapters of this thesis are succinctly summarized.

6.2.1 Introduction

(I) Expansive soil is a term that is widely used for soils that undergo significant volume changes due to the variation of the natural water content. The volume change behavior of expansive soils associated with water content changes contributes to several challenges in the design of several geotechnical infrastructures including the design of foundations.

Pile foundation is an effective method to reduce damages induced by expansive soils to ensure the safety of buildings constructed in expansive soil areas. Conventionally, piles are designed such that they can penetrate through the expansive soil layers to reach the bedrock or a firm soil layer that is not affected by the variation in the water contents. To design the pile in the expansive soil, the hydro-mechanical behavior of the pile should be thoroughly investigated.

(II) Prior to the infiltration of water, positive friction contribution arises along the length of the pile in expansive soils due to surcharge. The bedrock or the firm soil that is not affected by the variation in water content can offer the end bearing resistance. When there is an increase in water content due to rainfall or other modes of water infiltration, the expansive soil swells. Due to this reason, expansive soil moves in the upward direction relative to the pile. The positive friction may increase due to the increase in the relative movement between the soil and pile. The pile under the light loaded structure may get uplifted due to the increase in the positive friction. Therefore, the end bearing resistance of pile typically decreases due to the influence water infiltration.

(III) Three design methods (i.e. the rigid method, the elastic method, and the finite element method) are available for the design of the pile foundation in expansive soil. Research studies related to the finite element method are limited based on unsaturated soil mechanics. The key objective of this thesis is to employ the unsaturated soil mechanics into the finite element method to simulate the behavior of the pile foundation in unsaturated expansive soil upon infiltration. Abaqus is one of the most widely used commercial software to conduct numerical modeling in geotechnical engineering. Abaqus provides different types of user-defined subroutines whereby users can define the complex behavior of materials in a general way. Therefore, the commercial software Abaqus is used in this study to conduct the simulation. A three-dimensional coupled hydro-mechanical constitutive model for the unsaturated expansive soil and a model for the unsaturated pile-soil interface were developed in this thesis.

6.2.2 Literature review

(I) Three types of design methods; namely, the rigid methods, the elastic methods, and the finite element based methods are available for the design pile foundation in expansive soils.

Chen (1988) and O'Neill (1988) proposed the rigid pile method. In the rigid method, the pile is assumed as rigid and the displacement of the pile is not allowed. In other words, the displacement of the pile in the rigid method is zero. The uplift friction induced by the swelling of the expansive soil is considered equal to the summation of the negative friction in the soil layers below the active zone and the surcharge. The rigid method is simple for use in practice; however, it is conservative for the design of the pile. In the elastic design method, the displacement of the pile is allowed.

Poulos and Davis (1980) proposed a basic framework for the elastic pile method. In this method, the heave of the expansive soil is assumed to be linear in the active zone. Fan et al. (2007) assumed that the displacement of soil around the pile related not only to the depth but to the distance away from the pile axes. According to the displacement compatible condition, the displacement of soil at the radius of the pile radius should be equal to the displacement of the pile. Therefore, the pile displacement can be determined from the equation for the soil displacement. However, the elastic design method is suitable for the pile whose ratio between the length and diameter is less than 20. In addition, this method is only suitable for simple soil profile conditions.

The finite element method is an effective method to reduce these shortcomings of rigid and elastic methods. In the finite element method, the constitutive models for the expansive soil and the pile-soil interface can be included, which makes it possible to study the mechanical behavior of the pile in expansive soil under complex soil profiles and complex hydraulic conditions (e.g. initial water content, drain conditions, and so on). Some research studies were based on the finite element method, however, in these investigations, the unsaturated expansive soil model and the unsaturated pile-soil interface model were not included. Therefore, an unsaturated expansive soil model and a pile-soil interface model were developed in this thesis.

(II) Matyas and Radhakrishna (1968) were the pioneers who first introduced the concept of the state surface for rational explanation of the behavior of unsaturated soils. The state surface concept suggested that three-dimensional surfaces can be used to present the complete history of the void ratio and the water content of the unsaturated soils. The surfaces are contained by three axes showing the magnitude of the net normal stress, $(\sigma_n - u_a)$, the suction, $(u_a - u_w)$, and the void ratio, e or water content, w. Fredlund and Morgenstern (1976) proposed mathematical equations to formulate the constitutive relations for the void ratio and water content extending the concept of the state surface, considering net normal stress, $(\sigma_n - u_a)$, the suction, $(u_a - u_w)$, as independent stress state variables. The state surface model is simple and can be used to simulate the different stress states of the expansive soils. Therefore, in this thesis, the state surface model was employed to study the behavior of a single pile in expansive soils. The elastoplastic models are the second widely used constitutive model for the unsaturated soils. Most elastoplastic models are based on the Barcelona Basic Model (BBM) (Alonso et al. 1990). These models are capable of modeling complex stress paths. However, the parameters required for using these models are difficult to determine. Hence, these models may not be suitable in the conventional design of pile foundations by practicing engineers.

(III) In addition to the 3D state surface model, constitutive model for the unsaturated soil-structure interface model is required in the finite element method. These models are included in the elastic models, elastoplastic models, and the disturbed state models. The hyperbolic model is one of simplest and can fully simulate the mechanical behavior of the soil-structure interface. Zhang and Zhang (2012) proposed an equation that can simulate the degradation behavior of the shear stress in the pile-soil interface. This equation requires only three parameters (i.e. the peak stress, the relative displacement between the pile and soil with respect to the peak stress, and the ratio between the residual stress and the peak stress). This equation facilitates smooth transfer from the peak stress and residual stress. This advantage can contribute to the increase simulation efficiency of the finite element method; therefore, this model is employed in this study. Many elastoplastic and disturbed concept models were also proposed. Several parameters are required in these models are difficult to determine. Due to this reason, these models may not be suitable for use in conventional engineering practice.

6.2.3 Constitutive relationships of unsaturated soil and unsaturated soil-structure interface

(I) The constitutive models are required for performing the coupled hydro-mechanical analysis of the pile in the unsaturated expansive soils. The state surface model was used to achieve this objective in this thesis. In the state surface model, the constitutive relations for the soil structure and water phase of the unsaturated soil are formulated in terms of independent stress state variables; namely, net normal stress and suction. Fredlund and Morgenstern (1976) proposed the linear equations to describe the constitutive surfaces for the soil structure and water phase. The linear equations are valuable for formulating the nonlinear behavior of the unsaturated soils for infinitesimal stress and strain increments. These equations are simple in form and require only four parameters (i.e. the elasticity modulus for the soil structure with respect to the net normal stress, E, the elasticity modulus for the soil structure with respect to the suction, H, the coefficient of water volume change with respect to net normal stress, m_1^w or m_{1-1}^w, the coefficient of water volume change with respect to suction, m_2^w or m_{1-2}^w). When the constitutive surfaces of the void ratio and the water content are constructed, the elastic parameters can be determined by differentiating the constitutive surfaces.

Shuai (1996) measured the constitutive surfaces of the void ratio and water content for the Regina unsaturated expansive soil. Vu (2003) proposed equations for the same soil to fit the constitutive surfaces for the void ratio and water content; these equations were used to determine the elastic parameters. The flow law is also required in addition to the constitutive relations for the soil structure and water phase for a rational explanation of the flow behavior. In this model, Darcy’s law is assumed valid for unsaturated soils. The unsaturated hydraulic conductivity is required in Darcy’s law for the unsaturated soils. Shuai (1996) measured the hydraulic conductivity of unsaturated expansive soil and proposed an equation to formulate the hydraulic conductivity by using the saturated hydraulic conductivity, void ratio, and the soil-water characteristic curve.

(II) The differential governing equations are required to establish the equations for the fully coupled hydro-mechanical problems. The balance equations for the soil structure satisfy the requirement of the static equilibrium. The balance equation for the water phase satisfies the requirement of continuity. By incorporating the balance equations and the constitutive relations for each phase (i.e. soil structure and water phase), the governing equations for the coupled hydro-mechanical problems are established (Muraleetharan and Wei 1999). The governing equations can be solved and the solutions for the coupled hydro-mechanical problems can be obtained by specifying appropriate boundary conditions.

(III) The constitutive model for the unsaturated pile-soil interface is required in the finite element analysis of the pile foundation in the expansive soil. Zhang and Zhang (2012) proposed a hyperbolic model to formulate the relationship between shear stress and the relative displacement between the pile-soil interface. This model is capable of describing the hardening behavior and simulating the softening behavior of the pile-soil interface. Only three parameters (i.e. the peak shear strength, τ_{su}, the relative displacement with respect to the peak shear strength, S_{su}, and the ratio between the residual shear strength and peak shear strength, β_s) are included in this model. Hamid and Miller (2009) used the modified direct shear apparatus to control matric suction and study the shear strength of unsaturated soil-structure interface and proposed a mathematical equation to formulate the shear strength of the unsaturated pile-soil interface. This equation has a similar form to the equation for the shear strength of the unsaturated soils proposed by Vanapalli et al. (1996). Liu (2019) introduced this equation into Zhang and Zhang model to calculate the peak shear strength, which makes it possible to describe the mechanical behavior of the unsaturated pile-soil interface. The model proposed by Liu (2019) was employed in this study.

6.2.4 Implementation of constitutive and soil-structure interface models into Abaqus for modeling the pile behavior in unsaturated expansive soils

(I) The coupled hydro-mechanical model for the unsaturated expansive soil is implemented into Abaqus software. To develop the program, the similarity between the coupled thermo-mechanical analysis and the coupled hydro-mechanical analysis was exploited. In the coupled hydro-mechanical problems, the water flow follows Darcy's law. The water flow is directly proportional to the gradient of the hydraulic head as per Darcy's law. In the coupled thermo-mechanical problems, the heat transfer can be described by Fourier's law. As per Fourier's law, the heat flow is directly proportional to the gradient of the temperature. Therefore, Darcy's law is similar to Fourier's law in principle and form (Groenevelt 2003; Rose 2000). In the coupled hydro-mechanical problems for the unsaturated soils, the strain is induced by the variations in the external stress and the suction. In the coupled thermo-mechanical problems, the strain is induced by the variations in the external stress and the temperature. Therefore, the constitutive relations for the mechanical behavior of the unsaturated soil in the coupled hydro-mechanical problems are similar to the constitutive relations for the hydro-mechanical behavior of a matter in the coupled thermo-mechanical problems. Based on this similarity, the coupled hydro-mechanical problems can be simulated by extending similar approaches for analyzing coupled thermo-mechanical problems. In this thesis, the equations for the coupled hydro-mechanical problems are compared with the equations for the coupled thermo-mechanical problems. The comparison clearly shows the similarity between the equations for the hydro-mechanical problems and that for the thermo-mechanical problems. After establishing the similarity, the equations and the parameters in the coupled thermo-mechanical problems were used in the simulations of the coupled hydro-mechanical problems.

(II) Abaqus was used to conduct the coupled thermo-mechanical analysis and the coupled hydro-mechanical model for the unsaturated expansive soils and the constitutive model for the unsaturated pile-soil interface were developed into five user-defined subroutines. Abaqus/CAE (Computer Aided Engineering) is used to perform the main program. The main program is used to define the size of the model, the material properties, type of the elements and size of the meshes, soil-pile interface, initial conditions, boundary conditions, and analysis steps. The properties of soil and soil-pile interface defined in the main program are transferred into user-defined subroutines. Four user-defined subroutines were used to develop the coupled hydro-mechanical model of the unsaturated expansive soils. User-defined field subroutine (USDFLD) processes access to material point data such as stress state, strain, and temperature (pore-water pressure). These data are transferred into other user-defined subroutines. User-defined material subroutine (UMAT) is used to define the mechanical constitutive relationship. In UMAT, the elastic modulus with respect to net normal stress, E, was defined and the stress at the end of the increment was updated. User-defined thermal expansion subroutine (UEXPAN) is used to define the thermal strains (swelling strain of the unsaturated expansive soils). The coefficient of heat expansion, α, is calculated and the thermal strains are updated. User-defined thermal material subroutine (UMATHT) is used to define the thermal constitutive model of the material (hydraulic behavior of the unsaturated expansive soil). The internal energy per unit mass and the heat flux were updated in UMATHT. User-defined friction behavior subroutine (FRIC) is used to define the frictional behavior between contact surfaces. The friction stress in the pile-soil interface is updated in FRIC.

6.2.5 Modeling the experimental study results of a single model pile in unsaturated expansive soil

(I) The large scale model pile test was carried out at the University of Ottawa by Liu (2019). For analysing the model pile test results, several other tests were performed which include the soil properties test of Regina clay and the shear strength tests of saturated and unsaturated Regina clay and the pile-soil interface. The physical properties and the soil-water characteristic curve of Regina clay were measured. The saturated and unsaturated shear strength of Regina clay and the soil-pile interface were measured by using direct shear tests. The parameters (i.e. the effective friction angle of the shear strength for the saturated Regina clay and the saturated pile-soil interface, the friction angle with respect to the net normal stress for the unsaturated Regina clay and the unsaturated pile-soil interface, the friction angle with respect to suction for the unsaturated Regina clay and the unsaturated pile-soil interface, the cohesion for the unsaturated soil, and the adhesion for the unsaturated pile-soil interface) were given. In the model pile infiltration test, two steps including the static loading process and the infiltration process were conducted. In the static loading process, a total load with a value of 500N was applied to the pile head. After the displacement of the pile head was stable, the water was added manually to the soil and the soil was allowed to swell. During the test, the mechanical properties of the pile and the expansive soil including the pore water pressure, the displacement of the pile head and the soil surface, the shaft friction, the axial force of the pile, and the end bearing resistance were detected.

(II) The pile model test was simulated by Abaqus along with the developed subroutines. One-fourth of the model pile and soil were simulated. The pile was assumed as elastic and the values of the parameters were obtained from Liu (2019). The elastic modulus of the pile was input as 7×10^7kPa. The input value of the Poisson’s ratio was set as 0.3. Shuai (1996) measured the constitutive surfaces for the soil structure (void ratio) and water content (gravimetric water content) of Regina clay under the K_0-loading state by conducting the constant suction consolidation tests. Vu (2003) proposed a mathematical equation to fit these constitutive surfaces and presented the values of the fitting parameters. These values were used as the input parameters to simulate the mechanical behavior of Regina clay. Shuai (1996) measured the unsaturated hydraulic conductivity for Regina clay and proposed an equation to fit it. The values of these fitting parameters were used to simulate the hydraulic behavior of Regina clay. The sand below the Regina clay was assumed as elastic and the values of properties of the sand were available in Liu (2019) and were input in the numerical modeling. The shear strength parameters of the pile-soil interface were measured by Liu (2019) and these values were used to simulate the behavior of the pile-soil interface in simulation. The boundary conditions including the displacement conditions and thermal conditions were applied to the model at the initial state. The pile and soil (i.e. expansive soil and sand) are allowed to move in the vertical direction and the other two directions are constrained. The initial temperature (pore water pressure) is set as -1000K (-1000kPa). Two analysis steps were set in the simulation according to the pile model test. The first step is the static loading process. The applied total loading in the static loading process is 0.125kN and the time is 576,000s (160 hours). The second step is the infiltration process. The heat flux of 2×10^5 J/($m^2\times s$) was applied to the top surface of the expansive soil in simulation. The time of this process is set as 180,000s (50 hours).

(III) The simulation results are presented and compared with the experiment results. The results showed that the simulation results had a reasonably good agreement with the experimental results. The results illustrated that during the infiltration process there will be a decrease in the suction or the increase in the pore water pressure, which can result in a reduction in the shaft friction in the pile-soil interface. Due to the decrease in the shaft friction, more load was transferred to the pile and soil below the pile, which contributed to an increase in the axial force and the end bearing resistance of the pile. The variation of the shaft friction, axial force, and the end bearing resistance can result in a downward displacement of the pile. With more advanced programming tools in future, this model can simulate more complex stress and hydraulic conditions that are typically encountered in practice.

6.3 Main Conclusions

(1) For the rational design of pile foundations in expansive soils, the hydro-mechanical behavior of the pile in unsaturated expansive soil upon the infiltration should be fully understood. In this thesis, the finite element method was used as a tool to understand the behavior of the pile foundation in unsaturated expansive soil upon the infiltration.

(2) Abaqus was used to conduct the finite element analysis. However, in Abaqus, the coupled hydro-mechanical model for the unsaturated expansive soil and the constitutive model for the unsaturated pile-soil interface are not available. Therefore, a constitutive model based on the state surface model as well as the hydraulic model for the unsaturated expansive soil were developed for use in subroutines provided in Abaqus. A modified hyperbolic model for the unsaturated pile-soil interface was developed in a subroutine. To develop the subroutines, the similarity between the coupled hydro-mechanical problems and the coupled thermo-mechanical problems was employed and the equations for the coupled hydro-mechanical problems were transferred to the equations for the coupled thermo-mechanical problems. Five subroutines (i.e. USDFLD, UMAT, UEXPAN, UMATHT, and FRIC) were developed.

(3) A comprehensive model pile test performed by Liu (2019) was successfully simulated. The simulation results illustrated that during the infiltration process there will be a decrease in the suction, which can result in a reduction in the shaft friction in the pile-soil interface. Due to the decrease in the shaft friction, more load was transferred to the pile and soil below the pile, which contributed to an increase in the axial force and the end bearing resistance of the pile. The pile will move downward because of the decrease in the shaft friction and the increase in the axial force and the end bearing resistance.

REFERENCES

ABAQUS/Standard User's Manual (2014). Version 6.14, USA.: Dassault Systems Simulia Corp.

ABAQUS/CAE User's Manual (2014). Version 6.14, USA.: Dassault Systems Simulia Corp.

ABAQUS Theory Manual (2014). Version 6.14, USA.: Dassault Systems Simulia Corp.

Abhishek, and Sharma, R. K. (2019). "A Numerical Study of Granular Pile Anchors Subjected to Uplift Forces in Expansive Soils Using PLAXIS 3D." *Indian Geotechnical Journal*, 49(3), 304–313.

Adem, H. H., and Vanapalli, S. K. (2013). "Constitutive modeling approach for estimating 1-D heave with respect to time for expansive soils." *International Journal of Geotechnical Engineering*, 7(2), 199–204.

Al-Busoda, B. S., Awn, S. H. A., and Abbase, H. O. (2017). "Numerical modeling of retaining wall resting on expansive soil." *Geotechnical Engineering*, 48(4), 116–121.

Alonso, E. E., Gens, A., and Josa, A. (1990). "A constitutive model for partially saturated soils." *Geotechnique*, 40(3), 405–430.

Alonso, E. E., Vaunat, J., and Gens, A. (1999). "Modelling the mechanical behaviour of expansive clays." *Engineering Geology*, 54(1–2), 173–183.

Amir, J. M., and Sokolov, M. J. (1976). "Finite element analysis of piles in expansive media." *Journal of Geotechnical and Geoenvironmental Engineering*, 102(7), 701–719.

Bishop, A. W. (1959). "The principle of effective stress." *Teknik Ukeblad*, 39, 859–863.

Bishop, A. W., Alpan, I., Blight, G. H., and Donald, I. B. (1960). "Factors controlling the strength of partly saturated cohesive soils." *Proceedings of the ASCE Research Conference on Shear Strength of Cohesive Soils*, 503–532.

Borana, L., Yin, J.-H., Singh, D. N., and Shukla, S. K. (2016). "Interface Behavior from Suction-Controlled Direct Shear Test on Completely Decomposed Granitic Soil and Steel Surfaces." *International Journal of Geomechanics*, 16(6), D4016008.

Borana, L., Yin, J. H., Singh, D. N., Shukla, S. K., and Pei, H. F. (2017). "Influences of Initial Water Content and Roughness on Skin Friction of Piles Using FBG Technique." *International Journal of Geomechanics*, 17(4), 04016097.

Boulon, M., and Nova, R. (1990). "Modelling of soil-structure interface behaviour a comparison between elastoplastic and rate type laws." *Computers and Geotechnics*, 9, 21–46.

Bowers, S. A., and Hanks, R. J. (1962). "Specific heat capacity of soils and minerals as determined with a radiation calorimeter." *Soil Science*, 94(6), 392–396.

Cao, W., Chen, Y., and Wolfe, W. E. (2014). "New Load Transfer Hyperbolic Model for Pile-Soil Interface and Negative Skin Friction on Single Piles Embedded in Soft Soils." *International Journal of Geomechanics*, 14(1), 92–100.

Chen, F. (1975). *Foundations on Expansive Soils*. Elsevier, New York.

Chen, F. H. (1988). *Foundations on expansive soils*. Elsevier, Amsterdam.

Cheng, S., Zhang, Q., Li, S., Li, L., Zhang, S., and Wang, K. (2018). "Nonlinear analysis of the response of a single pile subjected to tension load using a hyperbolic model." *European Journal of Environmental and Civil Engineering*, 22(2), 181–191.

Cho, S. E., and Lee, S. R. (2001). "Instability of unsaturated soil slopes due to infiltration." *Computers and Geotechnics*, 28(3), 185–208.

Cui, W., Potts, D. M., Zdravković, L., Gawecka, K. A., and Taborda, D. M. G. (2018). "An alternative coupled thermo-hydro-mechanical finite element formulation for fully saturated soils." *Computers and Geotechnics*, 94, 22–30.

Cui, Y. J., and Delage, P. (1996). "Yielding and plastic behaviour of an unsaturated compacted silt." *Geotechnique*, 46(2), 291–311.

Cui, Y., Loiseau, C., and Delage, P. (2002). "Microstructure changes of a confined swelling soil due to suction controlled hydration." *Proc 3rd Int Conf on Unsaturated soils UNSAT. 2002.*, Recife, Brazil, Balkema, 593–598.

Curran, D. R. (1963). "Nonhydrodynamic attenuation of shock waves in aluminum." *Journal of Applied Physics*, 34(9), 2677–2685.

Desai, C. (2000). *Mechanics of Materials and Interfaces:The Disturbed State Concept*. CRC Press, New York.

Desai, C. S., and Ma, Y. (1992). "Modeling of joints and interfaces using the disturbed state concept." *International Journal for Numerical and Analytical Methods in Geomechanics*, 16(9), 623–653.

Desai, C. S., and Rigby, D. B. (1997). "Cyclic Interface and Joint Shear Device Including Pore Pressure Effects." *Journal of Geotechnical and Geoenvironmental Engineering*, 123(6), 568–579.

Ebrahimian, B., Noorzad, A., and Alsaleh, M. I. (2012). "FE simulation of shear localization along granular soil-structure interfaces using micro-polar elasto-plasticity." *Mechanics Research Communications*, 39(1), 28–34.

Fakharian, K., and Evgin, E. (2000). "Elasto-plastic modelling of stress-path-dependent behaviour of interfaces." *International Journal for Numerical and Analytical Methods in Geomechanics*, 24(2), 183–199.

Fan, Z., Wang, Y., Xiao, H., and Zhang, C. (2007). "Analytical method of load-transfer of single pile under expansive soil swelling." *J. Cent. South Univ. Technol. (Engl. Ed.)*, 14(4), 575–579.

Farhadi, B., and Lashkari, A. (2017). "Influence of soil inherent anisotropy on behavior of crushed sand-steel interfaces." *Soils and Foundations*, 57(1), 111–125.

Fredlund, D. G. (1973). "Volume Change Behavior of Unsaturated Soils." Ph.D. Dissertation, University of Alberta, Canada.

Fredlund, D. G. (1979). "Second Canadian Geotechnical Colloquium: Appropriate concepts and technology for unsaturated soils." *Canadian Geotechnical Journal*, 16, 121–139.

Fredlund, D. G. (1981). "Seepage in saturated soils. Panel Discussion : Ground water and seepage problems." *Proceedings of the 10th International Conference on Soil Mechanics and Foundation Engineering*, Stockholm,Sweden, 629–641.

Fredlund, D. G., and Morgenstern, N. R. (1976). "Constitutive relations for volume change in unsaturated soils." *Canadian Geotechnical Journal*, 13(3), 261–276.

Fredlund, D. G., Morgenstern, N. R., and Widger, R. A. (1978). "The shear strength of unsaturated soil." *Canadian Geotechnical Journal*, 15(3), 313–321.

Fredlund, D. G., and Rahardjo, H. (1993). *Soil mechanics for unsaturated soils*. John Wiley & Sons., Hoboken.

Fredlund, D. G., Rahardjo, H., and Fredlund, M. D. (2012). *Unsaturated Soil Mechanics in Engineering Practice*. John Wiley & Sons, Hoboken.

Gallipoli, D., Gens, A., Sharma, R., and Vaunat, J. (2003). "An elasto-plastic model for unsaturated soil incorporating the effects of suction and degree of saturation on mechanical behaviour." *Géotechnique*, 53(1), 123–135.

Gardner, W. . (1958). "Some steady state solutions of the unsaturated moisture flow equation with application to evaporation from a water-table." *Soil science*, 85(4), 228–232.

Geiser, F., Laloui, L., Vulliet, L., and Desai, C. S. (1997). "Disturbed state concept for partially saturated soils." *Numerical Models in Geomechanics*, 2–4, 129–134.

Gens, A., and Alonso, E. E. (1992). "A framework for the behaviour of unsaturated expansive clays." *Canadian Geotechnical Journal*, 29(6), 1013–1032.

Ghionna, V. N., and Mortara, G. (2002). "An elastoplastic model for sand–structure interface behaviour." *Géotechnique*, 52(1), 41–50.

Goodman, R. E. (1976). *Methods of geological engineering in discontinuous rocks.* West Publishing Company, San Francisco.

Groenevelt, P. H. (2003). "The Place of Darcy's law in the Framework of Non-Equilibrium Thernodynamics." *Henry PG Darcy and other pioneers in hydraulics*, 71–77.

Hamid, T. B. (2005). "Testing and Modeling of Unsaturated Interface." Ph.D. Dissertation, University of Oklahoma, USA.

Hamid, T. B., and Miller, G. A. (2008). "A constitutive model for unsaturated soil interfaces." *International Journal for Numerical and Analytical Methods in Geomechanics*, 32(13), 1693–1714.

Hamid, T. B., and Miller, G. A. (2009). "Shear strength of unsaturated soil interfaces." *Canadian Geotechnical Journal*, 46(5), 595–606.

Han, Z., Vanapalli, S. K., and Kutlu, Z. N. (2016). "Modeling behavior of friction pile in compacted glacial till." *International Journal of Geomechanics*, 16(6), D4016009.

Ho, D. Y. F. (1988). "The relationship between the volumetric deformation moduli of unsaturated soils." Ph.D. Dissertation, The University of Saskatchewan, Canada.

Hosseinali, M., and Toufigh, V. (2018). "A plasticity-based constitutive model for the behavior of soil-structure interfaces under cyclic loading." *Transportation Geotechnics*, 14, 41–51.

Hu, L., and Pu, J. (2004). "Testing and Modeling of Soil-Structure Interface." *Journal of Geotechnical and Geoenvironmental Engineering*, 130(8), 851–860.

Huang, Y. (1991). "A User-material subroutine incorporating single crystal plasticity in the ABAQUS finite element program." Ph.D. Dissertation, Harvard University, USA.

Jennings, J. E. B., and Burland, J. B. (1962). "Limitations to the use of effective stresses in partly saturated soils." *Geotechnique*, 12(2), 125–144.

Jiang, J., Hou, K., and Ou, X. (2020). "Analysis of the Bearing Capacity of a Single Pile Based on an Analytical Solution of Pile–Soil Interaction in Expansive Soil." *Geotechnical and Geological Engineering*, 38, 1721–1732.

Justo, J., Saura, J., Salamanca, J. E., Delgado Trujillo, A., and Jaramillo, A. (1984). "A finite element method to design and calculate pier foundations in expansive-collapsing soils." *Fifth International Conference on Expansive Soils*, Adelaide, South Australia, 119–123.

Khalili, N., and Selvadurai, A. P. S. (2003). "A fully coupled constitutive model for thermo-hydro-mechanical analysis in elastic media with double porosity." *Geophysical Research Letters*, 30(24), 1–5.

Kim, S., Jeong, S., Cho, S., and Park, I. (1997). "Shear load transfer characteristics of drilled shafts in weathered rocks." *Journal of Geotechnical and Geoenvironmental Engineering*, 125(11), 999–1010.

Koliji, A., Laloui, L., Cusinier, O., and Vulliet, L. (2006). "Suction induced effects on the fabric of a structured soil." *Transport in Porous Media*, 64(2), 261–278.

Koliji, A., Vulliet, L., and Laloui, L. (2010). "Structural characterization of unsaturated aggregated soil." *Canadian Geotechnical Journal*, 47(3), 297–311.

Lashkari, A. (2012). "A critical state model for saturated and unsaturated interfaces." *Scientia Iranica*, 19(5), 1147–1156.

Lashkari, A., and Kadivar, M. (2016). "A constitutive model for unsaturated soil–structure interfaces." *International Journal for Numerical and Analytical Methods in Geomechanics*, 40(2), 207–234.

Lashkari, A., and Torkanlou, E. (2016). "On the constitutive modeling of partially saturated interfaces." *Computers and Geotechnics*, 74, 222–233.

Likos, W. J., and Wayllace, A. (2010). "Porosity evolution of free and confined bentonites during interlayer hydration." *Clays and Clay Minerals*, 58(3), 399–414.

Lin, C.-J., Zhang, Q.-Q., Liang, F.-Y., Zhang, Q., and Liu, H.-L. (2014). "Analysis of bearing behavior of a single pile considering progressive failure of pile-soil system." *Yantu Lixue/Rock and Soil Mechanics*, 35(4), 1131-1140 (in Chinese).

Liu, Y. (2019). "Interpretation of Load Transfer Mechanism for Piles in Unsaturated Expansive Soils." Ph.D. Dissertation, University of Ottawa, Canada.

Liu, Y., and Vanapalli, S. K. (2017). "Influence of Lateral Swelling Pressure on the Geotechnical Infrastructure in Expansive Soils." *Journal of Geotechnical and Geoenvironmental Engineering ASCE*, 143(6), 04017006.

Liu, Y., and Vanapalli, S. K. (2019a). "Load displacement analysis of a single pile in an unsaturated expansive soil." *Computers and Geotechnics*, 106, 83–98.

Liu, Y., and Vanapalli, S. K. (2019b). "Prediction of lateral swelling pressure behind retaining structure with expansive soil as backfill." *Soils and Foundations*, 59(1), 176–195.

Liu, Y., Vanapalli, S. K., and Amina, W. B. (2017). "Load-deformation Analysis of a Pile in Expansive Soil upon Infiltration." *Proceedings of the 2nd World Congress on Civil, Structural,and Environmental Engineering(CSEE`17)*, Barcelona, Spain, ICGRE 157-1-ICGRE 157-9.

Lloret, A., and Alonso, E. E. (1985). "State surfaces for partially saturated soils." *Proceedings of the 11th International Conference on Soil Mechanics and Foundation Engineering*, San Francisco, USA, 557–562.

Long, Y., Chen, J., and Zhang, J. (2017). "Introduction and analysis of a strain-softening damage model for soil–structure interfaces considering shear thickness." *KSCE Journal of Civil Engineering*, 21(7), 2634–2640.

Lytton, R. L. (1977). "Foundations in Expansive Soils." *Numerical methods in geotechnical engineering*, McGraw Hill Book Company, New York, 427–457.

Mašín, D. (2013). "Double structure hydromechanical coupling formalism and a model for unsaturated expansive clays." *Engineering Geology*, 165, 73–88.

Matyas, E. L., and Radhakrishna, H. S. (1968). "Volume change characteristics of partially saturated soils." *Géotechnique*, 18(4), 432–448.

Miller, G. A., and Hamid, T. B. (2006). "Interface direct shear testing of unsaturated soil." *Geotechnical Testing Journal*, 30(3), 182–191.

Mohamedzein, Y. (2006). "Finite element analysis of piers in expansive soils." *Expansive Soils: Recent Advances in Characterization and Treatment*, Taylor & Francis, Leiden, 231–243.

Mohamedzein, Y. E. A., Mohamed, M. G., and El Sharief, A. M. (1999). "Finite element analysis of short piles in expansive soils." *Computers and Geotechnics*, 24, 231–243.

Muraleetharan, K. K., and Wei, C. (1999). "Dynamic behaviour of unsaturated porous media: Governing equations using the Theory of Mixtures with Interfaces (TMI)." *International Journal for Numerical and Analytical Methods in Geomechanics*, 23(13), 1579–1608.

Nelson, J. D., Chao, K. C., and Overton, D. D. (2007). "Design of Pier Foundations on Expansive

Soils." *Proc., 3rd Asian Conf. on Unsaturated Soils*, Science Press, Beijing, 97–108.

Nelson, J. D., Chao, K. C., Overton, D. D., and Nelson, E. J. (2015). *Foundation Engineering for Expansive Soils*. Wiley, New York.

Nelson, J. D., Thompson, E. G., Schaut, R. W., Chao, K. C., Overton, D. D., and Dunham-Friel, J. S. (2012). "Design procedure and considerations for piers in expansive soils." *Journal of Geotechnical and Geoenvironmental Engineering*, 138(8), 945–956.

Nelson, J., and Miller, D. J. (1997). *Expansive soils Problems and practice in foundation and pavement engineering*. John Wiley & Sons, New York.

Ng, C. W. W., Zhan, L. T., Bao, C. G., Fredlund, D. G., and Gong, B. W. (2003). "Performance of an unsaturated expansive soil slope subjected to artificial rainfall infiltration." *Géotechnique*, 53(2), 143–157.

Ni, P., Song, L., Mei, G., and Zhao, Y. (2017). "Generalized Nonlinear Softening Load-Transfer Model for Axially Loaded Piles." *International Journal of Geomechanics*, 17(8), 04017019.

Nowamooz, H., and Masrouri, F. (2010). "Suction variations and soil fabric of swelling compacted soils." *Journal of Rock Mechanics and Geotechnical Engineering*, 2(2), 129–134.

Nuth, M., and Laloui, L. (2008). "Effective stress concept in unsaturated soils: Clarification and validation of a unified framework." *International Journal for Numerical and Analytical Methods in Geomechanics*, 32(7), 771–801.

O'Neill, M. (1988). "Adaptive Model for Drilled Shafts in Expansive Clay." *Special Topics in Foundations*, ASCE, 1–20.

Oh, W. T., and Vanapalli, S. K. (2016). "Influence of Poisson's Ratio on the Stress vs. Settlement Behavior of Shallow Foundations in Unsaturated Fine-Grained Soils." *Soils and Rocks*, 39(1), 71–79.

Pelecanos, L., and Soga, K. (2017). "Innovative Structural Health Monitoring of Foundation Piles Using Distributed Fibre-optic Sensing relevant parameters for foundation piles." *Proceedings of the 8th International Conference on Structural Engineering and Construction Managment*, Kandy, Sri Lanka, 1–8.

Pereira, J. H. F., and Fredlund, D. G. (2000). "Volume change behavior of collapsible compacted geneiss soil." *Journal of Geotechnical and Geoenvironmental Engineering*, 126(10), 907–916.

Poulos, H. G. (1993). "Piled rafts in swelling or consolidating soils." *Journal of Geotechnical Engineering*, 119(2), 374–380.

Poulos, H. G., and Davis, E. H. (1980). *Pile Foundation Analysis and Design*. Wiley (John) & Sons, New York.

Puppala, A. J., and Cerato, A. (2009). "Heave distress problems in chemically-treated sulfate-laden materials." *Geo-Strata*, 10(2), 28.

Qi, S., and Vanapalli, S. K. (2015). "Hydro-mechanical coupling effect on surficial layer stability of unsaturated expansive soil slopes." *Computers and Geotechnics*, 70, 68–82.

Qi, S., and Vanapalli, S. K. (2016). "Influence of swelling behavior on the stability of an infinite unsaturated expansive soil slope." *Computers and Geotechnics*, 76, 154–169.

Rahardjo, H., and Fredlund, D. G. (1995). "Experimental verification of the theory of consolidation for unsaturated soils." *Canadian Geotechnical Journal*, 32(5), 749–766.

Rose, W. (2000). "Myths about later-day extensions of Darcy's law." *Journal of Petroleum Science and Engineering*, 26(1–4), 187–198.

Said, I., De Gennaro, V., and Frank, R. (2009). "Axisymmetric finite element analysis of pile loading tests." *Computers and Geotechnics*, 36(1–2), 6–19.

Seiphoori, A., Ferrari, A., and Laloui, L. (2014). "Water retention behaviour and microstructural evolution of MX-80 bentonite during wetting and drying cycles." *Géotechnique*, 64(9), 721–734.

Shahrour, I., and Rezaie, F. (1997). "An Elastoplastic Constitutive Relation for the Soil-Structure Interface under Cyclic Loading." *Computers and Geotechnics*, 21(1), 21–39.

Shen, J., and Karakus, M. (2014). "Three-dimensional numerical analysis for rock slope stability using shear strength reduction method." *Canadian Geotechnical Journal*, 51(2), 164–172.

Sheng, D., Fredlund, D. G., and Gens, A. (2008). "A new modelling approach for unsaturated soils using independent stress variables." *Canadian Geotechnical Journal*, 45(4), 511–534.

Shi, B., Jiang, H., Liu, Z., and Fang, H. Y. (2002). "Engineering geological characteristics of expansive soils in China." *Engineering Geology*, 67(1–2), 63–71.

Shuai, F. (1996). "Simulation of swelling pressure measurements on expansive soil." Ph.D. Dissertation, The University of Saskatchewan, Canada.

Shuai, F., and Fredlund, D. G. (1998). "Model for the simulation of swelling-pressure measurements on expansive soils." *Canadian Geotechnical Journal*, 35(1), 96–114.

Sinha, A., and Hanna, A. M. (2017). "3D Numerical Model for Piled Raft Foundation." *International Journal of Geomechanics*, 17(2), 04016055.

Skempton, A. W. (1960). "Terzaghi's discovery of effective stress." *From Theory to Practice in Soil Mechanics: Selections from the Writings of Karl Terzaghi*, 42–53.

Sorochan, E. A. (1974). "Use of piles in expansive soils." *Soil Mechanics and Foundation Engineering*, 11(1), 33–38.

Soundara, B., and Robinson, R. G. (2017). "Hyperbolic model to evaluate uplift force on pile in expansive soils." *KSCE Journal of Civil Engineering*, 21(3), 746–751.

Steinberg, M. L. (1998). *Geomembranes and the control of expansive soils in construction*. McGraw-Hill Professional, New York.

Tamagnini, R. (2004). "An extended Cam-clay model for unsaturated soils with hydraulic hysteresis." *Géotechnique*, 54(3), 223–228.

Tang, L., Cong, S., Ling, X., Xing, W., and Nie, Z. (2018). "A unified formulation of stress-strain relations considering micro-damage for expansive soils exposed to freeze-thaw cycles." *Cold Regions Science and Technology*, 153, 164–171.

Vanapalli, S., and Adem, H. (2013). "Estimation of the 1-D heave of a natural expansive soil deposit with a light structure using the modulus of elasticity based method." *Proceedings of the 1st Pan-American conference on unsaturated soils, Colombia*, 101–114.

Vanapalli, S. K., Fredlund, D. ., Pufahi, D. E., and Clifton, A. W. (1996). "Model for the prediction of shear strength with respect to soil suction." *Canadian Geotechnical Journal*, 33(3), 379–392.

Vu, H. Q. (2003). "Uncoupled and coupled solutions of volume change problems in expansive soils." Ph.D. Dissertation, The University of Saskatchewan, Canada.

Wang, G., and Wei, X. (2014). "Modeling swelling–shrinkage behavior of compacted expansive soils during wetting–drying cycles." *Canadian Geotechnical Journal*, 52(6), 783–794.

Wang, J., Ma, G., Zhuang, H., Dou, Y., and Fu, J. (2019). "Influence of diaphragm wall on seismic responses of large unequal-span subway station in liquefiable soils." *Tunnelling and Underground Space Technology*, 91, 102988.

Wang, Q., Cui, Y. J., Tang, A. M., Barnichon, J. D., Saba, S., and Ye, W. M. (2013). "Hydraulic conductivity and microstructure changes of compacted bentonite/sand mixture during hydration." *Engineering Geology*, 164, 67–76.

Wheeler, S. J., Sharma, R. S., and Buisson, M. S. R. (2003). "Coupling of hydraulic hysteresis and stress–strain behaviour in unsaturated soils." *Géotechnique*, 53(1), 41–54.

Wheeler, S. J., and Sivakumar, V. (1995). "An elasto-plastic critical state framework for unsaturated soil." *Géotechnique*, 45(1), 35–53.

Xiao, H., Zhang, C., Wang, Y., and Fan, Z. (2011). "Pile-Soil Interaction in Expansive Soil Foundation: Analytical Solution and Numerical Simulation." *International Journal of Geomechanics*, 11(3), 159–166.

Xue, Y., Li, Y., Shao, W., Xu, L., and Cai, F. (2018). "A simplified piecewise-hyperbolic softening model of skin friction for axially loaded piles." *Computers and Geotechnics*, 108, 7–16.

Yang, X., Yang, G., and Yu, T. (2012). "Comparison of Strength Reduction Method for Slope Stability Analysis Based on ABAQUS FEM and FLAC3D FDM." *Applied Mechanics and Materials*, Applied Mechanics and Materials, 170, 918–922.

Yu, Y., Damians, I. P., and Bathurst, R. J. (2015). "Influence of choice of FLAC and PLAXIS interface models on reinforced soil-structure interactions." *Computers and Geotechnics*, 65, 164–174.

Zemenu, G., Martine, A., and Roger, C. (2009). “Analysis of the behaviour of a natural expansive soil under cyclic drying and wetting.” *Bulletin of Engineering Geology and the Environment*, 68(3), 421–436.

Zhang, G., and Zhang, J. (2009). “State of the art: Mechanical behavior of soil-structure interface.” *Progress in Natural Science*, National Natural Science Foundation of China and Chinese Academy of Sciences, 19(10), 1187–1196.

Zhang, Q., Zhang, B., Li, L., Zhang, Q., and Li, S. (2015). “Analysis on Response of a Single Pile Subjected to Tension Load Using a Softening Model and a Hyperbolic Model.” *Marine Georesources & Geotechnology*, 33(2), 167–176.

Zhang, Q., and Zhang, Z. (2012). “A simplified nonlinear approach for single pile settlement analysis.” *Canadian Geotechnical Journal*, 49(11), 1256–1266.

Zhang, X. (2004). “Consolidation theories for saturated-unsaturated soils and numerical simulation of residential buildings on expansive soils.” Ph.D. Dissertation, Texas A&M University, USA.

Zhang, X., and Lytton, R. L. (2009a). “Modified state-surface approach to the study of unsaturated soil behavior. Part I: Basic concept.” *Canadian Geotechnical Journal*, 46(5), 536–552.

Zhang, X., and Lytton, R. L. (2009b). “Modified state-surface approach to the study of unsaturated soil behavior. Part II: General formulation.” *Canadian Geotechnical Journal*, 46(5), 553–570.

Zhang, Z., Zhang, Q., and Yu, F. (2011). “A destructive field study on the behavior of piles under tension and compression.” *Journal of Zhejiang University: Science A*, 12(4), 291–300.

Zhang, Z., Zhang, Q., Yu, F., and Liu, J. (2010). “Field performance of long bored piles within piled rafts.” *Proceedings of the Institution of Civil Engineers - Geotechnical Engineering - Geotechnical Engineering*, 163(6), 293–305.

Zhao, C., Lu, J., Sun, Q., Zhu, T., and Li, S. (2009). “Experimental study of load transmission property of large-diameter bored cast-in-situ deep and long pile in different soil layers.” *Yanshilixue Yu Gongcheng Xuebao/Chinese Journal of Rock Mechanics and Engineering*, 28(5), 1020–1026.

Zhao, M. H., Yang, M. H., and Zou, X. J. (2005). "Vertical bearing capacity of pile based on load transfer model." *Journal of Central South University of Technology (English Edition)*, 12(4), 488–493.

Zienkiewicz, O. C., and Chan, A. H. C. (1989). "Coupled Problems and Their Numerical Solution." *Advances in Computational Nonlinear Mechanics*, Springer, New York, 139–176.

Zienkiewicz, O. C., Taylor, R. L., and Zhu, J. Z. (2005). *The Finite Element Method : Its Basis and Fundamentals*. Elsevier, Burlington.